



TRC0506

# **Geosynthetic Drains for Slope Stability & Rehabilitation**

Norman D. Dennis, Jr., Hai Ngoc Nguyen

Final Report

2015

**Technical Report Documentation Page**

1. Report No.		2. Government Accession No.		3. Recipient's Catalog No.	
4. Title and Subtitle  <b>TRC0506 Geosynthetic Drains for Slope Stability and Rehabilitation  Final Report</b>				5. Report Date <b>Jan 2015</b>	
				6. Performing Organization Code	
7. Author(s) <b>Norman D. Dennis, Jr. Hai Ngoc Nguyen</b>				8. Performing Organization Report No.	
9. Performing Organization Name and Address <b>University of Arkansas, Department of Civil Engineering 4190 Bell Engineering Center Fayetteville, AR 72701</b>				10. Work Unit No. (TRAIS)	
				11. Contract or Grant No. <b>TRC0506</b>	
12. Sponsoring Agency Name and Address <b>Arkansas State Highway and Transportation Department P.O. Box 2261 Little Rock, AR 72203-2261</b>				13. Type of Report and Period covered <b>Final Report 1 July 2005 thru 30 June 2009</b>	
				14. Sponsoring Agency Code	
15. Supplementary Notes					
<p>16. Abstract</p> <p>According to Walkinshaw (1997) the State of Arkansas expended approximately \$600,000 per year on slope repairs for minor and major slides between 1986 and 1990. These slides were triggered primarily from rainfall events and saturated slopes. During the construction of interstate I-540 in Northwest Arkansas it is estimated that \$65,000 per lane mile was expended on slope repairs. Post construction, an additional \$32,000,000 was spent on repairs in the first four years of service. The vast majority of slope failures along I-540 were triggered by rainfall events and were the result of saturated soil conditions. Clearly, drainage, both surface and internal, is a key element for preventing or retarding slope failures.</p> <p>The objective of this study was to investigate the use of geosynthetic horizontal drains for increased slope stability in soils. The first year of this study devoted to defining the optimum drain type, drain configuration, drain spacing and construction equipment, through a review of the literature and parametric studies. Using the information determined during parametric study, a full-scale field demonstration was then implemented at a site on I-540. The site was monitored, and evaluated during the last 12 months of the project. The full-scale field test consisted of a control section, where no drainage features were installed and a test section where 18 pre-fabricated geosynthetic drains were driven into the slope near its toe. Slope movement and moisture conditions within the slope were monitored remotely using time domain reflectometry (TDR) techniques, which could be monitored remotely, along with more conventional equipment such as slope inclinometers and piezometers which had to be manually employed and read on a recurring interval. Additionally, an abbreviated weather station was installed to monitor rainfall events and temperature at the site. The volume of flow discharged by the drains was monitored using a tipping bucket rain gauge.</p> <p>The parametric study resulted in recommendations for drain spacing when considering soil type and slope geometry. Drain spacing recommendations ranged from 0.75 meters in both vertical and horizontal dimension for clay soils up to 4 m in only the horizontal direction for predominately sandy and gravelly soils. The results of the field investigation indicated that the drains were effective in reducing the moisture content in the soil, sometime by as much as 20 percent, when the drained section was compared to the control section. Through the discharge collection system it was determined that the drains responded almost immediately to a rainfall event and the discharge volume never exceeded the flow capacity of the drain. While movements in the drained section were always smaller than those in the control section and were generally lagging by about three weeks, the geosynthetic drains did not totally prevent movements in the slope as we had hoped. A cost analysis of the drain installation suggests the average cost per foot of drain was approximately \$4.25 which is substantially cheaper than the costs for PVC or galvanized pipe drains.</p>					
17. Key Words <b>Slope stability, wick drains, horizontal slope drains, slope remediation, intenal drains</b>			18. Distribution Statement <b>No Restrictions</b>		
19. Security Classif. (Of this report) <b>(none)</b>		20. Security Classif. (Of this page) <b>(none)</b>		21. No. of Pages <b>203</b>	22. Price



## Geosynthetic Drains for Slope Stability and Rehabilitation

### PROJECT BACKGROUND AND OBJECTIVES

According to Walkinshaw (1997) the State of Arkansas expended approximately \$600,000 per year on slope repairs for minor and major slides between 1986 and 1990. These slides were triggered primarily from rainfall events and saturated slopes. During the construction of interstate I-540 in Northwest Arkansas it is estimated that \$65,000 per lane mile was expended on slope repairs. Post construction, an additional \$32,000,000 was spent on repairs in the first four years of service. The vast majority of slope failures along I-540 were triggered by rainfall events and were the result of nearly saturated soil conditions. Clearly, drainage, both surface and internal, is a key element for preventing or retarding slope failures.

The objective of this study was to investigate the use of geosynthetic horizontal drains for increased slope stability in soils. The first year of this study devoted to defining the optimum drain type, drain configuration, drain spacing and construction equipment, through a review of the literature and parametric studies. Using the information determined during parametric study, a full-scale field demonstration was then implemented at a site on I-540. The site was monitored, and evaluated during the last 12 months of the project. The full-scale field test consisted of a control section, where no drainage features were installed and a test section where 18 pre-fabricated geosynthetic drains were driven into the slope near its toe. Slope movement and moisture conditions within the slope were monitored remotely using time domain reflectometry (TDR) techniques, which could be monitored remotely, along with more conventional equipment such as slope inclinometers and piezometers which had to be manually employed and read on a recurring interval. Additionally, an abbreviated weather station was installed to monitor rainfall events and temperature at the site. The volume of flow discharged by the drains was monitored using a tipping bucket rain gauge.

### FINDINGS

The parametric study resulted in recommendations for drain spacing when considering soil type and slope geometry. Drain spacing recommendations ranged from 0.75 meters in both vertical and horizontal dimension for clay soils up to 4 m in only the horizontal direction for predominately sandy and gravelly soils. The results of the field investigation indicated that the drains were effective in reducing the moisture content in the soil, sometime by as much as 20 percent, when the drained section was compared to the control section. Through the discharge collection system it was determined that the drains responded almost immediately to a rainfall event and the discharge volume never exceeded the flow capacity of the drain. While movements in the drained section were always smaller than those in the control section and were generally lagging by about three weeks, the geosynthetic drains did not totally prevent movements in the slope as we had hoped. A cost analysis of the drain installation suggests the average cost per foot of drain was approximately \$4.25 which is substantially cheaper than the costs for PVC or galvanized pipe drains.

### RECOMMENDATIONS

During the course of the field investigation a number of lessons were learned about the installation process that could possibly reduce the installation cost and the installation speed for the geosynthetic drains. Due to the time of year and the cost of rental installation equipment, fewer than the optimum number of drains were installed in the test section. It is hypothesized that improved installation procedures coupled with installation of the optimum number of drain would make this drainage method a viable remediation measure for moisture induced slope failures.

**R  
E  
S  
E  
A  
R  
C  
H**

**TRC- 0506**

# Geosynthetic Drains for Slope Stability and Rehabilitation

By

Norman D. Dennis

and

Hai Ngoc Nguyen

## Abstract

According to Walkinshaw (1997) the State of Arkansas expended approximately \$600,000 per year on slope repairs for minor and major slides between 1986 and 1990. These slides were triggered primarily from rainfall events and saturated slopes. During the construction of interstate I-540 in Northwest Arkansas it is estimated that \$65,000 per lane mile was expended on slope repairs. Post construction, an additional \$32,000,000 was spent on repairs in the first four years of service. The vast majority of slope failures along I-540 were triggered by rainfall events and were the result of nearly saturated soil conditions. Clearly, drainage, both surface and internal, is a key element for preventing or retarding slope failures.

The objective of this study was to investigate the use of geosynthetic horizontal drains for increased slope stability in soils. The first year of this study devoted to defining the optimum drain type, drain configuration, drain spacing and construction equipment, through a review of the literature and parametric studies. Using the information determined during parametric study, a full-scale field demonstration was then implemented at a site on I-540. The site was monitored, and evaluated during the last 12 months of the project. The full-scale field test consisted of a control section, where no drainage features were installed and a test section where 18 pre-fabricated geosynthetic drains were driven into the slope near its toe. Slope movement and moisture conditions within the slope were monitored remotely using time domain reflectometry (TDR) techniques, which could be monitored remotely, along with more conventional equipment such as slope inclinometers and piezometers which had to be manually

employed and read on a recurring interval. Additionally, an abbreviated weather station was installed to monitor rainfall events and temperature at the site. The volume of flow discharged by the drains was monitored using a tipping bucket rain gauge.

The parametric study resulted in recommendations for drain spacing when considering soil type and slope geometry. Drain spacing recommendations ranged from 0.75 meters in both vertical and horizontal dimension for clay soils up to 4 m in only the horizontal direction for predominately sandy and gravelly soils. The results of the field investigation indicated that the drains were effective in reducing the moisture content in the soil, sometime by as much as 20 percent, when the drained section was compared to the control section. Through the discharge collection system it was determined that the drains responded almost immediately to a rainfall event and the discharge volume never exceeded the flow capacity of the drain. While movements in the drained section were always smaller than those in the control section and were generally lagging by about three weeks, the geosynthetic drains did not totally prevent movements in the slope as we had hoped. A cost analysis of the drain installation suggests the average cost per foot of drain was approximately \$4.25 which is substantially cheaper than the costs for PVC or galvanized pipe drains.

During the course of the field investigation a number of lessons were learned about the installation process that could possibly reduce the installation cost and the installation speed for the geosynthetic drains. Due to the time of year and the cost of rental installation equipment fewer than the optimum number of drains were installed in the test section. It is hypothesized that improved installation procedures coupled with

installation of the optimum number of drain would make this drainage method an viable remediation measure for moisture induced slope failures.

## Table of Contents

Abstract	ii
Chapter 1 Introduction	1
Chapter 2 Background and Literature Review	5
Chapter 3 Research Methodology	48
Chapter 4 Results and Discussion	107
Chapter 5 Conclusions and Recommendations	184
Appendix A: Operating Principles of the Slope Inclinometer	188
Appendix B:	194



# CHAPTER 1

## INTRODUCTION

### 1.1 Problem statement

Throughout history, slope failures have caused major loss of life and heavy economic damage. In 1985 The National Research Council (Committee on Ground Failure Hazards, 1985) estimated that the total cost of slope failures in the United States was about \$1 to \$2 billion per year. Distributing this cost to the entire population at that time, results in an annual cost of \$5 to \$10 for every man woman and child in the United States. Walkinshaw (1992) reported that the total average direct costs for the repair and maintenance of landslide prone areas on 1.3 million km of state highways, was over \$106 million per year for the 5-year period from 1986 to 1990. Walkinshaw (1992) also found that in many states, for which detailed maintenance records had been kept, the cost of in-house maintenance exceeded annual contract repair costs. It should be noted that Walkinshaw's data represented only 20 percent of the entire US highway system at the time (Turner and Schuster, 1996), so the annual cost of all repairs could be much more than reported by Walkinshaw. As a result of these high costs many state Departments of Transportation (DOTs) are acutely aware of slope instability issues because of both budgetary and loss of service considerations.

On January 8, 1999, the final 69 km (43 mile) section of Interstate I-540 was finished, connecting Fayetteville to Fort Smith at a cost of \$440 million. This section of road represents a very expensive project for the State of Arkansas and for other rural areas in the United States. According to information taken from "State of Arkansas 2007

Hazard Mitigation Plan” (Arkansas Department of Emergency Management), approximately \$65,000 per mile per year was spent to repair active landslides during the construction period. The total cost of slope repairs along this segment of highway, both during construction and subsequent to its opening have exceeded \$42,000,000. This makes I-540 one of the most expensive highways that has ever been built in Arkansas, as well as one of the most expensive highways to maintain. The history of slope failures along I-540 and other highways in the State has made the Arkansas State Highway and transportation Department acutely aware of the need for proactive remediation procedures for both cut and fill slopes along its highway system.

The geologic features of the northwest Arkansas also have a major impact on failure potential. Hunt (1984) stated that the northwest region of Arkansas is located on the Ozark Plateau. The principal geologic feature of this region is mostly weak weathered soil overlying low permeability shale. The strength of these soil deposits usually decreases with the presence of water in the soil mass. Moreover, the terrain of the northwest region of Arkansas is mostly hilly. Thus, the failure potential of slopes in this region is very large. Coupled with the fact that over 62 active slides have been detected by the Arkansas Highway Transportation Department (AHTD) in the first 5-years of service along a 42-mile section of I-540, there is a need for an effective and economical method to stabilize active slides along this and other highways in the state of Arkansas, as well as other parts of the country.

Many slope failures stem from elevated pore water pressure in the soil mass, which results in reduced effective stresses and a loss of soil strength. Elevated pore water pressures in soil masses are due mostly to inadequate drainage within the soil mass (after

Dennis, personal communication, 2007). Currently, the most common strategy to repair slope failures in northwest Arkansas is to remove the poor quality soil and replace it with better quality material. Another alternative being used in this region is buttressing the failed material with rock at the toe of the slopes. However, these two methods are relatively expensive and sometimes the slopes still fail behind the repair. Therefore, the need for a more economical and effective remediation technique is needed.

Among the many techniques used for landslide hazard reduction, drainage is an effective and economical method (Natarajan, 1986). Not only is drainage effective in remediating failed slopes, it can also be used to enhance the stability of semi-stable slopes, thus reducing the probability of a future failure. The objective of this research is to evaluate the effectiveness of a specific drainage method. Namely, the use of horizontal geosynthetic wick drains to produce an effective solution for positive drainage in slopes consisting of relatively impermeable material. Once this method is proven, it might be used throughout the state as a cost-effective remediation measure that will eliminate the need to constantly repair slope failures.

## **1.2 Research objectives**

The intent of this research is to evaluate the effectiveness of horizontally-installed geosynthetic wick drains as a cost effective measure to prevent slope failures or to remediate failed slopes. In order to achieve that objective, a well designed experiment must be developed that couples field measurements with analytical work. The major tasks can be defined as:

- 1) Select a test site that consists of a slope that shows signs of movement.
- 2) Characterize the slope and material properties at the test site.

- 3) Determine the optimum configuration of the drains (spacing, length, and position) by analytical techniques using finite element method.
- 4) Evaluate the installation process by considering efficiency and cost of the installation to determine if it is an effective and economic method as desired.
- 5) Assemble and calibrate a suite of measuring equipment to monitor the performance to the remediated slope.
- 6) Evaluate the performance of the installed drainage system based on the data collected during the monitoring period.
- 7) Develop an implementation plan using the results of the study to establish the optimum configuration of the wick drain systems for various slope geometries and soil types, as well as establishing the best installation procedure.

## CHAPTER 2

### BACKGROUND AND LITERATURE REVIEW

#### 2.1 Overview of Stabilization Methods for Landslides and Slope Failures

A landslide, as defined by Cruden (1991), is “the movement of a mass of rock, debris or earth down a slope”. Xue and An (1986) stated that the first recorded landslide was in 1767 B.C. in the Hunan Province of central China. Since then many landslides have been recorded and analyzed, giving us a comprehensive understanding of the triggering mechanisms and sequence of movement of landslides, along with the resulting damage. Having a thorough understanding of landslide mechanics is very necessary to develop the principles or methods that can prevent or mitigate landslides and their damage.

According to Wieczorek (1996), there are many natural causes of a landslide such as intense rainfall, rapid snowmelt, external water level change, volcanic eruption, and earthquake shaking. Most of the natural causes cited above relate to the presence of water within the slope. Cai (1998) found that an increase in moisture level, even without increasing the level of the ground water table, leads to a reduction in the soil’s matric suction, resulting in a reduction in its shear strength. This loss of strength can ultimately cause a landslide. In some cases, such as in rapid drawdown of reservoirs, water inside the slope will generate positive pore pressures, resulting in reduced effective stress and a significant reduction in shear strength. When soil strengths are reduced below a certain level the slope becomes unstable. Keeping water out of the slope is therefore one of the

best methods to deal with landslides resulting from perched water inside the slope. A cost effective method to drain water out of slopes is the focus of this research.

Throughout history, landslides have caused great economic damage and loss of life whenever they occur. The cost of landslides can be described in terms of both direct and indirect losses to public and private property. According to Schuster (1996), the direct costs include the cost for repair, replacement or maintenance associated with property damaged by landslides, whereas indirect costs are the other costs of landslides such as:

- Loss of industrial, agricultural or forest productivity because of damage to transportation systems.
- Loss of human or animal productivity through death, injury, or psychological distress resulting from the landslide.
- Reduction in real estate values because of proximity to landslides.

In 1985 the National Research Council (Committee on Ground Failure Hazards, 1985) estimated that the total cost of slope failures in the United States was about \$1 to \$2 billion per year. By averaging these costs over the entire 1985 US population, the cost of slope failures was between \$5 and \$10 per capita per year. Walkinshaw (1992) reported that the total average direct costs for the repair and maintenance of landslide prone areas on 1.3 million km of state highways, was over \$106 million per year for the 5-year period from 1986 to 1990. Walkinshaw (1992) also found that in many states, the cost of in-house maintenance exceeded the annual contract repair costs. Even though these costs are significant, it should be noted that Walkinshaw's data represented only 20 percent of the entire US highway system at the time (Turner and Schuster, 1996), so the annual cost of all repairs could be much more than reported by Walkinshaw. The above

statistics show that the economic damage of landslides is very large; therefore, State DOTs should look for economical preventive measures to reduce potential direct and indirect costs associated with them.

There are many stabilization methods for both preventing potential landslides and remediating existing slope failures. According to Holtz and Schuster (1996), Gedney and Weber (1978) cited the most common methods for slope stabilization as those listed below. These methods are categorized in three main groups as follows:

1) Avoidance of a landslide problem.

- Relocating facility to a more stable site.
- Complete or partial removal of unstable materials from the site. This method is most appropriate when poor soils are encountered at shallow depths. However, it may be costly for landslides which require large amounts of excavation.
- Installing bridge. This alternative is best at hillside locations with shallow soil movements.

2) Reduction of driving forces.

- Flattening of slopes or reducing excavation depths, or through changes in line and grade for road systems
- Using drainage to remove water out of the slopes, thus reducing the weight of the mass tending to cause failures and increasing the strength of the soils within the slope.
  - Surface drainage. This method is the first approach to be considered in slope failure prevention since it requires minimal

engineering design. Sufficient surface drainage using diversion ditches and interceptor drains are commonly used for slopes in which large volumes of runoff are anticipated (Holtz and Schuster, 1996).

- Subsurface drainage. This alternative should be considered in the design if the initial site exploration indicates the presence of ground water within the slope. Subsurface drainage can help to control and lower the ground water, thus reducing the seepage force which is a cause of increased driving forces in a slope. Subsurface drainage can be applied by using blankets and trenches, wells, drain tunnels or drain galleries, and horizontal drains. This method is applicable in any slope where lowering groundwater can improve slope stability. However, the effectiveness of these methods are reduced when used in highly impermeable soils.
- Reduction of weight. Using lightweight backfill materials can reduce the gravitational forces which tend to cause slope instability. Therefore, this method is very useful to reduce driving forces and increase slope stability, especially in embankment constructions where a large amount of fill material is needed. The materials that have been used for lightweight backfill in highway embankments are: sawdust, dried peat, fly ash cinders, cellular concrete, expanded clay or shale, expanded polystyrene, shredded and chipped tires, and oyster shells and clamshells (Holtz and Schuster, 1996). This method can be applied at any existing or potential landslide.



However, it has a major drawback in that the cost of lightweight materials is high, especially when they may not be locally available. As a remediation measure this method also requires the excavation and disposal of large quantities of unsuitable material. Both of these issues could significantly increase the cost of the project.

3) Increasing resisting forces.

- Applying an external force at the toe of the slope to increase the resistance of the slope against failure.
  - Use of Buttresses, counterweight fills, and toe berms. Using these types of fills will provide additional dead load or restraints at or near the toe of the slope to prevent the movement of an unstable mass. A buttress must be heavy enough to provide the resistance needed for slope stability. At the same time it must be located on a firm foundation to prevent a bearing or overturning failure. These measures are usually constructed of blasted quarry rock, boulders and cobbles, and coarse gravel fills.
  - Structural retention systems. Conventional retaining walls and piles are more appropriate when physical constraints prevent the use of a buttress or the cost of a buttress or toe berm make them inappropriate choices to increase the resistance of the slope against sliding. Retention structures can be installed before excavation is carried out to help prevent slope movement. However, they cannot

tolerate large movements and the structures must penetrate deeper than the predicted sliding surface of the slope.

- Increasing internal strength
  - Soil reinforcement. This method will increase the tensile strength and shearing resistance of the soil mass against sliding. It is a cost-effective measure to improve the stability of a natural and embankment slope as well as to reduce the earth pressure against retaining walls and abutments. However, it is a method that is most effective for use during, not after construction.
    - Reinforced backfill. Reinforced-soil structures are used because of their advantages over the conventional retaining walls, mainly based on their ability to tolerate large movement, ease of construction, suitability of a wide range of backfill materials, and low cost compared to reinforced concrete retaining walls, especially for steep slopes. The reinforcements that have been commonly used are steel or polymeric strips or grids, geotextiles, and steel cables or bars attached to different anchor systems.
    - In situ reinforcement. These reinforcement methods include soil nailing and soil anchors. The materials used for soil “nails” are usually steel bars, rods, cables or steel tubes. These nails are either driven into the slope or grouted into boreholes that were previously drilled in the slope. Soil

nails develop tensile stress passively due to small movements in the soil, while anchor systems are actively stressed after installation.

- Vegetative and biotechnical stabilization. This technique helps to increase the stability of the slopes by providing reinforcement to the failure mass through the roots of the vegetation on the slope surface. This method also reduces the groundwater in the slope through rainfall interception and evapotranspiration. Grasses and woody plants are usually used in this biotechnical stabilization method.
- Chemical treatment. Lime, fly ash, Portland cement and calcium chloride are the chemicals normally used for soil modification to improve slope stability.
- Thermal treatment. Applying high thermal energy to dry out the soil and increase the soil shear strength can be used to reduce the sensitivity of the clay soils to the action of water. Additionally, ground freezing is very effective to increase the temporary stability of large excavations and tunnels. However, this technique is usually expensive and requires careful consideration in the design; therefore it is only used in some specific situations.

For slope stability issues related to water retention, such as those in Northwest Arkansas, the alternative of using drainage to stabilize a slope over other more costly and invasive techniques to is attractive. According to Natarajan, the use horizontal drainage

systems may be one of the most cost effective techniques for landslide hazard reduction (Natarajan, 1986).

## **2.2 Horizontal Drainage Method**

Horizontal drainage or sub-horizontal drainage is a technique whereby many drains are installed into a slope to convey water out and increase its stability (Forrester, 2001). The presence of water within a slope is a cause of reduced soil strength and slope instability. Removing water from the slope through the installation of horizontal drains can help to reduce driving stresses and increase the strength of the soil, thus improving the stability of the slope. This method can be applicable as a corrective or preventive measure for landslides, especially in cuts and embankments (Holtz and Schuster (1996).

The horizontal drainage method was developed and first used in 1939 by the California Division of Highways (Stanton, 1948). However, this method did not gain wide acceptance by highway engineers until many years later (Royster, 1980). Perforated steel pipes were used in the first applications of horizontal drains. These 102 mm (4 in) diameter steel pipes were perforated with 10 mm (0.4 in) diameter holes on 76 mm (3 in) spacing.(Royster, 1980). These pipes were installed into the slope using a drill rig called a “Hydrauger” (Eager, 1956). The Hydrauger was mounted on a tracked frame and the drill rod was advanced into the slope by a hand-operated ratchet. As the drill bit was advanced into the slope, water or air was pumped through the drill rod to cool the bit and flush the cuttings from the holes. The drilling process was continued until the desired depth was reached. Then a perforated steel pipe was jacked or otherwise advanced into the hole. Additional pipes were butt-welded to the first pipe section as the

operation proceeded, forming a continuous drain along the entire length of the bored hole (Stanton, 1948).

Since the first installation of metal perforated pipes, the equipment, materials and installation procedure have changed markedly (Royster, 1980). The availability of a wider variety of auger bits such as fishtail bit and later tri-cone roller bit were invented in 1949 so that the drilling could be made through stiffer material. While improvements to the drilling equipment were important in promoting the method, the most significant improvement in the horizontal drainage method was the development of a new drain material, polyvinyl chloride (PVC) pipes were introduced in the 1950s,(Royster, 1980). This type of material was unaffected by corrosion from the environment, and could extend the lifespan of the drain pipes to more than the 30-40 years that was usually obtained from the steel pipes. A PVC drain pipe is usually 5 cm (2 in.) in diameter and manufactured with a series of 0.25 mm (0.01 in) to 1.27 mm (0.05 in) wide slots distributed in a multi-slot configuration around the perimeter of the pipe at 6 mm (0.25 in) intervals. Figure 2-1 illustrates three PVC drain pipe samples with different slot widths ranging from 0.25 mm (0.01in.) to 1.27 mm (0.05 in.). Drill rigs with hollow stem augers were used to drill a nearly horizontal hole in soil or soft rock in order to install the PVC drain (Seegmiller, 1979). The slotted PVC pipe was inserted into the hole through the hollow stem after the desired drilling depth was reached. Then the auger stem was removed, leaving the drain behind in the hole.

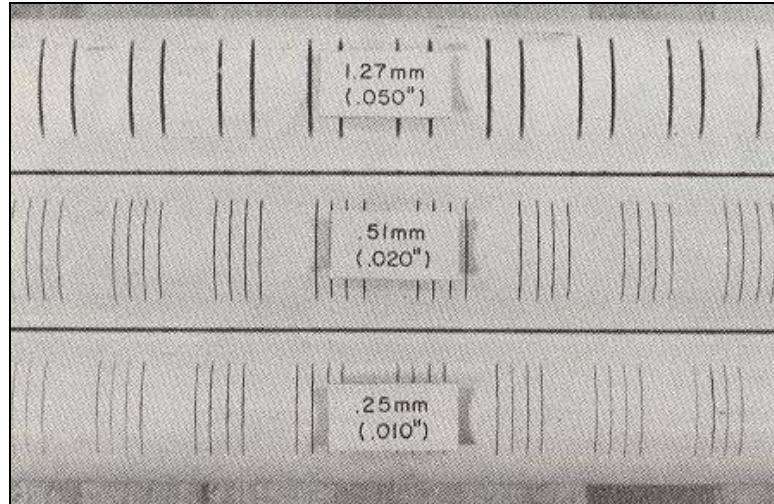


Figure 2-1: Conventional slotted PVC drain pipe (Royster, 1980).

Another new type of drain material, a geosynthetic wick, was first used for horizontal drains by Santi (1999). During the 1970's, wick drains were developed to replace conventional sand drains to accelerate the consolidation of soft soils.

Figure 2-2 illustrates a sample of wick drain currently available on the market. As shown in Figure 2-2, wick drains consist of a corrugated plastic core which is covered by a gray-colored nonwoven geotextile jacket. The grooved core of the wick drain provides a high flow capacity, which can be as high as 1.6 gallons per minute under 300 KPa confining pressure (American Wick Drain specification, 2008), while the geotextile jacket prevents clogging of the drain by serving as a filter to prevent the surrounding fine materials from entering the core. The conventional direction of wick drain installation for the acceleration of consolidation is vertical. Santi (1999) was the first researcher to document an experiment in which wick drains were installed in a horizontal direction to drain water from a slope. Since then a few studies have been conducted to evaluate the workability of this new type of material for horizontal drains. However, these

studies have not provided a thorough understanding of the important parameters for the design of horizontal wick drains systems.



Figure 2-2: Illustration of a typical wick drain.

### 2.2.1 Advantages of Horizontal Drains

The chief advantages of horizontal drains are listed by Seegmiller (1979) as:

- Installation rate of PVC (polyvinyl chloride) drains is rapid, and the installation process is quite easy.
- No power is required after installation since the drain system works by gravity.
- The cost of drain installation and maintenance is relatively low.

Singer (1990) also agreed that the installation of horizontal drains is a good method to stabilize slopes. More importantly, both authors emphasized the cost effectiveness of this remediation method. The economics of the horizontal drain method seems to be the most significant factor when comparing it to other remediation techniques. There is no requirement for skilled labor or specialized equipment for drain installation. Thus, the cost for equipment and labor for this method is relatively low. Moreover, the life span of the drains, usually made of PVC pipes or geosynthetic wicks, is very long, and it does not require any maintenance or repair once the installation is

completed. The cost of the material for this method is relatively low compared to the materials required for other remediation methods (Root, 1955).

## 2.2.2 Disadvantages of Horizontal Drains

Although the use of horizontal drains has a number of advantages, there are also some disadvantages. According to Santi (1999), the two biggest drawbacks of conventional horizontal PVC drains are the tendency for the drains to become clogged with fine materials which surround them. Secondly the cost of the PVC drain itself is between \$6 and \$11 per foot. However, Santi (1999) points out that these problems can be solved by using a wick drain. The inner corrugated polypropylene core of the wick drain can provide high drainage capacity while the outer nonwoven geotextile filter helps to prevent clogging from the surrounding fine materials. An additional benefit of wick drains is that the material cost is only approximately \$1-1.50 per foot (Santi, 1999), which is far cheaper than the cost of PVC pipe. The use of wick drains is therefore a good alternative to conventional horizontal drains based on cost alone.

## 2.3 Factors Affecting the Performance of Horizontal Drains.

### 2.3.1 Effect of Drain Length

Cai, Ugai, Wakai, and Li (1998) used three-dimensional finite element analyses to evaluate the effects of horizontal drains on slope stability under rainfall conditions. Their results showed that the discharge capacity ratio, which is the ratio of the discharge rate through the horizontal drains to the total rainfall falling on the slope face and slope crest, increases as the length of horizontal drains increases. Their conclusions focused on the following points:



- Increasing the length of drains improves the stability of a slope, but the rate of increase in stability is insignificant when the drain length is extended beyond a critical length. They defined the critical length as, “the distance between the slope toe and the slope shoulder” (Cai, Ugai, Wakai, and Li, 1998). This is because the stability of a slope is highly influenced by the pressure head in the zone along the slip surface, but it is independent of the pressure head at points which are far from the critical slip surface. Thus, extending the drains far beyond the failure surface is not useful in stabilizing a slope.
- When the length of the drains are shorter than the critical length, any reduction of the spacing between the drains or increase in the number of drains does not make as large of an improvement in stability as lengthening the drains. It is implied that increasing the drain length to the critical length is more effective than decreasing the drain spacing.

Lau and Kenney (1983) conducted a study which included a field experiment and a parametric study to analyze the parameters that affect the operation of horizontal drain pipes. The purpose of their fieldwork was to determine whether or not the drains would decrease the ground water pressure. The parametric study was conducted to analyze the factors that influence the effectiveness of the drain system in the stability of clayey soil slopes. The initial results of the field experiment showed that there was no clear evidence to indicate that the drains had any effect on lowering the ground water table (GWT) elevation. However, upon further investigation it was determined that the drains' zone of influence was smaller than the drain spacing and the placement of piezometer locations prevented them from recording the drains' effect on lowering the GWT. To supplement

the somewhat unsuccessful field study, the authors conducted a parametric study to determine the factors that affect the functionality of the drains. In their parametric studies, the authors investigated the influence of drain length, spacing, inclination, and elevation on slope stability. Many slope models were created with the aid of information obtained from the experimental study. From their research, the following conclusions were made:

- Drain spacing and drain diameter have an influence on the improvement of the stability of a slope. An increase in drain diameter and a decrease in drain spacing will help to enhance the factor of safety (FOS), hence increasing slope stability.
- The optimum drain direction is not necessarily horizontal (Lau and Kenny, 1983). The results from the analysis show that the effectiveness of inclined drains was only slightly less than that of the horizontal drains and the difference was insignificant.
- No additional benefit will be gained if the drains extend beyond the critical slip surface. This point is in agreement with the conclusions of Cai, Ugai, Wakai, and Li (1998).

### 2.3.2 Effect of Drain Position

Rahardjo, Hritzuk, Leong, and Rezaur (2002) (Nanyang Technological University, Singapore) conducted a parametric study to evaluate the influence of horizontal drain location on the stability of a slope. They used a finite element seepage program, Seep/W, for seepage analyses. Stability analyses were performed by the slope stability software, Slope/W, using the limit equilibrium method. Both of these programs were developed by GEOSLOPE International, Calgary, Alberta, Canada (Rahardjo, et.al.,

2002). A 30m-high slope model with a face inclination of  $45^\circ$  was created with three drain layers that were evenly spaced from the toe to the crest of the slope. Figure 2-3 illustrates the geometry of the modeled slope and the locations of the drain layers used in the model. To investigate the influence of drain location on the stability of the slope, five scenarios were created with different drain configurations. The first scenario was used as the control and had no drains installed. The next three scenarios were created with only one drain layer performing individually, and the last situation was the combination of the three drain layers working together..

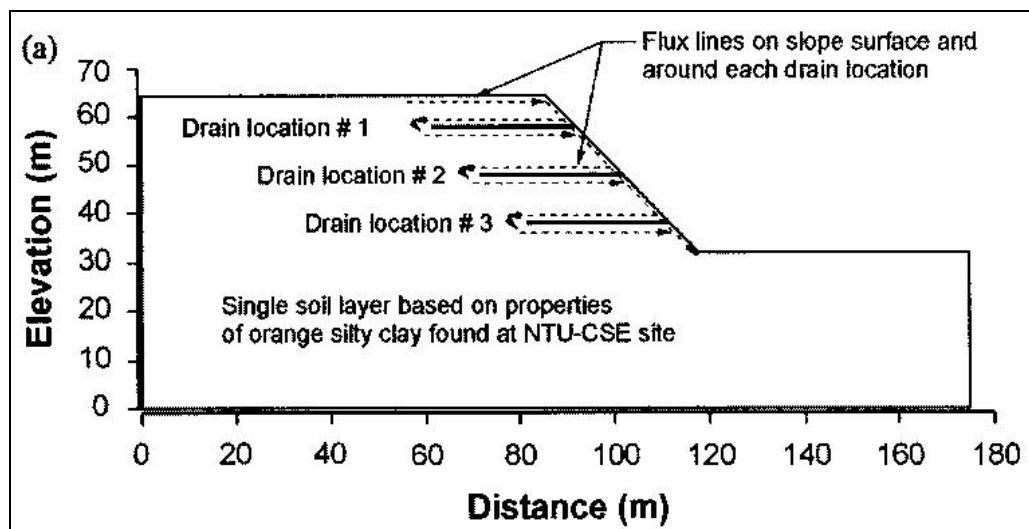


Figure 2-3: Slope geometry and drain configurations used in the research of Rahardjo, Hritzuk, Leong, and Rezaur (2002).

During the setup process, steady state conditions were developed for all drainage scenarios. The water table at steady state was set to an elevation below the drained zone, which was assumed to be 7m below the toe of the slope, to ensure that the initial conditions were independent of the drainage configurations. A rainfall with an intensity equal to the saturated hydraulic conductivity of the soil was then applied to the slope.

The hydraulic conductivity was previously measured at  $k_{sat} = 7.8 \times 10^{-7}$  m/s,. The analysis from the seepage program showed that it would take more than 20,000 days of continuous rainfall for the slope to reach equilibrium. This meant that the soil within the slope would never become saturated; however, the results were still helpful to evaluate the effect of drain location on slope stability. The profiles of pore water pressure head for each drainage scenario from the Seep/W analysis were transferred to the Slope/W program for the calculation of a factor of safety for each drainage condition. Flow was measured through any cross section of the model using the flux rate calculated by the program. Figure 2-4 presents the results of the measured flux from Seep/W in the last four drain scenarios and Figure 2-5 expresses the changes in the FOS as a function of time for each of the five scenarios .

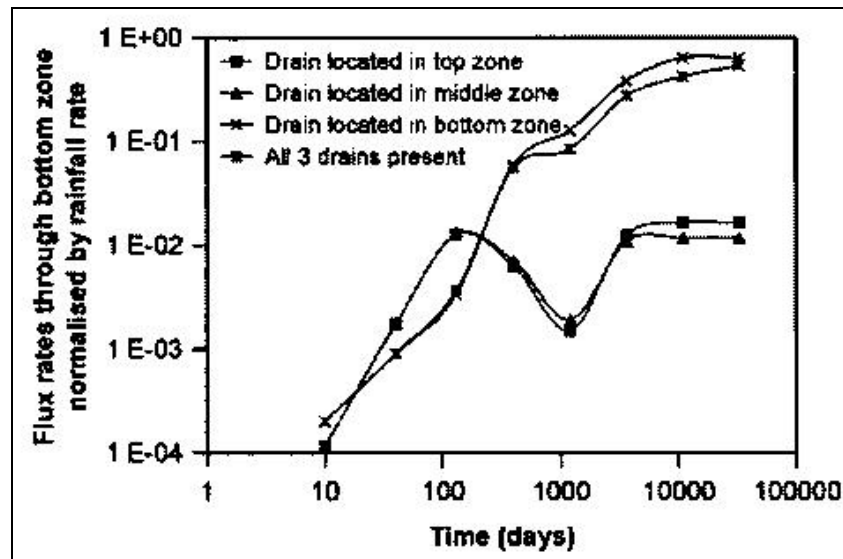


Figure 2-4: Summary of the computed flux through the bottom zone of the slope as a function of time for the various drain configurations (Rahardjo, et.al., 2002).

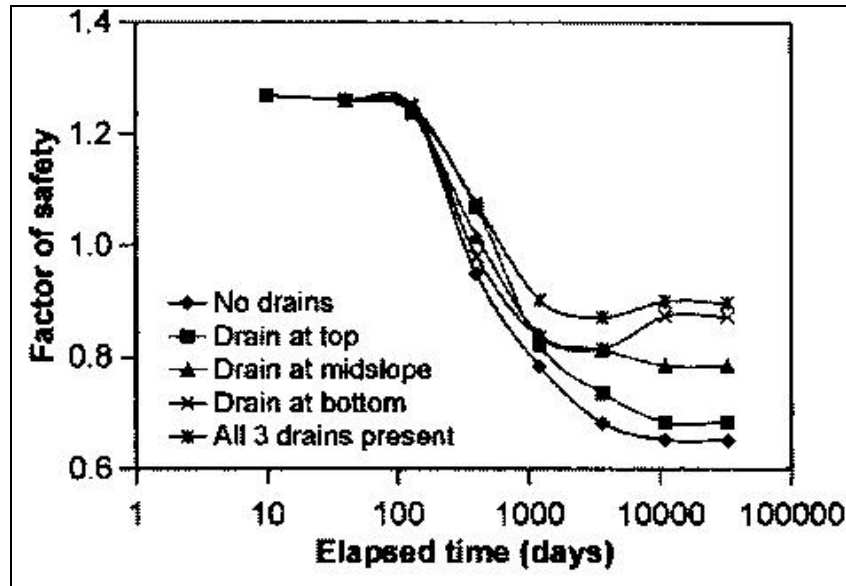


Figure 2-5: Summary of factor of safety as a function time for the model slope with different drain configurations (Rahardjo, Hritzuk, Leong, and Rezaur, 2002).

From the above figures, it is clear that the drains located in the upper parts of the slope give the least benefit, while more benefit is obtained from drains in the lower region of the slope. According to the authors, it was due to the fact that more water was attracted by the bottom drain. There is little additional benefit obtained by combining the bottom drains with other drains in the upper locations. Figure 2-5 reveals that the increase in the factor of safety for the case of combination drains is 3% over the single bottom drain. In Figure 2-4, the flux rates of the single bottom drain is nearly the same as that for the multiple drain scenario. The authors' conclusion was that drains installed in the lower region of a slope will play the most important role in increasing slope stability. As a result, the authors recommend that horizontal drains be placed as low as possible in the slope to gain more improvement in slope stability.

### 2.3.3 Factors Affecting the Drain Discharge Capacity

Kim, Park, and Jang (2003) conducted an experimental study to determine the factors which affect the discharge capacity of drains. Six different prefabricated horizontal drains were tested in this study. The drain cross-sections are illustrated in Figure 2-6.


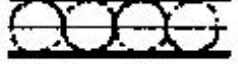




Drain types	Cross-section (mm x mm)	Shapes of core
Type-E	100 x 20	 Filament shape
Type-P	100 x 10	 Embossed shape
Type-O10	100 x 10	 Latticed shape
Type-O5	100 x 5	 Latticed shape
Type-VD	100 x 3	 Harmonica shape
Type-MD	50 (Diameter)	 Circular shape

Figure 2-6: Types and characteristics of drains used by Kim, Park, and Jang (2003).

The authors did not provide a verbal description of each drain type. However from information presented in Figure 2-6, the Type MD drain is most likely a 2" PVC pipe, and the shape of the Type VD drain is similar to a wick drain, which is used in the current study. The Type P, Type O10 and Type O5 drains could be classified as sheetdrains, which have a stiff waffle or egg crate core and a non-woven geotextile on one or both sides. The Type E drain is a filament-type geo-net. Due to its high drainage

capacity under low compressive stress, the Type-E drain is usually used as a drainage blanket or erosion control material in many environmental-related applications.

All of the drains were tested to evaluate the effect of hydraulic gradient, elapsed time, and confining pressure on their discharge capacity. Presented in Figure 2-7 are the normalized discharge capacities reported by the authors for each of the drain types.

Normalized discharge values were obtained by dividing the measured flow rate by the corresponding hydraulic gradient used in the test.

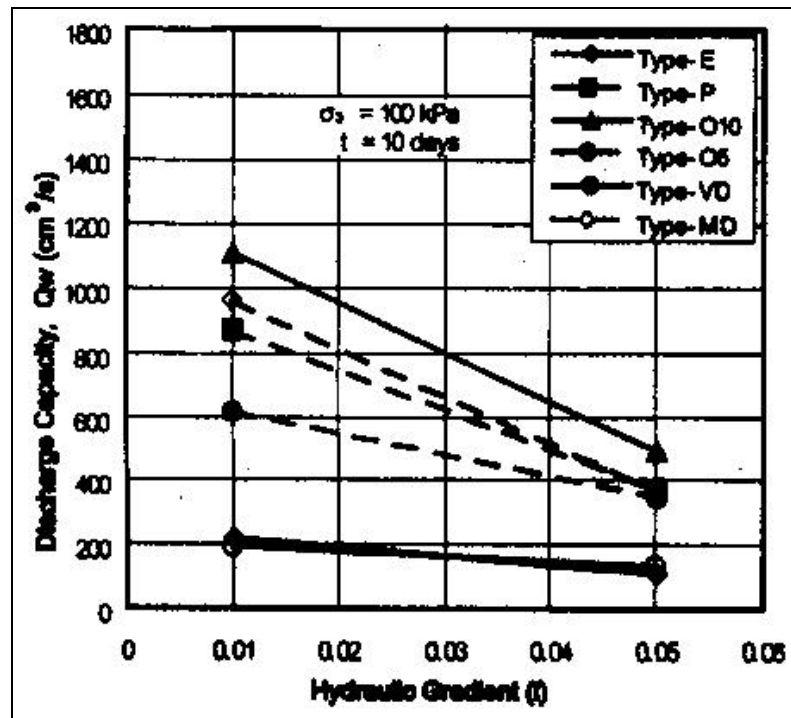


Figure 2-7: Effect of hydraulic gradient on discharge capacity for the drains in the study of Kim, Park, and Jang (2003).

Theoretically the discharge capacities reported in Figure 2-7 above should have remained unchanged for all of the drains because they were normalized by the hydraulic gradient. However, the results in Figure 2-7 show that there is a decrease in the normalized discharge capacity of all types of drains as the hydraulic gradient increases.

Kim, Park, and Jang (2003) explained that the increase in friction between water and the drain materials, coupled with turbulent flow inside the drains at a higher hydraulic gradient, caused a loss in flow energy, which led to a reduction in discharge capacity. Among the drains tested, the influence of hydraulic gradient on discharge capacity was the least for type E and type VD drains. This is because the Type E drain already had a large reduction of initial cross section after the confining pressure was applied, and the initial cross section of the Type VD drain was relatively small when compared to the cross sections of other drains. Thus, the E and VD type drains were not considered to be sensitive to changes in hydraulic gradient.

Kim and Park's test results showed that the discharge capacity of all drains decreased significantly during the first hour of the test but most achieved essentially steady state conditions beyond one hour. The exception to this behavior was drain type E which had a highly flexible filament-shaped core that was subject to creep deformation over time. On the other hand, drain type MD was least affected by time due to both its large cross sectional area and the resistance to creep of its rigid circular-shaped shell. Therefore, the type MD drain possesses the best characteristics for drainage applications.

Figure 2-8 illustrates the results of the study to determine discharge capacity as a function of confining pressure. All types of drains displayed a nearly linear decrease in discharge capacity when the confining pressure was increased. The discharge capacity of the Type E drain decreased most because its filament core was easily compressed by the confining pressure. On the other hand, the effect of confining pressure on the Type VD was insignificant. According to the authors, this was due to the relatively small initial



thickness of this type of drain, resulting in a relatively smaller reduction in cross sectional area under an increase of confining pressure. Also the discharge capacity of the Type MD

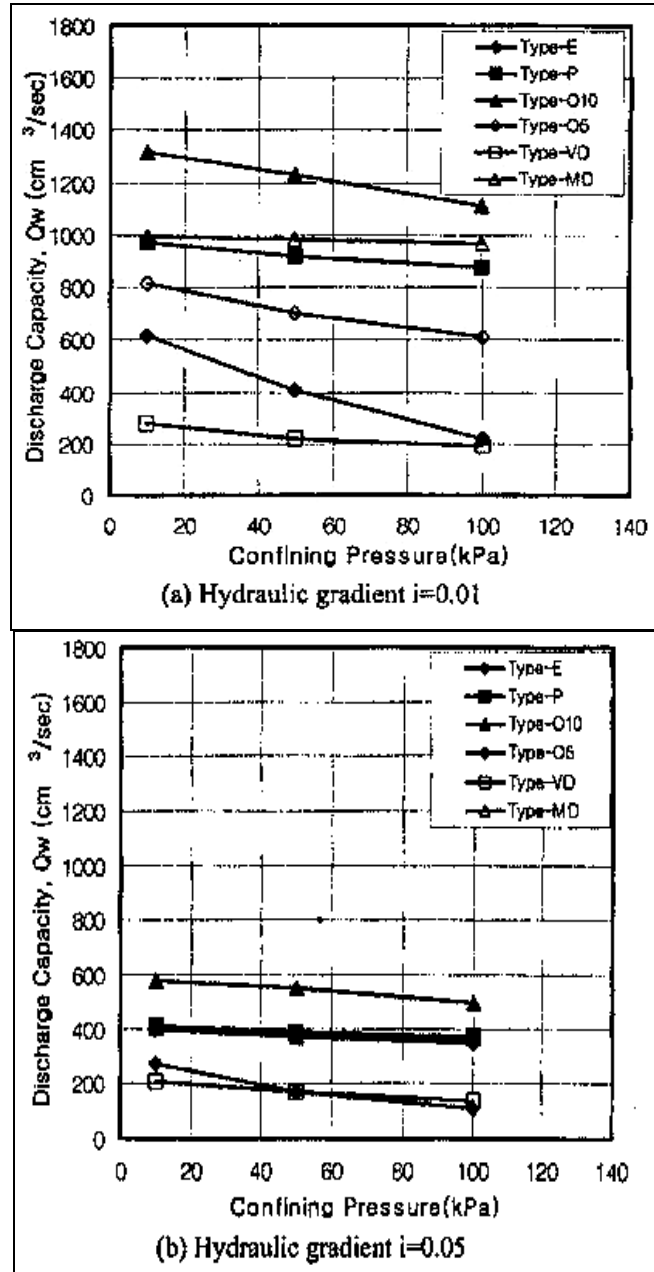


Figure 2-8: Effect of confining pressure and hydraulic gradient on the 10 day discharge capacity of the drains used in the study by Kim, Park, and Jang, (2003).

drain, which had a circular-shaped shell, was only slightly affected by increased confining pressure. The Type O-10 drain also yielded results similar to the Type MD drain.

Kim, Park, and Jang (2003) concluded that the core of a drain must be strong enough to maintain its cross sectional area over the time and pressures expected during its design life. Among the types of drains tested in the study, the Type MD drain with a circular shape and the Type VD drain were considered to have the best performance. The type MD drain is the conventional 2" diameter PVC pipes which has been used for horizontal drainage applications for decades while the type VD drain is the wick drain used in this study.

#### 2.3.4 Effects of Hydraulic Radius on the Discharge Capacity of Horizontal Drains

The hydraulic radius of a drainage channel, denoted by  $R$ , is defined as the ratio of cross section area to perimeter. According to Miura and Chai (2000), hydraulic radius is one of many factors that affect the discharge capacity of horizontal drains. To investigate the relationship between the hydraulic radius and the discharge capacity of horizontal drains, Chai, Miura, and Nomura (2004) conducted a study on four types of Prefabricated Vertical Drains (PVDs), three types of Prefabricated Horizontal Drains (PHDs) and one Dual Function (reinforcement and drainage) Geotextile (DFG). They found that the hydraulic radius had an influence on the drainage capacity ratio for all of the geosynthetic drains. The drainage capacity ratio was defined as the flow rate at a specific time divided by the corresponding initial value of flow rate. Their results showed that the discharge capacity of a drain increases in direct proportion to the hydraulic radius. Based on their results, Chai, Miura, and Nomura (2004) recommend the use of

drains which have strong cores and large values of hydraulic radius. They considered square and circular shapes to be the best shapes for drainage applications.

## **2.5 Design of Horizontal drains**

Because wick drains are relatively new to horizontal drainage applications, there is no literature relating to their use before the late 1990s. In 1999, Santi first attempted to install a wick drain in the horizontal direction to stabilize slopes. After the first successful experiment in an embankment at the University of Missouri - Rolla, Santi and his colleagues expanded their work and installed drains in Indiana, Missouri, and Colorado to obtain the necessary design parameters for the use of wick drains in slope stability applications. As a result of these studies a number of design parameters were empirically derived for the installation of horizontal wick drains.

### **2.5.1 Drain Layout Design**

There are two general drain layouts which are commonly used: a fan pattern with the radius initiated from a single installation point, and a parallel pattern resulting from a line of evenly spaced installation points. According to Santi, Elifrits, and Liljegren (2001), neither layout has dominating performance features over the other, and drain placement is usually decided by the access to the site and the site's geologic conditions. However, they point out that fanning of the drains from a single outlet position is usually more convenient and less disruptive than installing the drains in a parallel pattern. Thus, the fan layout is preferred by the authors.

### 2.5.2 Drain Length

According to the authors, in general, the deeper the drains are installed into the slope, the better they will perform in increasing slope stability. Long drains can convey more water out of the slope than short drains because they are more likely to intersect the water-producing zones. However, Santi, Elifrits, and Liljegren (2001) agreed with the conclusion from the study by Lau and Kenney (1983) in that little extra benefit would be gained if the drains extended far beyond the critical slip surface. The depth to which the drains were installed in Santi's experiments was limited. The maximum length of the drains which Santi and his colleagues were able to push into slopes were approximately 30 m (100 ft). In some situations, stiff material prevented the advancement of the drains into the slope. The authors believe that with more robust equipment the installation depth can reach 45 to 60 m (150 to 200 ft), even through stiff soils.

### 2.5.3 Drain Spacing

Drain spacing is a function many factors such as the soil's hydraulic conductivity, slope geometry, drain position, and drain discharge capacity. According to Santi, it is difficult to validate the results of these studies through theoretical analyses because they require soil homogeneity and isotropy as well as preciseness in drain location. These characteristics are rarely met in the field. Therefore, the drain spacing in the experiments were empirically decided based on the experience of the authors and some other factors such as site accessibility, topography, and geologic conditions.

### 2.5.4 Filter Size

Clogging is a drawback which can affect the performance of wick drains. Choosing an appropriate filter fabric that is properly matched to the soil type can help to

prevent the drains from clogging (Santi, Elifrits, and Liljegren, 2001). There are many design expressions available to assess the filter criteria for geosynthetic wick drains (Fahmy, Koerner, and Koerner, 1996). According to Koerner (2005), ASSHTO (Association of State Highway and Transportation Officials) recommends simple criteria, which relate to the percentage of soil passing the No.200 sieve (0.074 mm). AASHTO's criteria are as follows:

- For soil with  $> 50\%$  passing the No.200 sieve: AOS of the geotextile  $\geq$  No.50 sieve or  $O_{95} < 0.30$  mm.
- For soil with  $\leq 50\%$  passing the No.200 sieve: AOS of the geotextile  $\geq$  No.30 sieve or  $O_{95} < 0.60$  mm.

Where  $O_{95}$ , expressed in millimeters, is the opening size of the filter fabric corresponding to the particle size in which 95% of the soil particles would be retained. AOS (apparent opening size) is equal to  $O_{95}$  except that it is expressed as a sieve size number.

Atkinson and Eldred (1981) stated that the optimum pore size of the geotextile filter in clay soils should be from 10 to 20  $\mu\text{m}$ . However, Atkinson and Eldred's criterion can not be met due to the limited number of options for drain filter fabrics. The opening size of the geotextile for commercially available wick drains usually ranges from AOS 70 to 200, or  $O_{95}$  208 -75  $\mu\text{m}$  (Santi, Elifrits, and Liljegren, 2001). To choose the filter size for wick drains in clay soils, Santi and his colleagues suggested that the criteria proposed by Chen and Chen (1986), which were exclusively developed for prefabricated vertical wick drains, were the most appropriate. These criteria imply that a geotextile filter with AOS of No.70 sieve ( $O_{95} = 0.208$  mm) can be used for silt and clay soils which have a

high sand component ( $D_{85(\text{soil})} > 0.15 \text{ mm}$ ) and  $D_{50(\text{soil})} > 0.02 \text{ mm}$ ). Also, wick drains with AOS of No.100 sieve to No.200 sieve filters ( $O_{95} = 0.150\text{-}0.075 \text{ mm}$ ) are more appropriate for pure silt and clay soils ( $D_{85(\text{soil})} > 0.05 \text{ mm}$  and  $D_{50(\text{soil})} > 0.007 \text{ mm}$ ).

## **2.6 Installation Method for Horizontal Drains**

Compared to the installation method for horizontal steel pipes or PVC pipes, the installation process for geosynthetic wick drains, as developed by Santi, Elifrits, and Liljegren (2001) is quite different. Instead of drilling a hole and inserting a drain pipe the wick drains are installed by driving a carrier pipe into the slope. The installation equipment includes the following:

- A bulldozer or a tracked excavator (trackhoe) to apply a load to push the drive pipe into the slope.
- Sacrificial Drive Plate: A drive plate is made from 12-to-18-gauge (1.3-to-2.7 mm thickness) sheet steel which is welded to a short piece of #4 rebar or a bolt that contains a washer on the opposite end as illustrated in Figure 2-9.
- Drive pipes: The drive pipe should have minimum inner diameter of 32 mm (1 ¼ in) to accommodate the rolled wick. A larger diameter drive pipe will allow it to tolerate larger driving forces, and allow the pipe to advance farther in hard materials.
- Drive head: The drive head is used to transmit the pushing loads from the driving machine to the drive pipe. An additional function of the drive head is to protect the female threads of the drive pipe and reduce the tendency of the pipe to slide off the equipment.

- Pulling head: The pulling head is used to pull the steel pipe out of the soil after the drain is driven

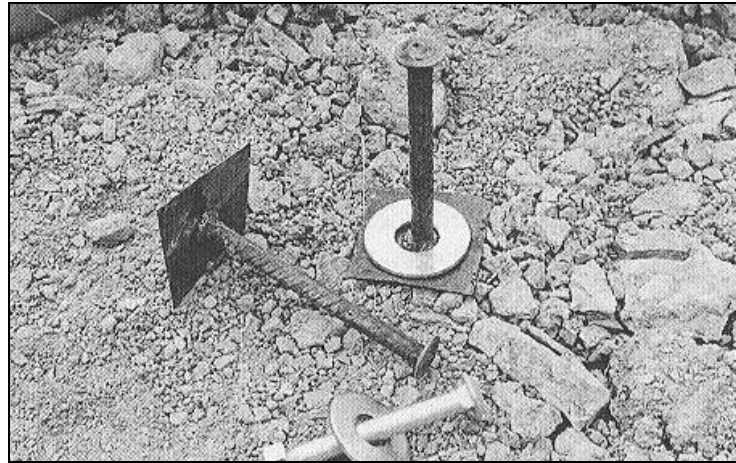


Figure 2-9: Drive plate with a supporting washer (top) used in the installation method of Santi, Elifrits, and Liljegren (2001).

Prior to installation, precut lengths of the wick drains that are slightly longer than the length of the drive pipe are preloaded or imbedded inside the sections of drill pipe as illustrated in Figure 2-10.



Figure 2-10: Wick drains are embedded inside steel pipes (Santi, personal communication, 2006).

The sacrificial drive plate is then placed at the front of the first steel pipe section to be installed as illustrated in Figure 2-11, and is attached to the front end of the wick drain using a hose clamp. Next, the drive head is placed over the back end of the first pipe, and the wick drain is folded out of the way as shown in Figure 2-12.



Figure 2-11: A sacrificial plate is attached to the first steel pipe (Santi, personal communication, 2006).

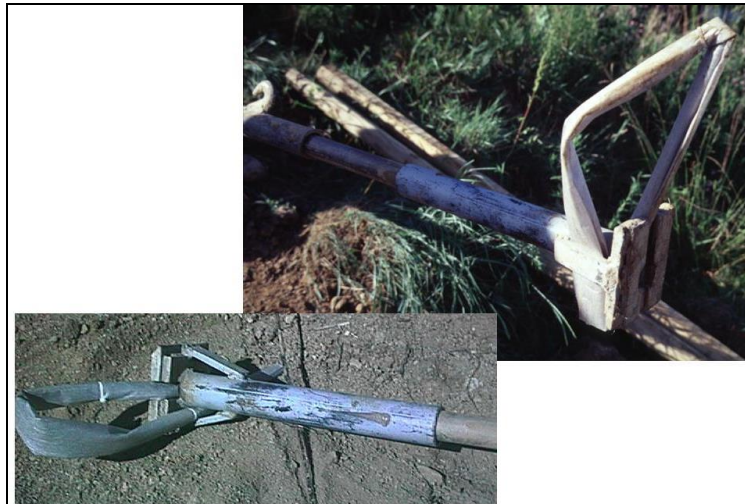


Figure 2-12: A drive head is attached to the steel pipe (Santi, personal communication, 2006).



After being aligned, the first pipe is pushed into the slope by a bulldozer or the bucket of a tracked excavator as illustrated in Figure 2-13. Additional sections of drain are installed by splicing the protruding wick sections together with a stapler, as shown in Figure 2-14, threading the pipes together, and repeating the driving. When the desired depth is reached, the pulling head is attached to the protruding end of the pipe and, the pipe is gently pulled out of the slope by the bulldozer or trackhoe with the use of a chain, as illustrated in Figure 2-15. Because the sacrificial drive plate anchors the wick in place and provides resisting force against withdrawal, the wick drain remains inside the slope as the pipe is removed.



Figure 2-13: Pushing the steel pipe by the bucket of a trackhoe (Santi, personal communication, 2006).



Figure 2-14: The drains are spliced by a stapler (Santi, personal communication, 2006).



Figure 2-15: The pipe is pulled out through a chain connected to the pulling head (Santi, personal communication, 2006).

According to Santi, Elifrits, and Liljegren (2000), the new installation technique represents a significant improvement in the rate of drain installation. The installation speed can range from 12 to 21 m of wick drain per hour, with the cost of the installation

of the wick drain ranging from \$9 to \$20 per linear meter. By contrast, the total cost of installing PVC drain pipe ranges from \$20 to \$36 per linear meter.

## **2.7 Study cases**

Natarajan, Murty, and Gokhale (1986) documented many successful applications of horizontal pipe drains during the period 1940 to 1983. Outside the U.S., horizontal pipes drains are mainly utilized in Canada, where 12 sites were stabilized by the use of horizontal pipe drains (Mekechuck, 1992). In 1999, Santi first tested and installed horizontal wick drains into a slope in Rolla, Missouri. Since the use of wick drains for slope stabilization is relatively new, only a few applications of horizontal wick drains have been reported. Among the reported cases, several successful applications of horizontal drains are described in the following sections.

### **2.7.1 Case Study 1: First Experiment of Using Horizontal Wick Drains**

In order to investigate the feasibility of using horizontal wick drains for slope stabilization, Santi (1999) conducted an experiment in an embankment in Rolla, Missouri. The embankment consisted of approximately 60 cubic yard of sandy clay, and the inclination of the front face was 1V:1H. Six wick drains were installed by a bulldozer into one half of the slope that was referred to as the drained section, while the other half of the slope had no drains and was referred as the control section. An initial ground water table (GWT) was established through the seepage of water from a trench located at the back of the slope. In order to simulate rainfall during the time of the experiment, many sprinklers were used to produce a 100-year 24-hour rainfall (approximately 0.31"/hour). Six piezometers, 16 soil moisture meters, and 20 survey

markers were installed to measure the change in moisture content and GWT within the slope. During the experiment, water level, flow rate, and slope movement were recorded.

The important results of this are summarized as follows:

- 1) The flow capacity of the drains was approximately 10 gallons per hour. The flow rate was below the expected value, which was estimated at 96 gallons per hour. It was believed that the low permeability of the soil had an effect on the flow rate of the wick drains (Santi,1999).
- 2) The piezometers showed that there was a reduction of the GWT in the vicinity of the drains as illustrated in Figure 2-16.

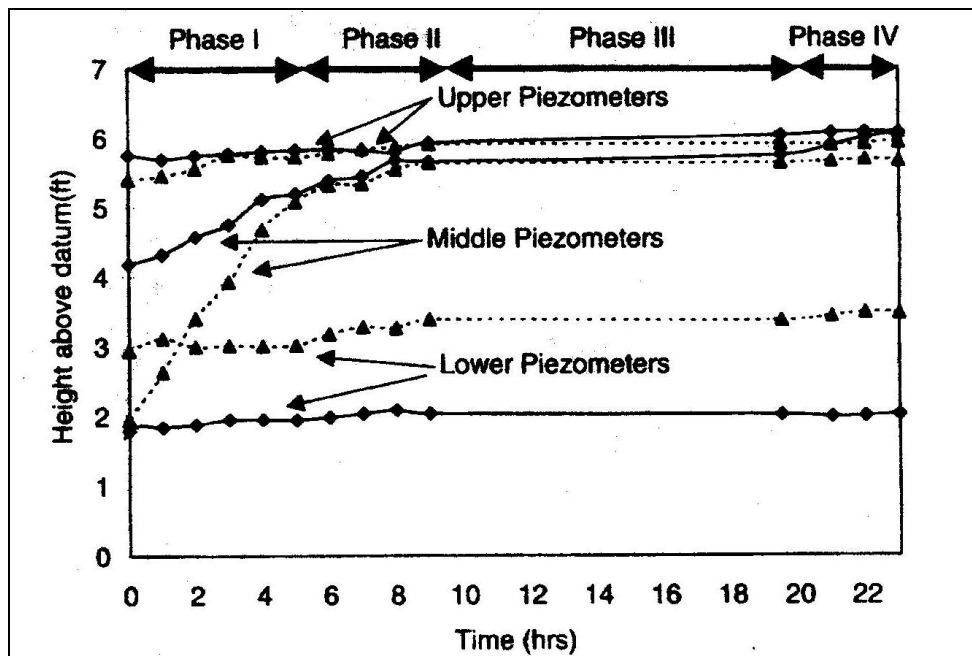


Figure 2-16: Change in water table during the experiment of Santi (1999).

In Figure 2-16, the solid line expresses the GWT within the drained section and the dashed line represents the GWT within the control section. Through Figure 2-16, it can be seen that in the lower portion of the slope, the GWT in

the drained- section was lowered 1 foot compared to the control section.

However, in the upper regions of the slope, the effect of the horizontal wick drains was insignificant. Moreover, the results also showed that the rise in water level in the drained section was less than half of that in the control section. From these results, Santi (1999) concluded that the drains in the lower part and near the face of the slope were more effective in controlling the water level in both the long term and short term than the drains in the middle or at the top of the slope.

- 3) During the experiment, the survey stakes showed slightly less movement in the drained section when compared to the control section. The movement of the drained section was less than 0.45 ft throughout, and less than 0.2 ft in the area close to the drains. Whereas the movement in the control section ranged from 0.4 to 0.6 ft.

Based upon the results obtained from this study, Santi (1999) concluded that wick drains were effective in controlling the water table within natural slopes and existing embankments. Moreover, the installation cost of a foot of drain was in range of \$3-5 with no requirement for experienced operators for the installation. Therefore, he considered horizontal wick drains as an effective and economical method to stabilize slopes (Santi, 1999).

### 2.7.2 Case 2: Demonstration projects using wick drains to stabilize landslides

After the technique to install horizontal wick drains into a slope was developed in 1999, Santi and his colleagues installed more than 170 drains with the total length of 2,600 m (8,600 ft) at eight sites in Missouri, Colorado, and Indiana to evaluate the

effectiveness of this horizontal drainage method. At three of the eight sites the drains were installed at a density and layout which was considered appropriate for full-scale slope stabilization (Santi, Crenshaw, Elifrits, 2003). Several inclinometers and piezometers were also installed to monitor the movements of the slope and the changes in ground water tables during the investigation period. After drain installation, slope stability was analyzed for each of the three sites using the modified Bishop method with the help of the program PCSTABL5. In the computer analysis, three conditions were evaluated: (1) Stability of the slope under normal ground water conditions without drains, which were assumed for the dry period during the summer, (2) Stability of the slope under high ground water conditions with no drains installed, which simulated periods of heavy rainfall and (3) Stability of the slope under high ground water conditions with wick drains installed. The third case was used to evaluate the effectiveness of the drains for the worst water level condition. A summary of the important statistics from the three full-scale sites are described below.

### **Jasper, Indiana**

This site was on the east side of State Highway 545, 3 miles south of Dubois, IN, which was near to the larger town of Jasper, IN. The slope was above State highway 545, and its movement had uplifted the shoulder of the highway. There was a small retaining wall, constructed in the late 1980s, at the toe of the slope. The north end of the wall had overturned because of insufficient embedment of the supporting piers (Santi, Crenshaw, Elifrits, 2003). The soil of the slope consisted of residual clay and clay overlying weathered limestone, shale, and sandstone. Many scarps and tension cracks were found on the surface of the slope, which allowed water to enter the landslide area, resulting in

further instability of the slope. Therefore, a drainage method to remove the water from the slope was necessary.

Forty four drains with total length of 800m (2,613 ft) were installed by a Komatsu PC200LC trackhoe during a 9 day period in June 2000. Sixteen drains were observed to convey water immediately after installation, nineteen drains produced water after rainfall, and nine drains remained permanently dry. The data recorded from the inclinometers and piezometers showed that there was less than 4 mm of total movement near the top of the slope and less than 2 mm of movement near the middle of the slope. No movement at the toe of the slope was recorded.

The results of the FOS analyses for all three water conditions for this slope's geometry are illustrated in Figure 2-17. The dashed lines in the figure express the water levels corresponding to three conditions applied to the slope with W1 standing for condition 1 as explained earlier, and so forth. As can be seen in Figure 2-17, the factors of safety (FOS) for the three scenarios are 1.24, 0.99, and 1.42, respectively. This means that during the dry months with normal GWT location, the FOS is 1.24, and the slope is stable. Whenever a heavy rainfall occurs, the stability of the slope drops below unity which can cause a landslide. However, when the drains are installed in the slope, described by condition 3, the FOS is increased 11% over the dry season condition and 43% over the critical high GWT condition. This represents a significant improvement in slope stability, supporting the effectiveness of the horizontal wick drain in slope stabilization.

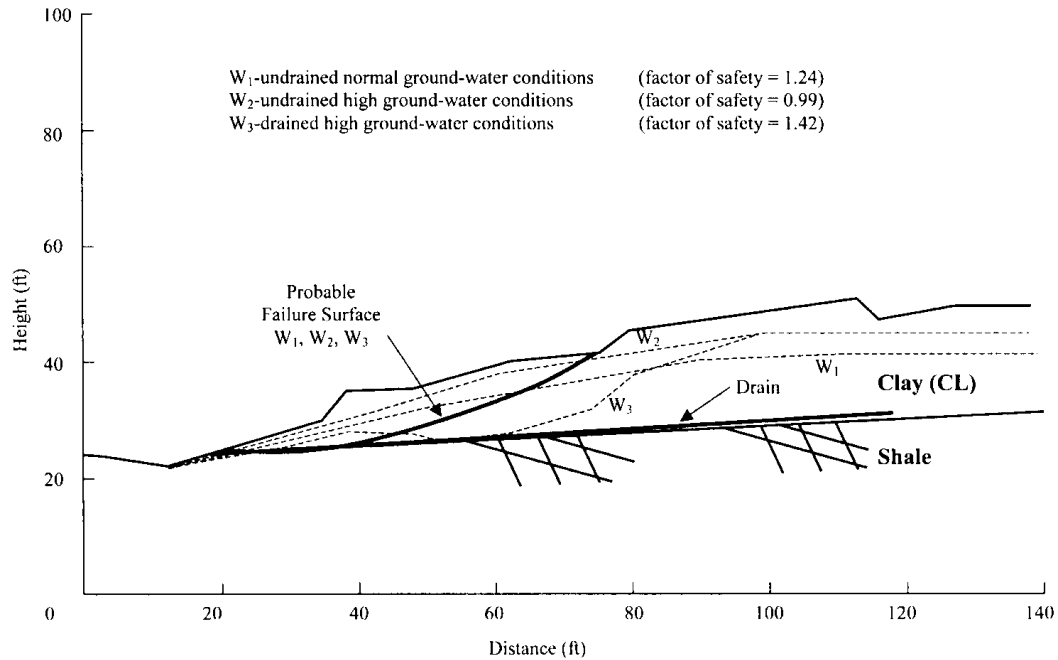


Figure 2-17: Results of slope stability analyses for the slope at the Jasper, IN site, (Santi, Creenshaw, and Elifrits, 2003).

### Boonville, Missouri

This site was located on the south side of the east bound lanes of Interstate 70. The slope of this site dropped off below and to the south of eastbound I-70. A failure surface at the top of the slope damaged the asphalt in the shoulder of the interstate highway. The slope consisted of 5.5m of mixed sandy clay and clay fill, overlying an irregular, sloping cobble and boulder fill layer. The cobble fill was used to fill a valley and to provide a level surface for the roadway. Beneath this fill layer were a layers of shale and then limestone.. The landslide was very steep with an approximate slope of 1.5H:1V. The slope face was highly vegetated during the spring and summer, which indicated the existence of water near the surface of the slope (Santi, Creenshaw, and



Elifrits, 2003). Therefore, horizontal wick drains were installed to lower the GWT and improve slope stability.

On December 2<sup>nd</sup> and 3<sup>rd</sup>, 1998, ten drains with total length of 76 m (249 ft) were installed at three levels near the middle of the slope by a Case 550E bulldozer and a Case 9030B trackhoe. Two drains at the upper level began conveying a small volume of water overnight. Two inclinometers and two piezometers were installed to monitor the changes in slope movement and GWT. The results from the inclinometers showed less than 5 mm of movement by the end of December 2000. Later, 36 drains totaling 558 m (1,832 ft) in length were installed during the period May 21<sup>st</sup> to May 25<sup>th</sup>, 2001, by a Case 580 SuperL Extendahoe. Two of the drains produced water right after the installation, and several other drains were moist. During the 5 days of the installation, the results from the piezometers showed a constant water level at the lower drain position. But the water table at the upper part of the slope dropped 0.85 m (2.8 ft) as a result of drainage through the wick drains.

Through the computer analysis, the FOS's against sliding for this slope under the three conditions described earlier were 1.14, 0.99, and 1.08, respectively as illustrated in Figure 2-18. Like the landslide in Jasper, IN, the status of this slope in normal dry condition is safe, but it can become unstable when the soil gets wet from heavy rainfalls, leading to a potential failure. At this site, the FOS of the drained slope using wick drains and a high GWT is not high. The increase in slope stability over the undrained high water condition was about 10%. The small improvement was believed to be due to the fact that the wick drains could not all be pushed past the cobble layer; therefore, many of the drains could not function to their full potential (Santi, Greenshaw, and Elifrits, 2003). A

FOS of 1.08 is usually not acceptable for transportation projects. However, according to the authors, the results are acceptable due to the conservative parameters used in the analysis. Therefore, the improvement in slope stability is expected to reduce the potential for landslides.

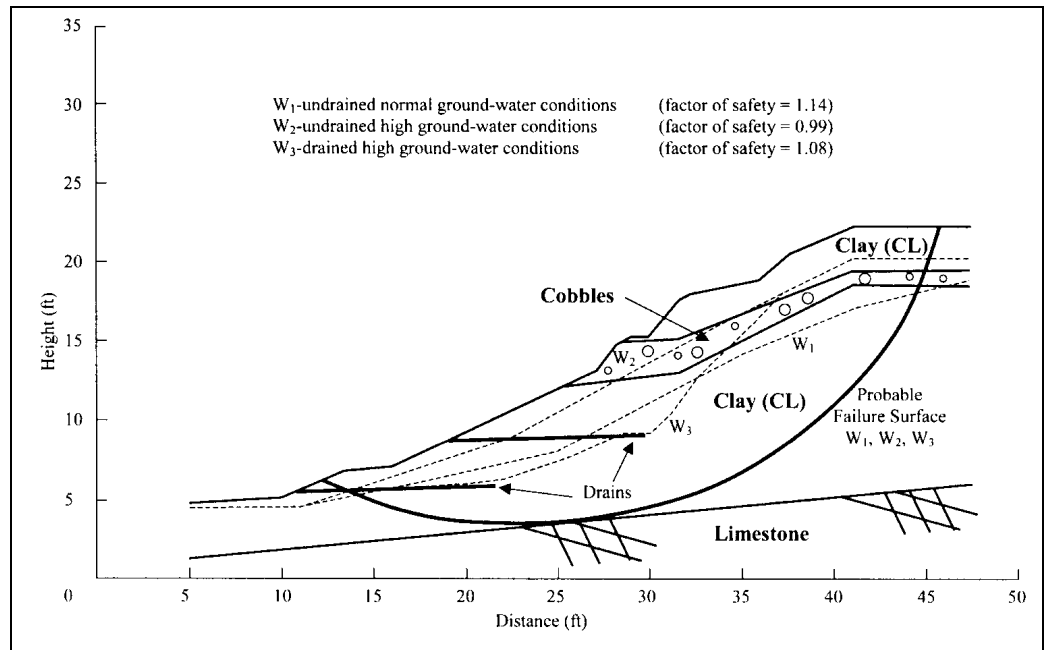


Figure 2-18: Results of slope stability analyses for the Boonville, MO site (Santi, Greenshaw, and Elifrits, 2003).

### Meeker, Colorado

This site was located north of Meeker, Colorado on State Highway 13. The slope dropped off below and to the east of northbound lanes of State Highway 13, and the failure at the top of the slope caused the asphalt in the roadway to crack. The failure occurred in a layer of fill soil consisting of clay and silty clay. This fill soil, which was approximately 6 to 15 m (20 to 50 ft) thick, was used to fill a valley and to provide a level roadway surface. There was a 1.5m (5ft)-thick layer of silty gravel overlying this fill soil. Siltstone and claystone bedrock were encountered beneath the fill. Slope movement

mainly occurred during the spring period due to a rise of the GWT from snowmelt. Horizontal drains were installed to remove water from the slope and increase stability.

From June 11 to June 14, 1999, six drains with a total length of 111 m (365 ft) were installed in a fan pattern by a Caterpillar D4C XL bulldozer. Several of the drains were reported to produce water immediately, and the discharge rate of one of the drains was as high as 20 L/min (5 gallons/min) (Santi, Greenshaw, and Elifrits, 2003). Three years after the installation, the drain outlet pipe still produced water.

Later, from June 4 to June 7, 2001, 27 additional wick drains, totaling 576 m (1,891 ft.) in length, were installed to the Meeker, CO site by the same bulldozer. Twelve of them started to remove water right after installation, and several others produced water a few days later. In this slope, the average length of the drains was more than 21 m (70 ft.), and the drain installation was typically terminated at the bedrock.

Three piezometers were installed into the slope in the mid-1990s by the Colorado DOT to evaluate the overall movement. The data recorded in May, 2000, showed the water level at 6.4 m to 8.2 m (21 to 27 ft.) below the roadway surface. Theoretically, the data are useful for slope stability analyses. However, because the piezometers were installed too far away from the wick drains, the influence of the drains on slope stability could not be validated. As a result, a number of additional piezometers were installed during the spring of 2001 to monitor the drain performance.

The same conditions were used to evaluate the effectiveness of the drains in the Meeker slope as were used for the Jasper and Boonville landslides. The results of the computer analyses for this site are shown in Figure 2-19 below.

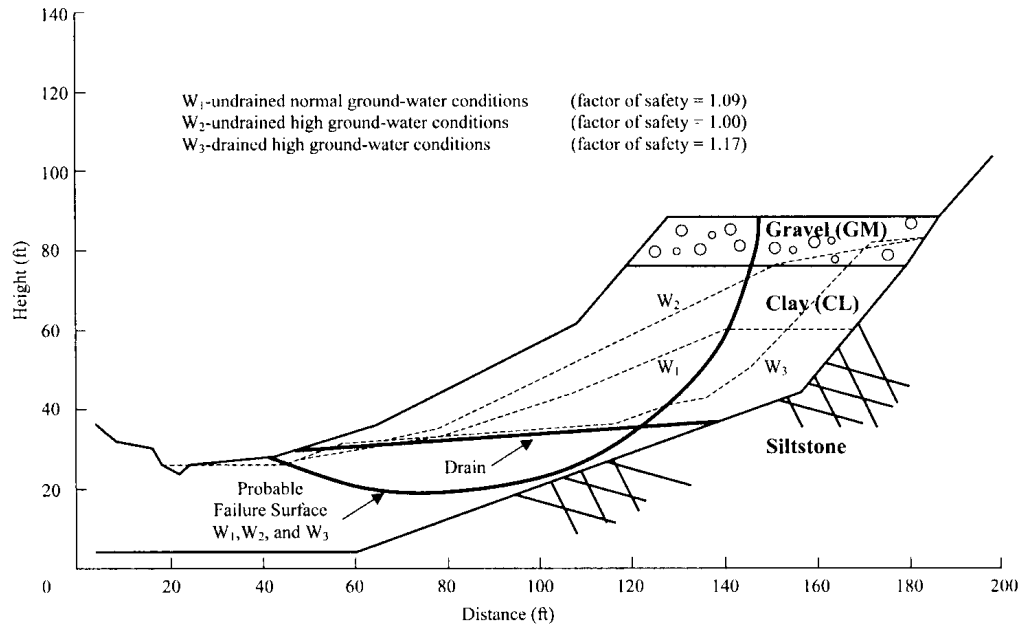


Figure 2-19: Groundwater conditions and results of slope stability analyses for the Meeker, CO site (Santi, Creenshaw, and Elifrits, 2003).

Figure 2-19, illustrates the significant effect the long drain had on the water table. The GWT in the drained condition, condition 3, nearly coincided with the level of the drain. Compared to the FOS of the first two scenarios, the FOS for the drained slope during high GWT was increased to 1.17, which represented a considerable increase in slope stability.

According to Santi et al. (2003), none of the three sites had a long-term monitoring program, so it was difficult to decisively evaluate the long-term effects of the horizontal wick drains on slope stability with field data. However, none of the sites have shown any significant slope movement since the drains were installed. Many of the drains began to convey water immediately after drain installation, and most of the drains produced water during the period of the investigation, even during the dry years. Moreover, computer stability analyses indicated a clear increase in slope stability when

horizontal wick drains were installed. All of these case studies support the concept that drains lower the water table within a slope, and improve slope stability.

According to Santi et al. (2003), this method may be applied in specific cases which require relatively short drains (30-45 m, or 100-150 ft) and a wide range of materials ranging from soft to very stiff clay (up to 30 blow counts/ft from the standard penetration test).

Using data from the demonstration projects Santi et al, estimated the total costs, associated with this drainage method, . Assuming that the average installation rate was 18m/hour, the total cost for each meter of drain installation (including the cost of material) was \$8 per meter (2001 dollars) or \$2.50/ft, which was much cheaper than conventional PVC horizontal drains, Santi et al. (2003).

### 2.7.3 Case 3: Bluff Stabilization by Using Horizontal Wick Drains

In this case study, horizontal wick drains were used by Bahner and Jackson (2007) to stabilize bluffs along the western shore of Lake Michigan. The results were reported in the 1<sup>st</sup> North American Landslide Conference in Colorado, June 2007. The bluffs have been historically unstable or marginally unstable. The geologic profile of this area is dominated by soil deposits from the late Wisconsin glaciation period (Bahner and Jackson, 2007). Problematic slope geometry, the impact of freezing/thawing, erosion at the toe due to wave action, and “erosion caused by ground water from glacial outwash deposits within the bluff profile” are the major reasons for instability of the bluffs, (Bahner and Jackson, 2007). Among these reasons, erosion from seepage along with the buildup of hydrostatic pressures in the soil strata contributed most to the instability. The

instability of the bluffs affected the value of adjacent private property, because of the perceived potential for major damage to structures on the property.

There were a numbers of challenges in the installation of the drains in the lake bluffs. The biggest challenges were the heavy vegetative cover and steepness of the bluffs coupled with the narrow beaches which would not allow the staging of the work. In addition, there was poor or non-existent access to the beaches. As a result it was necessary to use modern Horizontal Direction Drilling (HDD) technology to install the drains from the top of the bluffs. The installation procedure was designed and patented by Bahner and Jackson (2007).

Using the Bahner and Jackson installation approach, a host pipe was drilled with polymer drilling fluid through the overburden soil to the discharge point, which was about 3 to 5 ft above the toe of the bluff. Then, a wick drain was advanced downward through the host pipe. Once the drain was seen at the bluff toe and threaded into a discharge pipe, the host pipe was removed from the bluff, leaving the drain inside the slope. The polymer drilling fluid decomposed to plain water soon after installation. The removable host pipes also helped to prevent any damage to the wick drains during installation process.

Over a 5-year period, seven projects were installed with a total of 80 drains having lengths of 300-400 ft. The discharge capacity of the drains approached 120 gallons per hour. No plugging of the drains was observed during the period of the study. At the Duckworth site, located in Lake Forest, IL, the initial bluff slope was actively sliding, and significantly damaging retaining walls and other structures on the bluff crest. After the drains were installed, survey measurements showed that the slope movement

slowed and eventually stopped. As a result, the bluff was stabilized, and repairs of the damage and site improvements at the crest of that slope could be made.

Based upon the results of their work, Bahner and Jackson (2007) conclude that the horizontal wick drains installed by using HDD methods is a cost-effective method to improve drainage and stabilize slopes where typical installation methods can not be used because of limited site access, slope geometry, and subsurface conditions. This case study represents another successful application of using horizontal wick drains to improve slope stability.

## **CHAPTER 3**

### **RESEARCH METHODS**

#### **3.1 Introductory**

Prior to the installation of the wick drain system at the test site, some preparatory work such as laboratory soil testing, parametric analyses, equipment calibration, and programming for of data collection devices was completed. The pre-fieldwork activities, along with installation procedures for drains and monitoring equipment are described in this chapter.

#### **3.2 Site conditions**

The site selected for this study was located at mile marker 38 on the east side of the north bound lanes of interstate I-540. The study location is within a cut slope that was excavated during the construction of Interstate I-540. The slope had a height of 6 m (20 ft) and a slope angle of 3:1 (H:V). Figure 3-1 displays the location of the chosen slope in the primary highway system of the state of Arkansas. An aerial view of the site is illustrated in Figure 3-2, and the initial geometry of the slope is shown in Figure 3-3. There was initially some vegetation on the surface of the slope. This vegetation was dry in the winter as illustrated in Figure 3-3 but was very densely vegetated and green in the spring and summer, indicating the presence of water within the slope. Moreover, there was a slope failure in the vicinity of the selected site. These indicators of instability caused the study team to believe that there would be a slope failure at this site if remediation measures were not taken, (Dennis, personal communication, 2006). Since



the failure potential for this slope was considered to be high, it was a good candidate to evaluate the effectiveness of the geosynthetic wick drains in preventing a slope failure.



Figure 3-1: Location of the study within the Arkansas Highway system.  
(Source: [http://www.fhwa.dot.gov/planning/nhs/maps/ar/ar\\_arkansas.pdf](http://www.fhwa.dot.gov/planning/nhs/maps/ar/ar_arkansas.pdf))



Figure 3-2: Aerial view of the study location. (Source: Image taken from Google Earth at



Figure 3-3: Initial geometry of the slope used in the study..

To support parametric analyses for drainage and stability, soil samples were taken to the University of Arkansas to determine both index and engineering properties of the soil at the site. The test regimen included the following tests:

- Index properties
  - Specific gravity
  - Particle size distribution
  - Plastic limit
  - Liquid limit
  - Maximum dry density and optimum moisture content
- Engineering properties:
  - Hydraulic conductivity

Prior to conducting the testing, the soil sample was air-dried at room temperature. Then it was preliminarily classified into two types based upon the differences in color and soil texture. Visually, the upper layer of soil at the site was brown sandy clay with some light grey shale fragments. This soil was very sticky when it got wet. The lower layer of soil was dark gray highly weathered shale with some light gray clay inclusions. This soil was less sticky in wet condition and more friable in dry condition than the soil in the upper layer. Both soil types were subjected to the same tests. All tests were conducted in accordance with ASTM (American Society for Testing and Materials) Standards. A summary of the results of these tests are displayed in Table 3-1, while the particle size distribution curves, moisture density relationship curves, and the results of the Atterberg limit testing are illustrated in Figures 3-4 to Figure 3-6.

Table 3-1: Summary Soil Properties for the test site.

Properties	Abbreviation	Brown clay	Gray clay
Specific gravity	$G_s$	2.772	2.729
Plastic Limit	$PL$	27	26
Liquid Limit	$LL$	55	52
Plasticity Index	$PI$	28	26
Maximum dry density	$\gamma_{dry\ max}$	15.96 (KN/m <sup>3</sup> ) [ 101.5 (pcf) ]	16.19 (KN/m <sup>3</sup> ) [ 103 (pcf) ]
Optimum moisture content	$w_{opt}$	21%	20%
Hydraulic conductivity	$K$	$2.3 \times 10^{-7}$ (cm/s)	$3.5 \times 10^{-7}$ (cm/s)

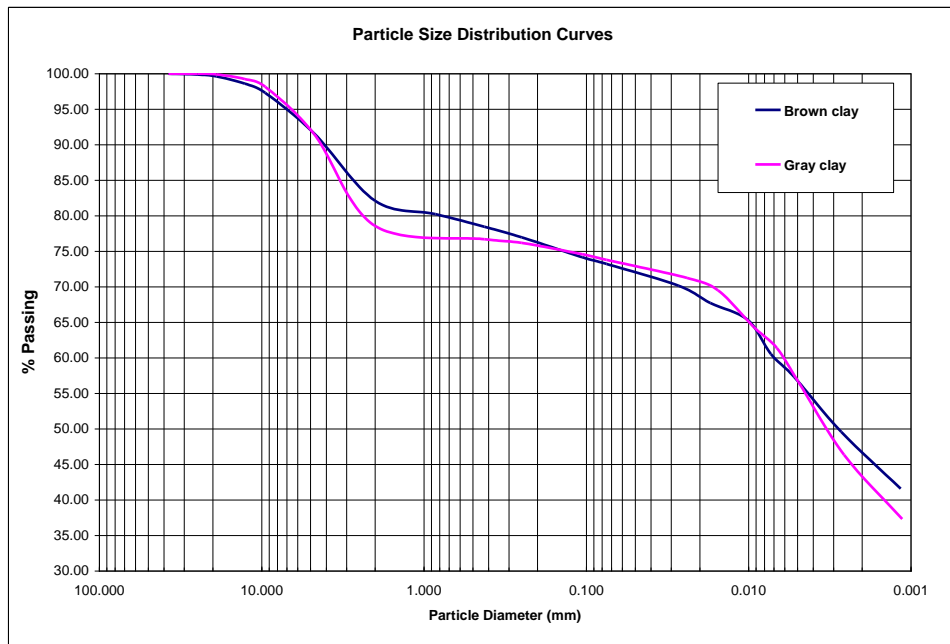


Figure 3-4: Particle size distribution curves of the soils at the site.

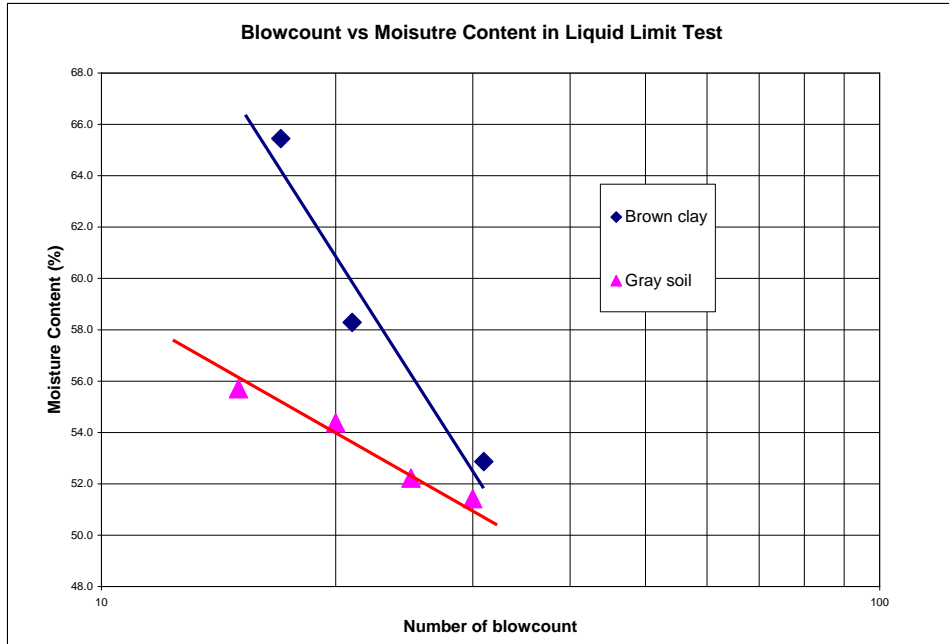


Figure 3-5: Flow Curves from liquid limit testing of the test site soils..

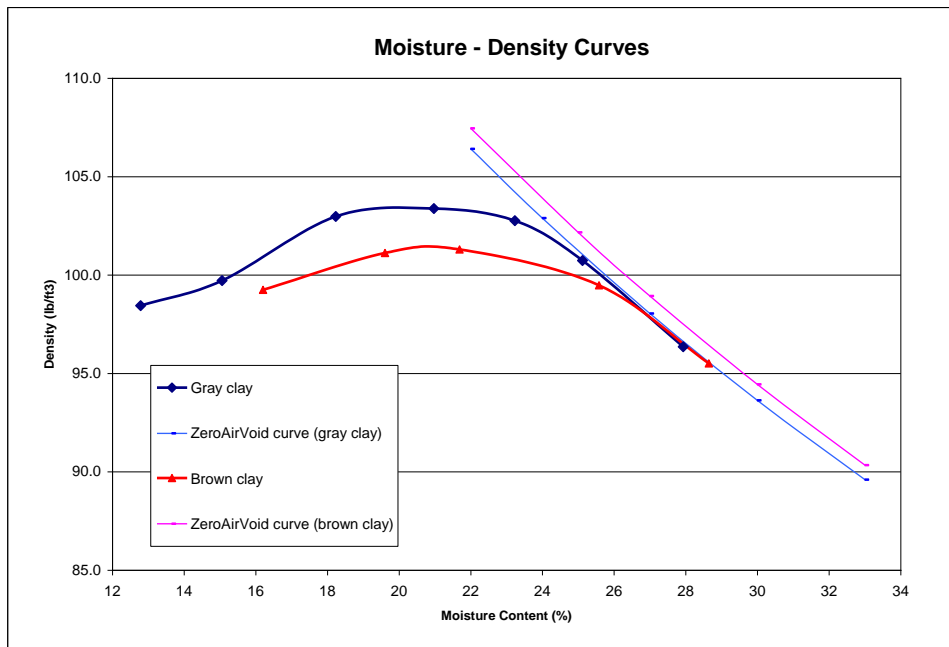


Figure 3-6: Moisture-Density curves of the soils at the site, created using standard effort in accordance with ASTM D-698..

According to the ASTM D-2487, both of these soils were classified as high plasticity clay (fat clay) with gravel. Since the properties of these two soil types were

very similar, it was decided that an average value of the properties measured in these tests could be in the parametric studies without any significant loss in accuracy..

### **3.3 Parametric Analyses**

A portion of the scope of this study was to determine the parameters of the drain installation such as drain length, drain spacing and drain position through a parametric analysis. The determination of the optimum configurations of the drain system was done with a software program called Plaxflow (Version 1.5). This software is produced by Delft University of Technology and PLAXIS b.v., the Netherlands. Plaxflow is a finite element based seepage program that is used for geotechnical applications (Plaxflow user manual). Through this software, soil models can be created to simulate both transient and steady-state flow through porous media under both saturated and unsaturated conditions (Plaxflow manual). The graphical user interface allows the user to create the geometry of a soil model by either using the mouse to position movable crosshairs on the computer screen or by importing the geometry coordinates from a spreadsheet or ASCII text file. A sample of a slope model created using the mouse is illustrated in Figure 3-7. Plaxflow has a soil library that contains many soil types with pre-defined properties. These pre-defined soils are stored in the software's global database. While it is a convenience to have these pre-defined soils, their properties are fixed and cannot be changed by the user. However, Plaxflow also allows users to create a soil type by assigning soil properties based upon their own testing. The user defined soil types can be set up by using common soil properties for a seepage analysis such as particle size distribution, horizontal/vertical hydraulic conductivity, and void ratio. The program then matches more complex soil characteristics, such as the soil moisture characteristic curve to them. Alternatively, the

more complex properties such as matric suction and unsaturated hydraulic conductivity can be entered by the user. Plaxflow allows the user to name and save their user defined soils in the “global database” for future modeling efforts. Figure 3-8 illustrates the slope model with the soil property setup window and the “global” soil library in Plaxflow.

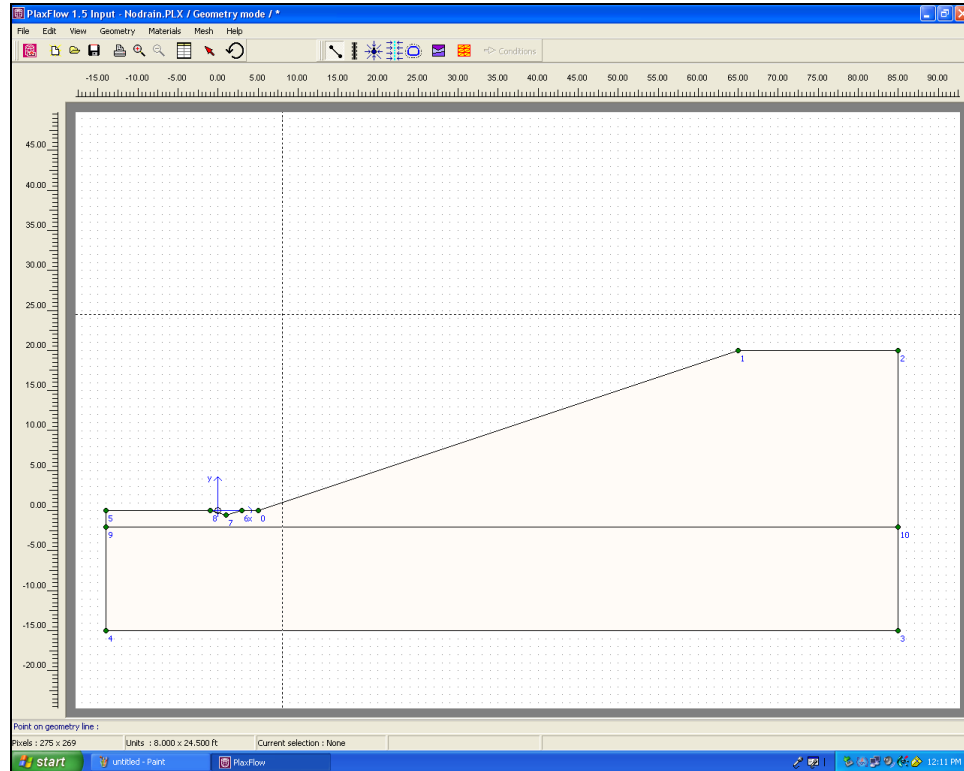


Figure 3-7: A slope geometry model created in Plaxflow by using the mouse crosshairs.

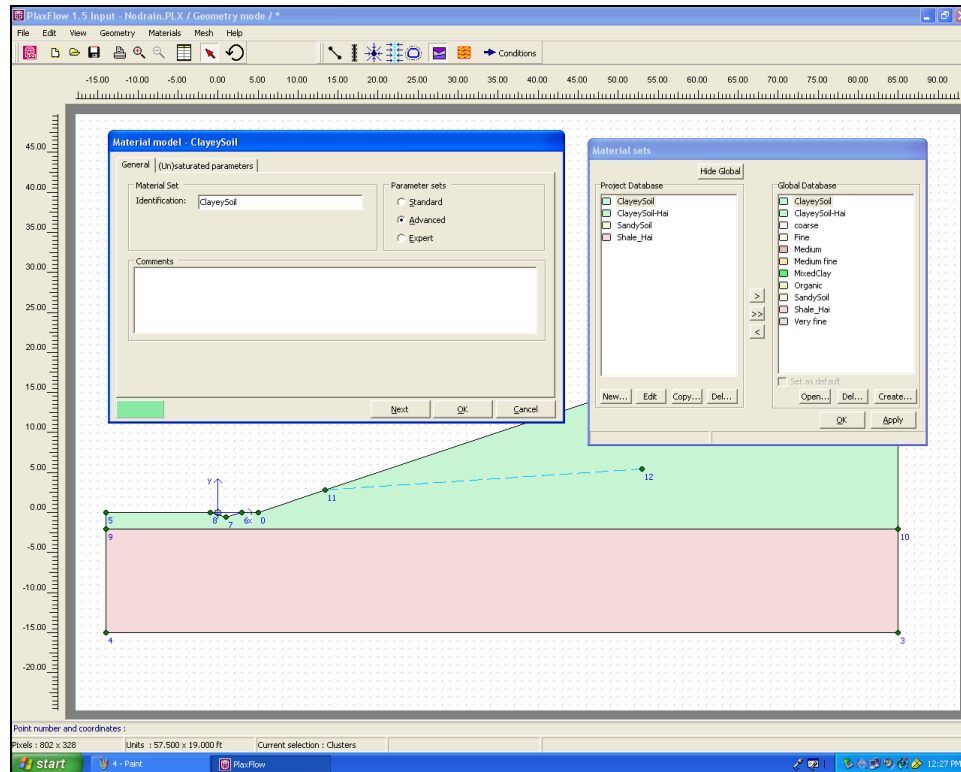


Figure 3-8: Soil property setup windows in Plaxflow.

Normal drainage boundaries for the model can be assigned as being either a well or a drain. This type of boundary condition is presented as the dashed straight line within the slope model illustrated in Figure 3-8. Impervious tunnels and screens are other drainages boundaries that can be assigned in Plaxflow but they were not used in this study. Other boundary options provided by Plaxflow include a phreatic surface, the water table location, precipitation boundaries, and boundary flow condition settings. In order to model transient conditions a series of time phases must be established, each having potentially differing boundary conditions prior to proceeding with a seepage analysis. The first phase is always the steady-state condition representing the initial condition before new fluids are introduced to the analysis. Subsequent phases can be created using either steady-state or transient inflow or outflow conditions. Depending on the user setting, transient phases can be analyzed over any time period, but more computer



memory and longer process times are required for long-term analyses. After seepage calculations are completed, the results are displayed in an output window as shown in Figure 3-9. There are many output options for presentation of the results to include water head, active pore pressure, degree of saturation, or a flow flux field. These outputs can be expressed through shadings, contour lines, or principle stress directions. A legend can be displayed on the right side of the model, as illustrated in Figure 3-9, to inform the user of the magnitude of the user selected output.

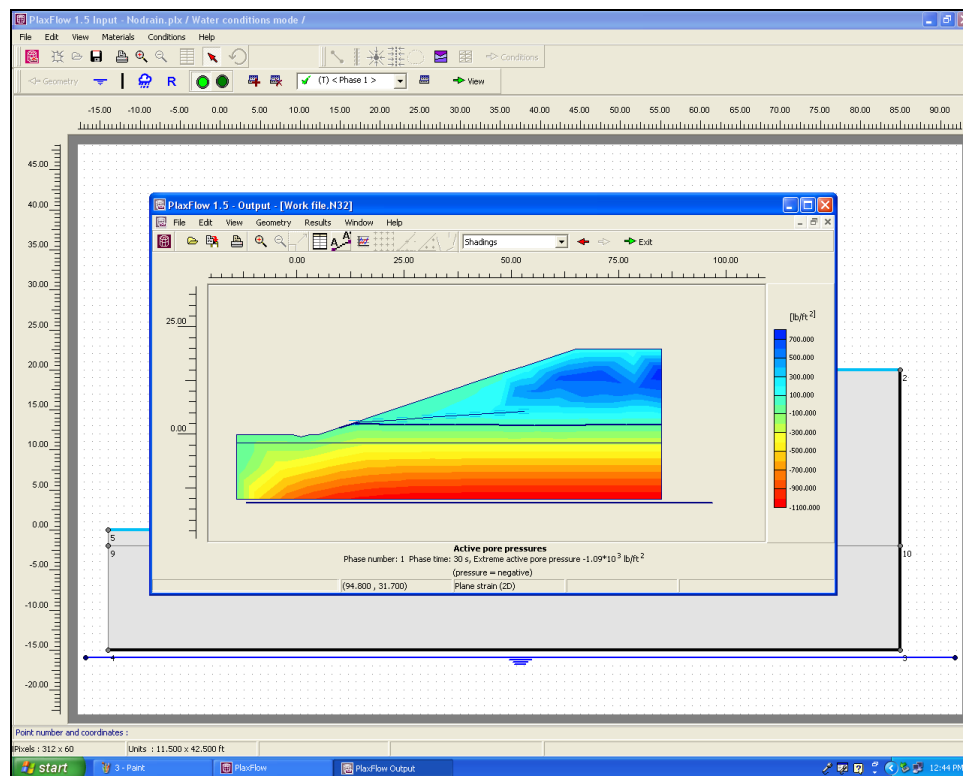


Figure 3-9: Output window of Plaxflow.

### 3.4 Overview of field work

The field work in this study included the installation of the wick drains and the monitoring equipment. The monitoring equipment included the following devices:

- TDR based moisture probes for moisture content monitoring.

- Grouted inclinometer casings and grouted TDR (Time Domain Reflectometer) cables to measure slope movement.
- Tipping bucket rain gauges to measure rainfall intensity at the site and the discharge of the wick drain system.
- Piezometers for monitoring the ground water table.
- Automated data acquisition and telecommunication equipment

The field site for this study was broken into two sections referred to as the drained section and the control section. Wick drains were installed into the portion of the slope referred to as the drained section, while an area adjacent to the drained section acted as the control section. The control section had no wick drains installed but did have a toe drainage system consisting of large, open graded, rock that was installed in a previous repair to the slope. Prior to the drain installation, the drain parameters such as drain length and drain spacing were determined so that the drain system would function at its theoretical maximum performance. The drain spacing was determined using a finite element based seepage program called Plaxflow. The results of these analyses will be presented in Chapter 4.

## **SENSORS and CALIBRATION**

All of the monitoring devices were calibrated prior to installation to ensure accurate conversion of voltage readings to engineering measurements. For this study the equipment calibration included the following devices:

- **Coaxial TDR** The cable selected for this study was type RG8 produced by Belden Inc. It is a 12.5 mm (½ inch) O.D., PVC jacketed, coaxial cable with a solid copper inner conductor and a braided steel outer conductor. The

manufacturer cites the propagation velocity of the cable, but often times this velocity can be different due to variations in manufacturing and materials. In order to pin-point the location of slope movement using TDR cable probes the exact propagation velocity had to be measured in the lab. For this calibration a known length of cable was connected to the TDR100 cable tester and a pulse was sent down the cable with the propagation velocity set equal to 100 percent of the speed of light. The time required for the signal to traverse the cable twice (down and back) was used to calculate the indicated length of the cable. The indicated length was divided by the actual length to determine the actual propagation velocity for this system.

- **Moisture probes.** Soil from the test site was compacted in a 151 mm diameter by 310 mm high concrete cylinder at various known moisture contents. The TDR probe was inserted into the compacted soil and a volumetric moisture content reading was taken using a program created by Campbell Scientific Inc called PCTDR. This program was specifically designed to measure volumetric moisture contents measured using the CS-615 moisture probe. The reported volumetric moisture content was plotted against the measured gravimetric moisture content.
- **Rain gauges** The rain gauges used in this study were TE525 tipping buckets produced by Texas Electronics. Their accuracy was 0.01 inches with a tipping volume of 4.73 ml/tip. The accuracy of these gauges was plus or minus one percent for rainfalls up to an intensity of one inch per hour. As intensity increased to 3 inches per hour the accuracy degraded to minus five percent.

### 3.5 Wick Drains

The wick drain material used in this study was **AmerDrain® 407**, which was purchased from the American Wick Drain Company, Monroe, North Carolina., The properties of this of wick drain material are described in Table 3-2 and an image of the material is presented in Figure 3.10.

Table 3-2: Properties of the wick drain used in this research.(American Wick Drain Company)

<b>Properties</b>	<b>Typical US value</b>	<b>Typical SI value</b>	<b>Test Method</b>
Material (Filter)	Polypropylene	Polypropylene	
Material (Core)	Polypropylene	Polypropylene	
AOS (Apparent Opening Size)	80 sieve	180 micron	ASTM D-4751
Permeability	0.016 in/sec	0.041 cm/sec	ASTM D-4491
Discharge rate	1.6 gal/min	6 L/min	ASTM D-4716
Roll length	1000 ft	305 m	
Roll width	4 in	102 mm	
Roll weight	52 lbs	23.6 kg	

Inspection of the particle size distribution curves in Figure 3-4 reveals that the soil at the site had more than 50% of its particles finer than the No.200 sieve (0.075 mm). As mentioned in the literature review, the ASSHTO specification recommends that the opening size of the geosynthetic filter should be smaller than 0.3 mm (or AOS > No.50 sieve) for the soils having more than 50% of their particles passing the No.200 sieve

(Koerner, 2005). Thus, the AOS of the selected filter fabric satisfied the ASSHTO specification.

In order to install the drains they had to be rolled into a cylindrical shape so that they could be inserted into the carrier drill pipe. As fabricated, the drains were four inches by one quarter inch and were shipped to University of Arkansas in 1000-ft rolls as illustrated in Figure 3-10. The drains were rolled into a cylindrical shape and bound at one-ft. intervals along their length by a wire tie as illustrated in Figure 3-11. The fabricated drains were transported to the site in 30 foot sections.



Figure 3-10: Wick drain material used in this study.

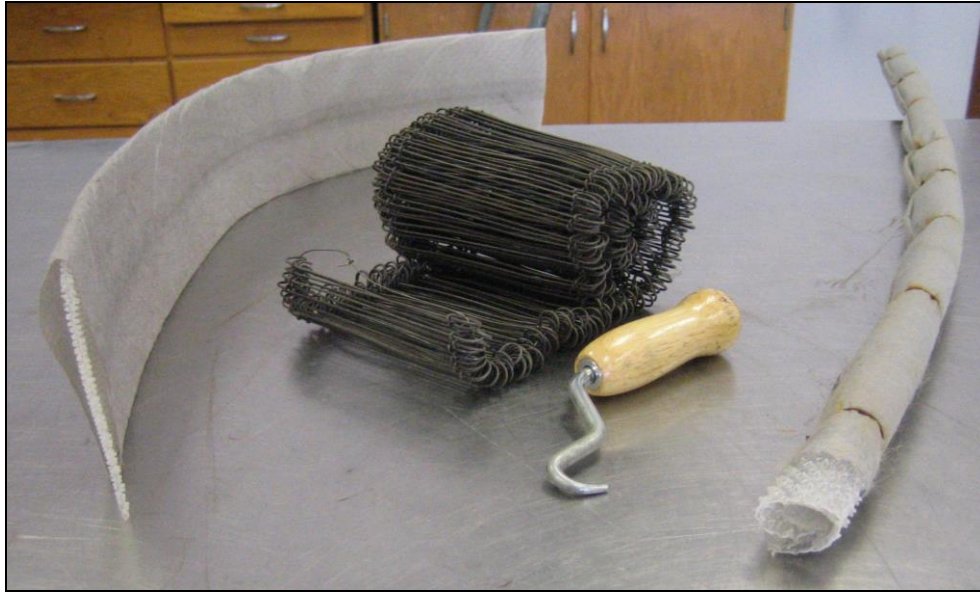


Figure 3-11: (from left to right) Original flat wick drain, malleable reinforcing steel ties, and a sample of the finished drain rolled and tied at 1-ft intervals.

### **3.6 Equipment**

#### **3.6.1 Datalogger CR10X**

Figure 3-12 displays a CR10X datalogger manufactured by the Campbell Scientific Company, Logan, Utah. It is equipped with many control ports which can be used for various applications depending on the devices which are connected to them. According to CR10X Measurement and Control System Operator's Manual (2000), the devices which can be connected to the CR10X include thermocouples for temperature measurement, tipping bucket rain gauges for rainfall intensity or flow capacity measurement, anemometers for wind velocity measurement, etc. In general you can connect devices that produce a voltage signal or a voltage pulse. You cannot directly connect strain gages, TDR devices or other instruments that have special circuit balancing or accurate timing requirements. In order for the connected devices to produce and record an engineering measurement, specific commands must be programmed into

the datalogger. These commands are programmed by many instructions in the *Edlog* module of LoggerNet software, which will be described later. Through the use of a software program called Loggernet, users can create and load control programs in the onboard memory of the data logger to execute a specific control functions or sampling processes. These operations include sending power to the measuring devices through the control ports, timing of measurements, and storage of the acquired data. Data were stored in the 2-megabytes of built-in memory, which allowed for the storage of about a week's worth of data before it was transferred to a computer for later analyses.



Figure 3-12: A datalogger CR10X used in the research.

### **LoggerNet Software Used for Datalogger CR10X**

Illustrated in Figure 3-13 is the opening screen and action menu of LoggerNet (version 3.1.5), a software program used to communicate with and control the operation of the CR10X datalogger.

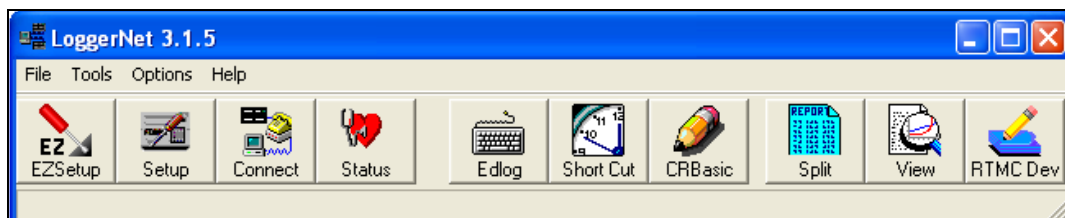


Figure 3-13: LoggerNet version 3.1.5 toolbar.

Loggernet was developed by the Macrovision Corporation; it has ten modules that control various features of data acquisition. Seven of the ten modules were used for data acquisition in this study and are described below:

- (1). *EZSetup*: This module provides the user the quickest and easiest way to make a connection between a PC and a datalogger. This module will help the user to set up the basic communication between a computer and the datalogger such as datalogger type, port location of connection.
- (2). *Setup*: This module allows the user to set and adjust the connection with the datalogger in detail. Through this module, the user can set the schedule of data acquisition such as the time of data collection, collection interval, and storage location in which the data will be stored after each measurement.
- (3). *Connect*: This module will launch a connect screen of the datalogger which is in use. The user can send the programs that contain the commands to execute and control the operation of the connected devices. Through this Connect function, the user can also collect the data, which were recorded from the previous measurements and store them inside the datalogger memory.
- (4). *Status*: This module expresses the status of the communication and the data collection of the devices which are registered with the program. This feature displays the quantity of the data collected, and the user can also collect data, turn on schedule calls or stop collecting data through the Status window.



- (5). *Edlog*: This module will bring up a window that allows the user to program the commands which will control the functions of the datalogger as well as the measuring devices. These commands are made through many instructions. Each instruction has its own function in controlling and executing the operation of the datalogger and the devices. A program can be created by one or many instructions, and this program is loaded into the datalogger through the *Connect* module.
- (6). *Split*: This module is used to process the data collected from a datalogger. Through the *Split* window the user can sort the data from the files based on the device ID, the date, and the time of the measurements. After being sorted and classified, the data are then saved in many categories or folders so that the analyses in the later parts can be done easily.
- (7). *View*: This module will open a window that displays the results of data collected.

The remaining modules are used to help the users who are new to the LoggerNet software to program the commands and provide instruction on how to handle the software properly.

### **3.6.2 Time Domain Reflectometer (TDR)**

#### **Operating principle of a TDR**

According to Wong (2004), time domain reflectometry is an electrical measurement whose operating principles are based on the transmission line theory. Essentially TDR is like radar except the energy is transmitted within a waveguide rather than in space. A step pulse of energy is transmitted through a wave guide and an

abnormality within the guide will cause a portion of the energy to be reflected back to the source. With accurate timing and receiving devices one can determine the following using TDR:

- Locate the faults in the conduit and determine the cause of the energy reflections.
- Measure the dielectric property of the materials.

Cogdell (1996) pointed out the following major properties of transmission lines which are important to the time domain reflectometry:

- The speed that an electromagnetic signal or an electrical conduit travels in a transmission line depends on the dielectric constant of the materials between the conductors.
- Any change in impedance in the transmission line also affects the traveling wave inside it. The changes can be geometric or in the dielectric constant of the materials. When there is a change in the transmission line, part of the signal is transmitted and part is reflected.

A TDR includes three main components: an electrical pulse generator, a sampler, and an oscilloscope (Wong, 2004). First, the electrical pulse generator will emit a fast rise-time electromagnetic step pulse into the transmission line at a specific interval. In this case the transmission line is the TDR coaxial cable. Then the amplitude of the electrical pulse and the total time between the pulse emission of and arrival of the reflected pulse are recorded accurately by a high precision voltmeter and a high precision timing device built inside the sampler (Wong, 2004). The function of the oscilloscope is to perform the simultaneous measurements of time and voltage from the sampler in the

configuration of a waveform. This waveform is then known as the “signature” of the cable for a specific measurement.

The electromagnetic pulse travels through the coaxial cable after generated by the pulse generator with a propagation velocity,  $V_p$ . The propagation velocity is defined as the speed of a wave traveling through a transmission line, and  $V_p$  is a function of the dielectric constant of the material of the transmission line (Wong, 2004). Generally the wave travels with the speed of light ( $3 \times 10^8$  m/s) in a vacuum, but its velocity will alter when the transmission line is made of other materials with different dielectric constants. For instance, if the transmission line is made of polyethylene, the speed of the signal traveling through that material is about 60% of the speed of light (Wong, 2004).

According to Wong (2004), for a normal coaxial cable the electromagnetic pulse travels to the end of the cable, and then it propagates in the reverse direction without any change of impedance along the cable. The voltmeter in the sampler also measures the voltage between the shield and the conductor of the cable as a function of time. If there is a change in geometry or dielectric constant of the cable, such as short circuits, breaks, or water ingress, the impedance of the cable will be affected and some or the whole of the electromagnetic pulse will reflect to the sampler. In this case the voltmeter will measure and detect the voltage change of the reflected pulse and express it as a reflection coefficient  $\rho$ . The reflection coefficient is the ratio between the reflected voltage to the input voltage as in Equation 3-1. The waveform configuration of the coaxial cable will be expressed by the reflection coefficients, and any changes in geometry or dielectric constant along the cable will be detected based upon the changes of reflected coefficient (Wong, 2004).

$$\rho = \frac{V_r}{V_i} \quad (\text{Eq.3-1})$$

Where  $V_r$ : reflected voltage

$V_i$ : input voltage

### **Types of TDR application**

The TDR is now used widespread in many geotechnical applications and other engineering applications such as environmental subsurface pollutant detection or monitoring water contents of subgrade (Wong, 2004). According to Wong (2004), the applications of the TDR mainly focus on the two following purposes:

- 1) Measure and locate the deformation or fracture of the slope at the experimental site.
- 2) Measure the moisture content of the soil within the slope.

In the application of slope movement detection, a TDR cable is installed into a borehole within the slope passing the suspected slip zone and grouted with a mixture of cement and bentonite. After the installation of the TDR cable is completed, an initial waveform, or cable signature, is obtained before any slope movement occurs and is used as the baseline for future comparison. This signature expresses no change in geometry of the cable whereas any change in geometry of the cable due to slope failures or slope movements is characterized by a difference of the reflection coefficient in the later readings compared to the initial signature. An example of many TDR signatures indicating slope movement is illustrated in Figure 3-14 below.

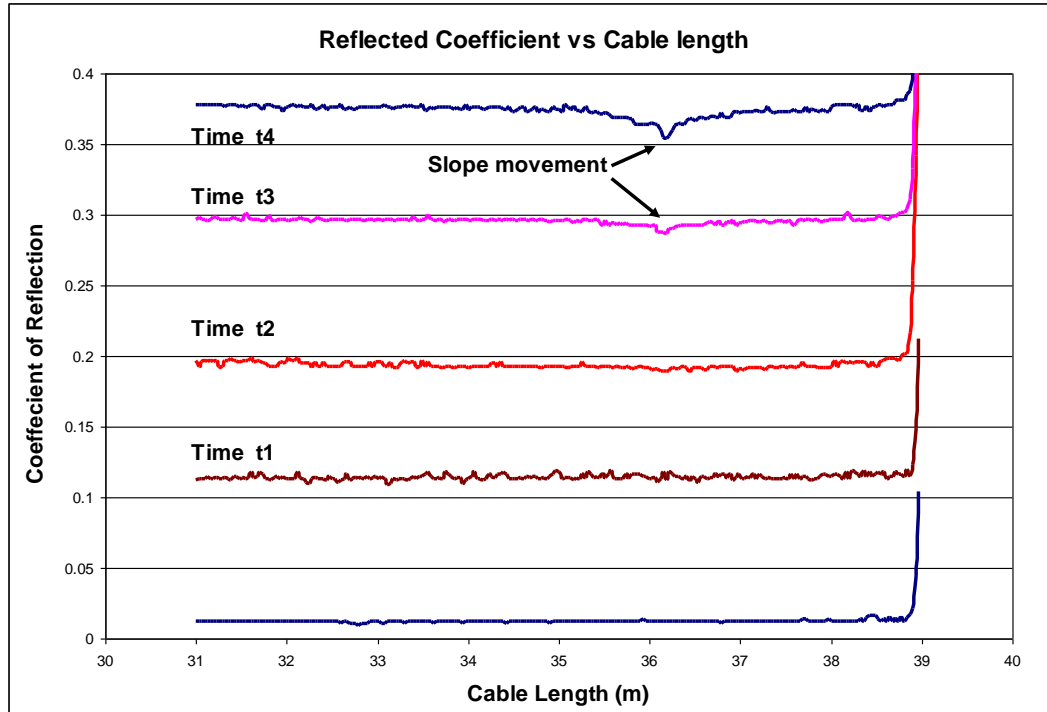


Figure 3-14: Typical TDR cable signatures in slope movement detection.

In the above figure, the bottom blue line is used as the baseline. This base line was recorded at the first time of the measurement. It should be noticed that its flat and smooth geometry expresses no change in geometry of the slope. The two signatures corresponding to the time t1 and t2 also show that the slope has no movement or failure. However, these two signatures are not as smooth as the first one. This could be because of during the consolidation of the soil within the slope, some rock fragments of the soil crimped or crushed onto the cable, affecting the geometry of the cable. These small changes in geometry of the cable were recorded and displayed in some small spikes along the length of the cable. The signature at the time t3 shows a clear spike compared to the previous signatures. This spike displays a fracture on the slope, and the position of the spike is also the place where a crack occurs. The later signature corresponding to the time t4 clearly shows a large spike in the signal which is related to deformation of the cable

resulting from shear displacement in the slope at that location. One can observe a similar spike in signature t3 at the same location. The amplitude of the spike quantifies the movement of the slope.

### **TDR100 Reflectometer**

Figure 3-15 illustrates the TDR100 used in this study. This device is produced by the Campbell Scientific Company, Logan, Utah. The TDR100 is a combination pulser-receiver that is used to acquire a cable waveform that can be used to measure the moisture content of the soil, using a moisture probe, or to locate the position of a failure surface and the magnitude of movement along that surface using a TDR cable probe.



Figure 3-15: A Campbell Scientific TDR100 used in the research.

### **Control Software for the TDR100**

The software program used to control the TDR 100 is called PCTRD. It is provided with the purchase of the TDR100 by the Campbell Scientific Company, Logan,

UT. The version of the software used in this study was 2.05. The main function of the software is to display the wave form of signature travelling along the TDR probe (Wong, 2004). The display screen of the PCTDR software is shown in Figure 3-16. Through this interactive screen the user can detect changes in cable geometry along the length of a cable or in the dielectric constant for a moisture probe. These changes are expressed as changes in reflection coefficients. The user can also get the bulk electrical conductivity (EC) or the water content (volumetric moisture content) of a porous medium through this PCTDR program in the same window. The program contains both the Topp and Ledieu equations for determining volumetric moisture content based of the measured cable signature and allows the user to select either equation or to define a custom equation for making moisture content predictions.

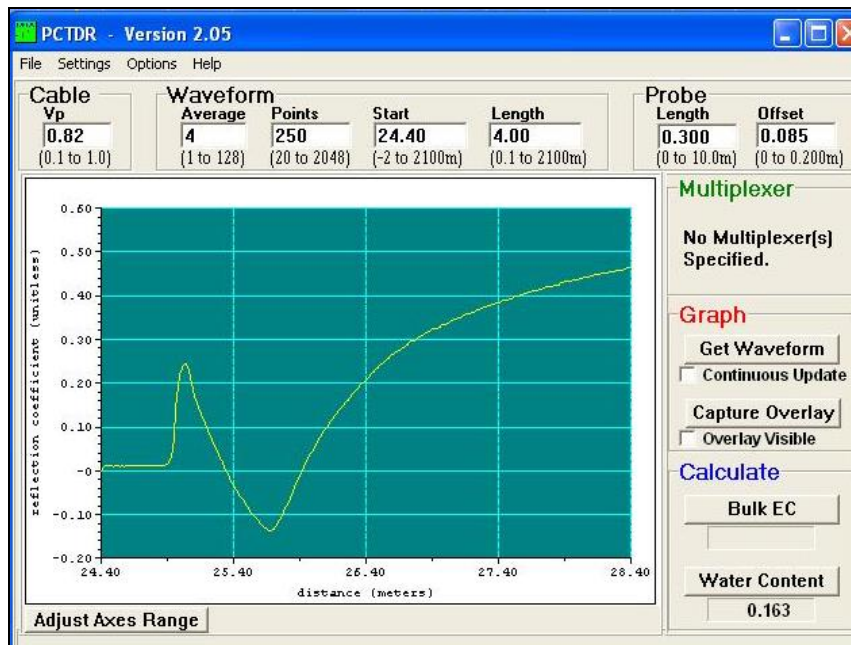


Figure 3-16: The PCTDR- Version 2.05 window screen.

There are seven parameter boxes across the top of the screen in which the user can use to specify what parameters to control how the real time capture of a waveform or signal is recorded by the TDR100. The first box is the *Cable Propagation Velocity* box where the propagation velocity of the cable attached to the TDR100 is entered. This property is needed so that the timing of the signal measured by the TDR100 can be related to distance along the cable. As defined earlier in chapter 2, the propagation velocity ( $V_p$ ) is the speed of a wave traveling through a transmission line, and  $V_p$  is a function of the geometry and materials in the transmission line. When an incorrect value of  $V_p$  is used, the time-space relation of the signal will be incorrect, and the dielectric constant measurement or signal location results will be inaccurate. This in turn will lead to inaccuracies in fault locations and incorrect moisture contents.

There are two methods to determine the propagation velocity of a cable. In the first method, the propagation velocity is provided by the product specification of the manufacturer. This method is the easiest one as the propagation velocity of the cable is usually provided by the manufacturer when a purchased is made. When a cable with unknown propagation velocity is used, however, the user can use the TDR100, cable of known length and special software to and obtain the correct  $V_p$ . The methodology of the second method will be discussed in the later part of this chapter.

The next four boxes in Figure 3-18 are the Waveform Parameters Boxes. According to the TDR100 manual, the *Average* box will set the number of signal measurements that are averaged to produce the final waveform appearing on the screen. Averaging is helpful if noises of random nature, or from power sources, are superimposed on the reflected waveform. A value of 4 is highly recommended by the



manufacturer. When a value of 4 is entered in the Average box, four measurements are collected at a given distance before measurements are taken at the next specified distance increment.

The *Points* box specifies the number of points to be collected to describe the waveform. A value of 251, which is recommended by the Campbell Scientific, will break the waveform into 250 measuring increments. A higher value of collected data points can be used for better resolution but more data storage capacity is required. The number of points recommended by Campbell Scientific is a good balance between resolution and storage requirements.

The *Start* box establishes the position along the TDR cable where measurements of the cable or moisture probe signature will begin. The length of cable or probe over which measurements will be made is specified in the *Length* box. For example, in Figure 3.18 the *Start* value is 24.4 m and the *Length* value is 4 m, so the displayed waveform, measured four times at 251 discrete points, is displayed on the screen from 24.4 m to 28.4 m.

The last two parameter boxes are used only when a moisture probe is connected to the TDR100 and the program is used for volumetric moisture content measurement. Since these two parameters are directly related to the physical characteristics of the moisture probe (rod length and connection head length), they are usually provided by the manufacturer. For the CS615 moisture probe used in this study, the length of the three roDoS are 30 cm, which will be entered as 0.3 in the *Probe Length* box, and the value of 0.085 m probe offset, provided by Campbell Scientific Inc., is input in the *Probe Offset* box. When all of the parameters are set, PCTDR will automatically measure the reflected

coefficients along the cable and display them in the form of a waveform, or the value of volumetric moisture content can also be determined.

### 3.5.3 Multiplexer SDMX50

The TDR100 has only a single port and if measurements from more than one probe are to be measured its capacity must be expanded. In this study a SDMX50 multiplexer, manufactured by the Campbell Scientific Company was used to expand the capacity of the TDR 100. A multiplexer allows more than one cable or moisture probe to be connected to the TDR100. As shown in Figure 3-17, the SDMX50 multiplexer has one output, or common, plug and eight input plugs. Each input plug can be connected to a TDR cable or a moisture probe, or to an the common plug of another multiplexer.. According to the TDR100 manual (2005), three levels of multiplexers can be addressed which creates a total of 512 ports for attachment of TDR devices. A three level multiplexer arrangement is illustrated in Figure 3-28.



Figure 3-17 A Campbell Scientific SDMX50 multiplexer used in this study.

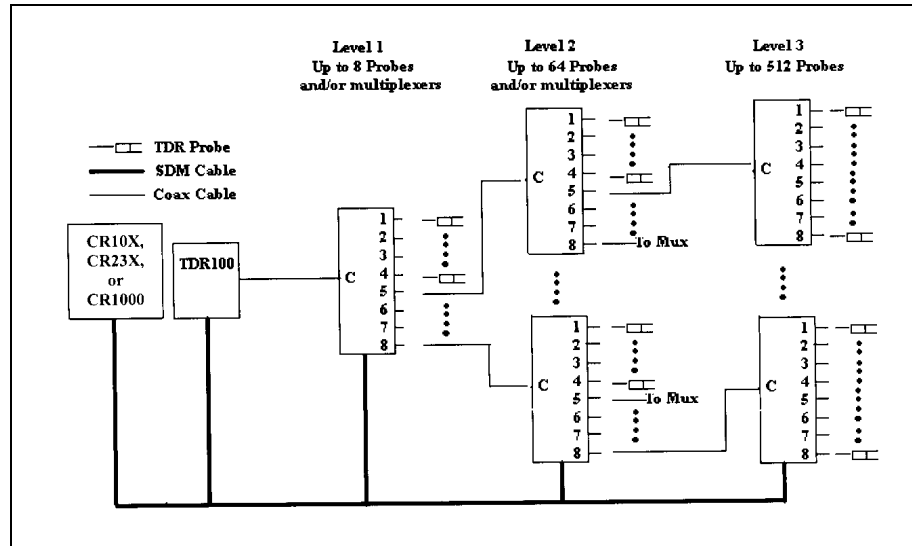


Figure 3-18: Diagram of a 3-level SDM50 multiplexer (Campbell Scientific TDR100 Manual, 2005).

In this study, two SDM50 multiplexers were used to provide a total of 15 connections. This allowed for a suitable number of connections for the TDR cables and the CS615 moisture probes at the test site.

### 3.5.4 Coaxial TDR cables

Coaxial cables are normally used as the transmission line for TDR systems used in slope movement monitoring (Wong, 2004). A coaxial cable consists of an inner conductor and an outer conductor which are separated by a layer of dielectric material at a constant distance. This dielectric material plays a role as the insulation layer between the conductors that does not conduct electricity (Wong, 2004). The outer conductor is protected by a water-proof outer jacket, which is usually made of polyvinyl chloride (PVC). There are many types of coaxial cables on the market, and they are classified based on the differences in the types of outer and inner conductor as well as the types of material for the insulator. Based on the recommendations of Wong (2004), RG8 coaxial cable was selected for the TDR transmission line and probes in this study. This

cable was purchased from Belden Incorporated, St. Louis, Missouri in 500 foot rolls. The cable roll is illustrated in the main picture in Figure 3-19 and the detail component layers of the RG8 coaxial cable are shown in the inset picture at the bottom-left corner of Figure 3-19. In this study four TDR cable probes were used to monitor slope movement, two in the drained section and two in the undrained section.



Figure 3-19: The RG8 TDR coaxial cable used in the research.

### 3.5.5 CS-615 moisture probe

The moisture probes used to measure soil moisture content within the slope in this study were the Model CS615, manufactured by Campbell Scientific Company, Logan, Utah. As illustrated in Figures 3.20 and 3.31, this type of moisture probe has three 1ft (30cm) stainless steel rods connected to a polycarbonate head. The probe is connected to the TDR100 or a multiplexer with RG8 coaxial cable, as illustrated in Figure 3-20. In this study, ten CS615 moisture probes were used to monitor the changes in moisture content

of the soil within the slope. Five were installed in the drained section and five were placed in the control section.

The CS-615 can be polled by the TDR100 at a rapid frequency (every hour in this study) and thus has the ability to provide an almost continuous record of moisture content of the soil at any depth of installation without the need to collect a soil sample or use some manual technique to obtain a measurement. This sensor type treats the soil between the metal rods as a dielectric material. As the moisture content of the soil between the rods changes its dielectric properties change and the electronic signature of the probe changes. Figure 3.22 illustrates a typical cable signature for the CS-615 moisture probe. The distance between the two spikes in the cable signature indicate the apparent length of the metal rods of the probe. When this length is compared to the actual length of the rods the soil's dielectric constant can be determined by Equation 3.2 which is based on electromagnetic pulse theory. Once the dielectric constant of the soil is known the volumetric moisture content can be empirically correlated using either Equation 3.3 or 3.4.

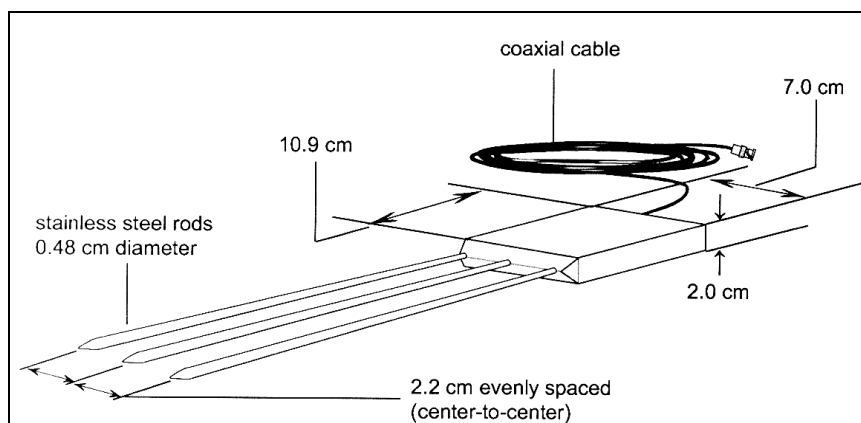


Figure 3-20: Schematic of the Campbell Scientific CS-615 moisture probe (TDR100 manual).



Figure 3-21: A CS610 moisture probe used in the study.

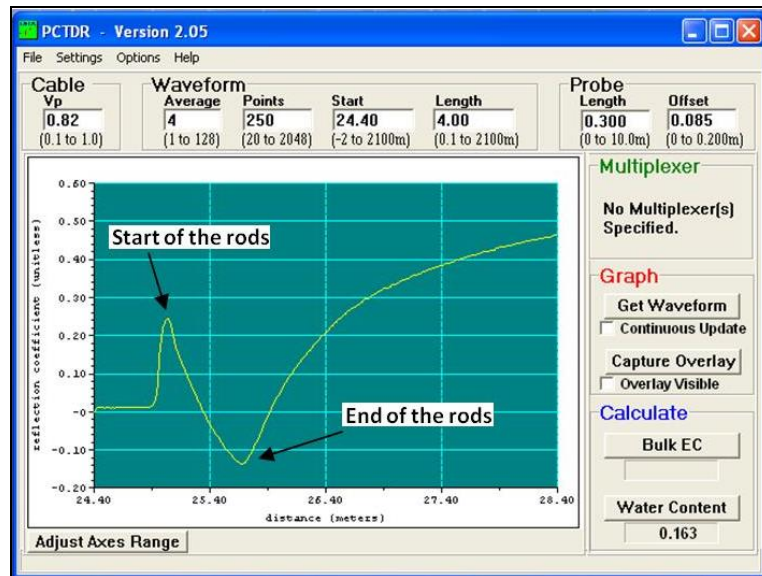


Figure 3-22: A typical TDR waveform for moisture content measurement.

$$\sqrt{K} = \frac{L_a}{L} \tag{Eq.3-2}$$

Where: K = Dielectric coefficient of the Soil

La = Apparent rod length

L = Actual rod length

The TDR100 instruction manual (2005) recommended either the Topp and Ledieu equation for predicting volumetric moisture content. Both empirically express the relationship between the dielectric constant, K, and the volumetric moisture content of the soil,  $\theta$ , as follows:

- Topp's equation:

$$\theta = -5.3 \times 10^{-2} + 2.92 \times 10^{-2} * K - 5.5 \times 10^{-4} * K^2 + 4.3 \times 10^{-6} * K^3 \quad (\text{Eq.3-3})$$

- Ledieu's equation:

$$\theta = 0.1138\sqrt{K} - 0.1758 \quad (\text{Eq.3-4})$$

According to the TDR100 instruction manual (2005), these formulas have been shown to be appropriate for nearly all soil applications and their accuracy is equivalent. However, the Ledieu equation is less complicated than the Topp equation. Thus, the Ledieu expression was used in this study to convert the dielectric constant of the soil to the volumetric moisture content. The volumetric moisture content was converted to the gravimetric moisture content, which is more familiar to geotechnical engineers.

### **3.5.6 Telecommunication system**

A telecommunication system was used in this study to transfer the data that was recorded and stored in a datalogger at a remote location to a base computer located in Bell Engineering Center. Without this component, an engineer must visit the site to collect data manually at least once a week. The telecommunication system included dual band cellular antenna, a data translation device and a cellular digital modem as shown in

Figure 3-23. The antenna operated at frequencies of 900 and 1900 MHz, which are the two frequencies utilized by the AT&T cellular system. The data translation device was a Campbell Scientific produced serial cable that was used to convert data signals from the Campbell Scientific logic used by the CR10X datalogger to standard RS-232 logic used by the communication industry and standard computers. This device served as the interface between the datalogger and the modem. The cellular modem was Raven II, Manufactured by Airlink Communications, San Jose, CA. It was designed to operate on AT&T's GSM system and could transmit data at a Baud rate of 9600 cps. When powered on the modem could automatically call a polling computer or could be called by a polling computer.



Figure 3-23: The telecommunication system used to in the study.

### **3.5.7 Rain gauge and thermocouple**

Two rain gauges were used in this study. One of them was used to measure the rainfall intensity at the site for the duration of the study, and the other was used for measuring the flow coming from the embedded horizontal wick drains. A thermocouple was used to measure the in situ temperature air temperature as a part of a partial weather



station. Figure 3-24 illustrates the model TR-525USW rain gauge, manufactured by Texas Electronics, that was used in this study. This device contains a calibrated bucket that tips when 0.01 of an inch of rainfall is collected in the collection funnel. Each tip creates a voltage pulse that is sent to the data logger. The voltage pulses are counted by the datalogger as a function of time so rainfall intensity can be recorded as inches of precipitation per unit of time.

In order to use this device as a flow measuring device the exact amount of liquid required to make the tipping bucket tip had to be established. In addition the maximum pulse rate that the data logger could count had to be ascertained as described earlier.



Figure 3-24: Model rain gauge used in the study.

### **3.5.8 Enclosure and Power Supply System**

All of the components in the monitoring system required either 12 or 5 Volt DC power to operate. In the absence of a source of commercial power an autonomous power supply was required to supply the system with power during the study. A system,

comprised of a 12 Volt storage battery and a 20 Watt solar panel was created to fill this need. The major components of this system are illustrated in Figure 3-25. Figure 3-26 shows the weather-resistant enclosure used to contain the data acquisition system, communication system and the 12-V battery with charge controller. This enclosure was a Fiberglass Reinforced Plastic Model PS3030A case, produced by Vynckier Enclosure Inc, Houston, TX. Its function was to prevent damage to the equipment by weather or other sources (manmade or natural) that might jeopardize the study.



Figure 3-25: Solar panel and 12-V battery used to supply power to the TDR system.



Figure 3-26: A weather-resistant enclosure housing the data collection system.

### **3.5.9 Slope Inclinometer**

#### **Inclinometer probe and readout unit**

The complete operating principles of a probe inclinometer is described in Appendix A. The traversing inclinometer probe used in this study was manufactured by Slope Indicator, Inc. and was purchased from the Stone Mountain, GA office. Figure 3-30 shows the 30 inch long stainless steel traversing probe. The force accelerometers for this probe are located at the wheel locations which are 24 inches apart. The power supply/data recorder mated to this probe is a Digitilt DataMate® also produced by Slope Indicator, The DataMate is shown in Figure 3-31. According to the manufacturer's specifications, the maximum storage capacity of this readout unit is 2,500 readings, which translates to about 40 casing surveys. Data must be offloaded to a computer when

the device is full because it will not overwrite older data. The data must also be offloaded to a computer for further analysis to in order to produce an inclinometer report.



Figure 3-30: The Slope Indicator inclinometer probe and its container.



Figure 3-31: The Digitilt DataMate® readout unit (After Slope Indicator).

### **Data cable and pulley assembly**

Illustrated in Figure 3-32 is the 100 foot control cable and the pulley assembly used for the inclinometer surveys in this study. The pulley assembly attaches to the top of the inclinometer casing and helps to position and hold the inclinometer probe in place within the casing while making a measurement. The cable has rubber depth markers fused to the jacket at 2 foot intervals. Using the depth markers the operator knows the exact position of the middle of the inclinometer probe, referenced from the top of the inclinometer casing, at each measurement location.



Figure 3-32: The control cable and the pulley assembly for inclinometer system.

### **Inclinometer casing**

The ABS plastic casings that were grouted into the slope at the study site were 70 mm (2.75 inches) in diameter and were also produced by Slope Indicator, Inc. Standard inclinometer casing comes in standard lengths of 5 and 10 feet and can be connected

together in the field with the snap-together connection to create casings of any length. The quick connect casing used in this study are produced in two sizes 85 and 70 mm in diameter. The 70 mm diameter casing diameter was used in this study because of the shallow depth of study and the anticipated small movements in the slope. The casings are grouted into a vertical borehole using grout or gravel that has approximately the same stiffness as the surrounding soil. As the slope moves the grout column and casing are deformed and this deformation is detected by the probe inclinometer.



Figure 3-32: Quick Connect (70 mm) inclinometer casings used in the study.

### **Software used for Slope Inclinometer**

After the readings are stored in the readout unit, they are transferred to a computer using a software called the DMM (Data Mate Manager) program. This software, produced by Slope Indicator Company, is used to establish serial communication between the Digitilt® DataMate readout unit and a computer. Its function is mainly to retrieve the

readings stored in the readout unit and store them on a computer in Microsoft Access® data base format for further analysis. This software also allows the user to check and adjust the readings obtained during the inclinometer survey. For example the orientation of the inclinometer probe can be rotated in 90 degree increments to account for the fact that the probe may have been inserted backwards for a particular set of readings.

Once the readings are transferred to a computer, they can be manipulated and plotted in graphical displays using the DigiPro software program. This program helps to illustrate the movement of the slope in a variety of ways by plotting the readings from multiple surveys on the same graph so that the user can easily identify the shear zone and magnitude of the movement as a function of time. According to Slope Indicator the slope movement profile can be displayed by DigiPro in the four common format types (in either English unit or Metric units): Inclinometer surveys can be displayed in four different formats:

- 1) *Incremental Deviation*: The change in deviation (angle of tilt) of subsequence readings for each interval relative to the baseline reading
- 2) *Incremental Displacement*: The change in lateral displacement of subsequence readings for each interval relative to the baseline reading
- 3) *Cumulative Deviation*: The change in deviation of all readings over the length of the casing
- 4) *Cumulative Displacement*: The change in lateral displacement of all readings for each interval over the length of the casing.

A typical DigiPro screen shot, depicting incremental displacement and cumulative displacement of a slope are illustrated in Figure 3-34. In this figure the two plots in the

left window illustrate the incremental displacements in both the A and B-directions (down slope and cross slope), respectively. The right panel illustrates the cumulative displacements in the A and B-directions. All plots show a progression of movement with time by superimposing inclinometer surveys taken at different times. Figure 3-34 (left pane) illustrates a distinctive shear plane developing at a depth of approximately 8.5 feet beneath the surface. While in the right pane one can see that movement actually starts at about 11 ft and becomes a maximum magnitude at about 8 ft. Normally, cumulative displacement is reported for the purposes of monitoring mass movements. For the purposes of this study the location of the shear plane was the desired parameter, so most illustrations will use incremental displacement which portrays that parameter better.

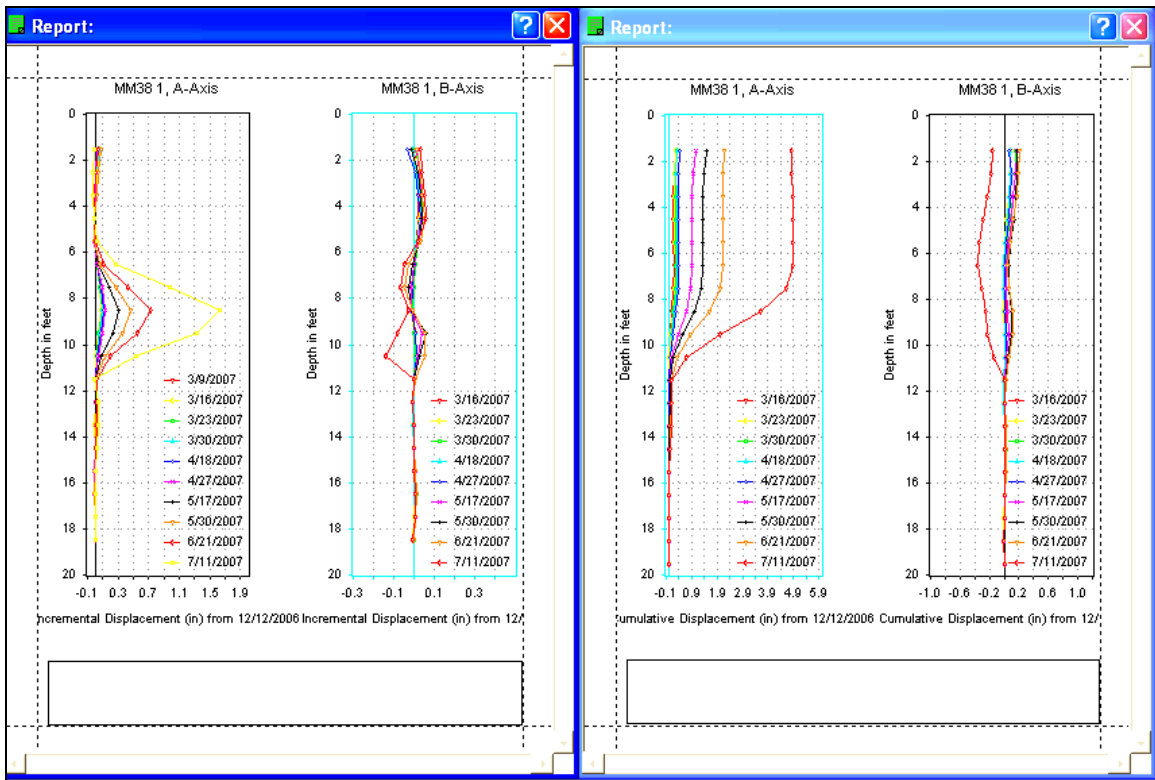


Figure 3-34: A typical DigiPro ® report of slope movement produced using traversing probe inclinometer survey data.



### 3.5.10 Piezometer

The piezometer, manufactured by Onset Computer Corporation, used for monitoring the position of the ground water table (GWT) within the slope is illustrated in Figure 3-35. This device is self-contained, autonomous, recorder that can be lowered into a borehole to continuously monitor the location of the GWT. According to the manufacture specifications, the on-board memory capacity of this piezometer is about 64K bytes, which allows storage of up to 21,700 readings, and the battery life can sustain continuous recording for up to 5 years with data being taken at one-minute intervals. These piezometers were placed in the modified inclinometer casings to maintain a record of the water level in the slope during this study. The inclinometer casings were modified by cutting a series of evenly spaced (4 in the radial direction) 3mm x 8 mm slots at 6mm intervals along the length of the lowest 5 feet of the casing. The casings were then backfilled with pea gravel to within 3 feet of the surface. The final three feet of the



Figure 3-35: A piezometer used in the study.

borehole was sealed with a bentonite powder to prevent surface runoff infiltration into the borehole.

To communicate with the piezometer, a software program called HOBOWare™ and an optical reader were used. The software, produced by Onset Computer Corporation, will poll a piezometer through the optical reader and collect the data which are recorded and stored in the piezometer's memory. This software can also be used to program the piezometer so that the user can establish the timing of each measurement, and the parameters of the measurements such as absolute pressure and temperature.

For the piezometers used in this study, only absolute water pressure was recorded. The data were converted into values of water level and plotted as a function of time in HOBOWare™ as illustrated in Figure 3-36. The data could also be off loaded from the piezometer in ASCII format and imported into Excel® for further manipulation of the data.

### **3.5 Installation procedure**

#### **3.5.1 Drains installation**

The installation method for the wick drains in this study represents a series of modifications to the method proposed by Santi (2001). The method proposed by Santi employed a bull dozer to push a steel pipe containing the rolled wick drain into the slope. Santi's procedure required a significant amount of level area for the dozer to operate in which may not always be available when working near highways. For this study an attempt was made to use longer sections of drill pipe and reduce the required operating area. Initially a specially designed pipe pusher was used in combination with a tracked excavator to advance the drill pipe into the slope.

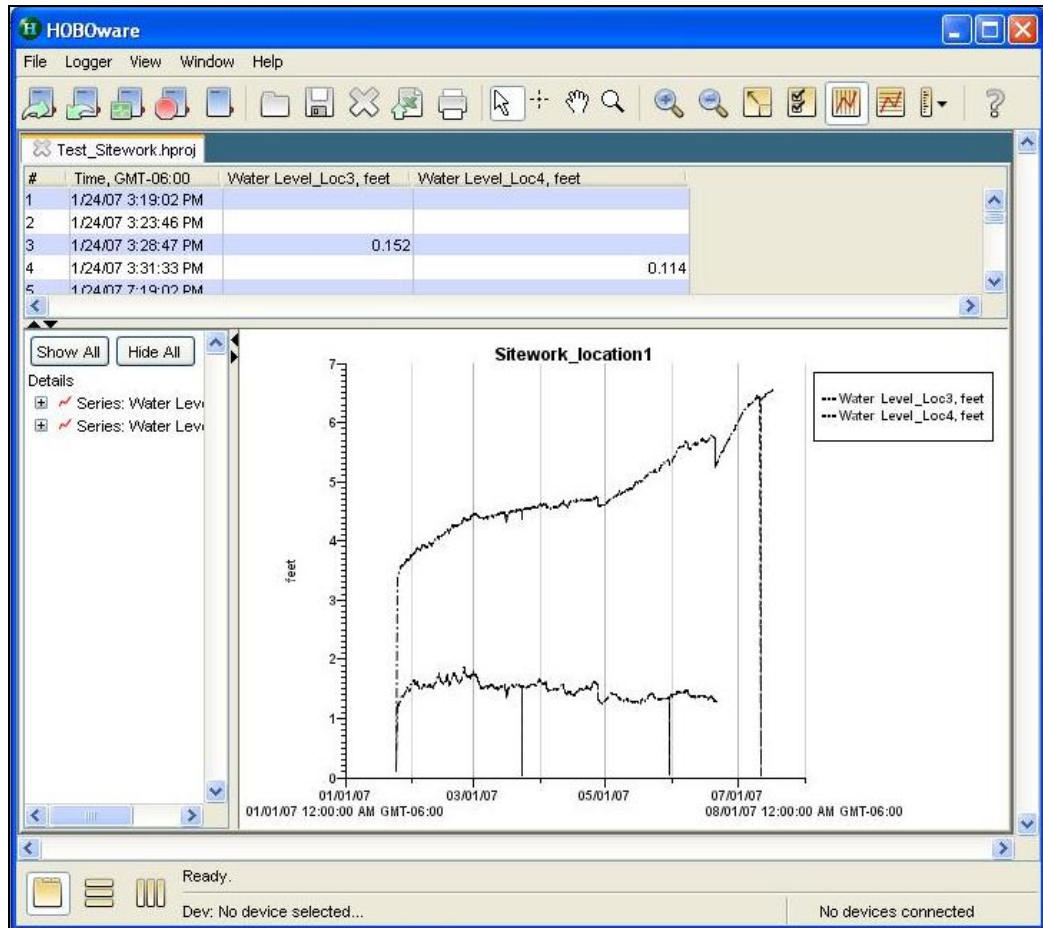


Figure 3-36: A typical plot of water level versus time created in HOBOWare™.

When it was discovered that this method could not advance the drill pipe to the desired distance into the slope a paving breaker was attached to the tracked excavator and the combination of the static push of the excavator arm and dynamic energy of the paving breaker was used to advance the drill rod. Each method will be described in the sections to follow.

#### Paving Breaker Method

The equipment required for the installation using this method includes the following devices:

- A track hoe to push the steel pipes into the slope, as shown in Figure 3-41.

- 2-5/8 in-diameter by 10 ft-long steel pipes (NWJ rod) for housing the drains.
- Steel cones to protect the head of the steel pipes during the installation.
- A slotted drive tube and a drive head to transfer the energy from the paving breaker and tracked excavator to the steel pipes while preventing the drive tube from damaging the wick drain.
- A pulling-end to be connected to the tracked excavator arm or a bulldozer winch to pull the steel rod out of the slope when the drain insertion is completed.

Illustrated in Figure 3-41 is the final equipment configuration used to drive the drill rod into the slope and install the wick drains. Each piece of equipment and segment of the



Figure 3-41: The track hoe and paving breaker used for wick drain installation. installation operation are described in the ensuing photographs. In Figure 3-42 the pulling-head, drive head, steel cone drive point, and the slotted drive tube the for wick drain installation are illustrated. At the conclusion of driving the drive tube is removed

and the pulling head is threaded into the tail of the drill string. A cable is attached to the eye in the pulling head and either the arm of a tracked excavator or a bulldozer winch is used to extract the drill string from the slope. The drive head is a device that is attached to the maul point of the paving breaker and slips over the drive tube of the drill string to transfer energy from the paving breaker to the drill string. The drive tube threads into the female end of the drill rod and contains a slot so that the wick drain can be routed out the rear of the rod assembly and not damaged by the driving operation. The drive point is constructed from a splitting wedge whose driving head has been machined so that it fits the inside diameter of the drill rod.



Figure 3-42: From left to right, pulling-head, drive head, steel drive point, and slotted drive tube used in the wick drain installation.

The rear of the drive point is tapped so that a carriage bolt can be screwed in. The wick drain is attached to the carriage bolt that is threaded into the driving point.

To start the drain installation the rolled wick drain had to first be threaded through each section of drill rod, as illustrated in Figure 3-43. The leading edge of the drain was

then attached to the carriage bolt of the sacrificial drive point using two hose clamps, as illustrated in Figure 3-44. The drive tube was threaded into the rear of the first section of drill rod and the wick drain was pulled through the slot and moved out of the way as illustrated in Figure 3-45. The first section of pipe was now ready to be inserted into the slope. As illustrated in Figure 3-46 the drill pipe was properly positioned and the drive head, which was attached to the maul point of the paving breaker, was slipped over the drive tube. The combination of static force of the excavator arm and the dynamic force of the paving breaker was then used to drive the first section of drill rod into the slope at an angle that was nearly horizontal. Once the first section of pipe was driven all the way into the slope the excavator was disengaged, the drive tube was removed and the wick drain was threaded through a second section of drill pipe. This section of drill pipe was threaded to the first section, as illustrated in Figure 3-47 and the driving was resumed. This process was repeated until the drill pipe had been driven to the desired depth or until the pipe could be advanced no further. At this point the drive tube was removed from the rear of the drill pipe and replaced with a pulling-head as illustrated in Figure 3-48. A cable was attached to the pulling head and the drill pipe was extracted from the slope using the winch of a bulldozer as illustrated in Figure 3-49.

Theoretically, the drain was supposed to remain anchored in the slope by the sacrificial drive point when drill pipe was extracted from the slope. However, when the drill pipe was removed the drain came out together with the drill pipe because it either pulled loose from the anchor or it got stuck inside the pipe broke at some location inside the drill pipe. As a result, the drain installation had to be refined so that the drains would stay inside the slope. Fortunately, after the drill pipes were pulled out of the slope, the

holes remained straight and smooth and the soil around them did not collapse into the hole. After a few trials it was discovered that a drain could be inserted to the hole produced by the drill rod by hand when it was attached to a fiberglass rod that was the same length as the depth of the hole. With the first successful drain insertion in this manner, the remaining drains were inserted into the slope by hand and not threaded through the drill rod. This increased the installation rate substantially. When the drain installation was complete, a short section of 3 inch PVC pipe was placed over each drain end as illustrated in Figure 3-50. These pipes were used to seal the end of the drain into the slope and direct any flow from the drain to the collection manifold rather than allowing the drainage to escape to the face of the slope.. Each drain outlet was connected to the manifold system illustrated in Figure 3.56 so that the total discharge from all drains could be measured by the tipping bucket rain gauge located at the discharge end of the manifold.



Figure 3-43: Drill rod pre-loaded with wick drain.



Figure 3-44: The leading edge of wick drain attached to the driving point.





Figure 3-45: Wick drain extended through the driving tube.



Figure 3-46: Driving the drill rod into the slope using a paving breaker.



Figure 3-47: Threading drain through additional drill rod section.



Figure 3-48: The pulling-head attached to final section of drill rod.



Figure 3-49: Extracting section of drill rod with the bulldozer winch.



Figure 3-50: Drain end sealed in the slope with a PVC pipe drain termination.

A total of 18 drains with approximately 234 m (767 ft) of length were installed into the drained section of the slope on Dec 11 and Dec 12, 2006. Among these drains, 16 drains were installed perpendicularly into the slope to a maximum depth of 12 m (40 ft).

The remaining two drains were installed into the slope at an acute angle, resulting to a deeper penetration of 21 m (70 ft). Therefore, the maximum depth of the drains installed with a right angle to the slope was about 12m (40ft), which was about three-fourths of the desired length.

### 3.5.2 Monitoring equipment installation

#### Inclinometer casing, TDR cables, and moisture probes

The installation of the inclinometer casings, TDR cables, and moisture probes began after the wick drain installation was finished. Instrumentation was installed in both the drained section and the control section to evaluate the drain performance. The TDR cables, inclinometer casings and moisture probes were installed in two locations in both the control and drained sections of the slope. One location was in the top-half near the slope crest and the other was near the toe of the slope resulting in a total of four locations as illustrated in Fig 3-51.

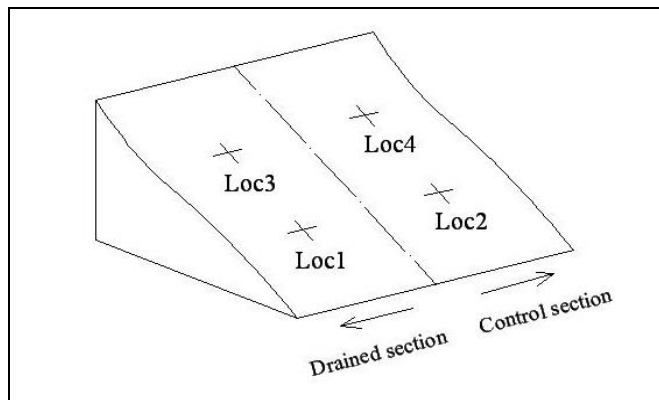


Figure 3-51: Schematic of the four instrumentation locations at the test site.

Three bore holes were drilled by an AHTD drill rig format each location. The first and the second holes were advanced with 200 mm (8 in) diameter drill to install the inclinometer casing and the moisture probes. The third hole was advanced with a 100 mm

(4 in) auger for the TDR cable installation. All boreholes were advanced well into the stable clay shale formation. Boreholes in the upper locations were advanced 20 feet from the ground surface while those at the lower locations were advanced 15 feet. Immediately after the boreholes were created at a location the inclinometer casing and the TDR cable were inserted to the bottom of the holes. The inclinometer casing was previously perforated with a series of small holes so that it could collect water from the slope and function as a monitoring well for determining the ground water location. Pea gravel was poured to fill the borehole to more than half of the depth of the inclinometer casing then a cement-bentonite grout mixture was poured into the remaining annular space to fill the hole. The grout mixture for the inclinometer casing consisted of a 47 lb. of Portland cement, 13 lb. of powdered bentonite, and 30 gallons of water. The TDR cable completely grouted with a grout mixture consisting of 94 lbs. of cement, 10 lbs. of powdered bentonite, and 30 gallons of water. The grout mixture for the inclinometer casing was designed to have a similar stiffness as the surrounding soil. The grout mixture for the TDR cable was intended to be stiffer than the surrounding soil so it would shear rather than deform if the earth moved. The TDR mixture also had to be strong enough to deform the TDR cable. In the remaining 200 mm (8 in) diameter borehole, two or more moisture probes were lowered to desired depths, and the borehole was filled with native soil to replicate the insitu unit weight of the soil. The installation of the TDR cables, inclinometer casings, and moisture probes at the other locations were completed in the same manner as the first location. Figure 3-52 illustrates the partially completed

installation of the inclinometer casings and TDR cables.



Figure 3-52: Inclinometer casing and TDR cable boreholes filled with grout.

A total of four TDR cables, four inclinometer casings and 10 moisture probes were installed at the site. Half were installed in the drained section and half in the control sections. A schematic of the instrumentation layout is presented in Figure 3-53. It was decided to use two moisture probes at in the lower sections of the slope (Loc1 and Loc2). These probes were placed at depths of 5 ft and 12 ft from the ground surface. The probes are labeled as MP1 and MP2, respectively in the drained section and MP3 and MP4 in the control section. For the upper locations (Loc3 and Loc4) three moisture probes were placed at depths of 3 ft., 9 ft., and 19 ft. from the ground surface and marked as MP5, MP6, MP7 for the drained section and MP8, MP9, and MP10 for the control section.

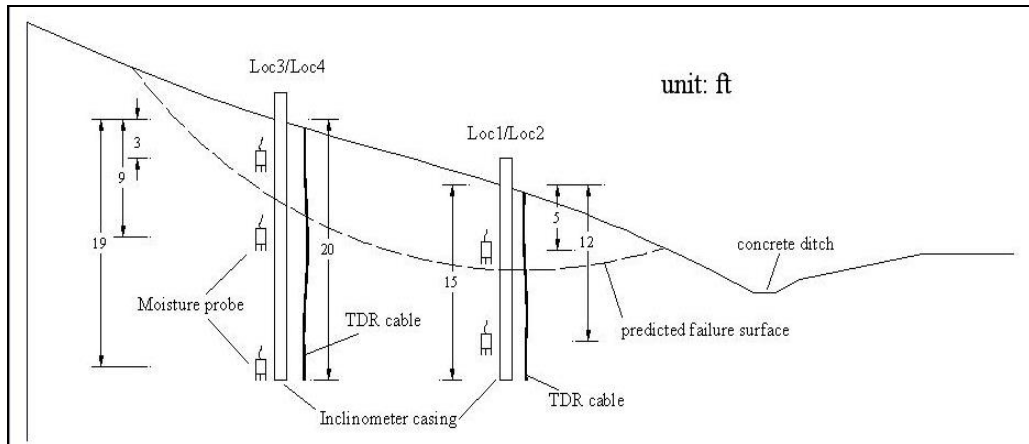


Figure 3-53: Side view of the slope with the installed monitoring equipment.

The weather-resistant enclosure containing the TDR system was installed at the crest of the slope by mounting it on two 4”x4” posts that were embedded in three feet of concrete. The solar panel, weather station and cellular modem antenna were mounted on steel pipes attached to the enclosure mounting posts. The completed equipment enclosure is illustrated in Figure 3-55.

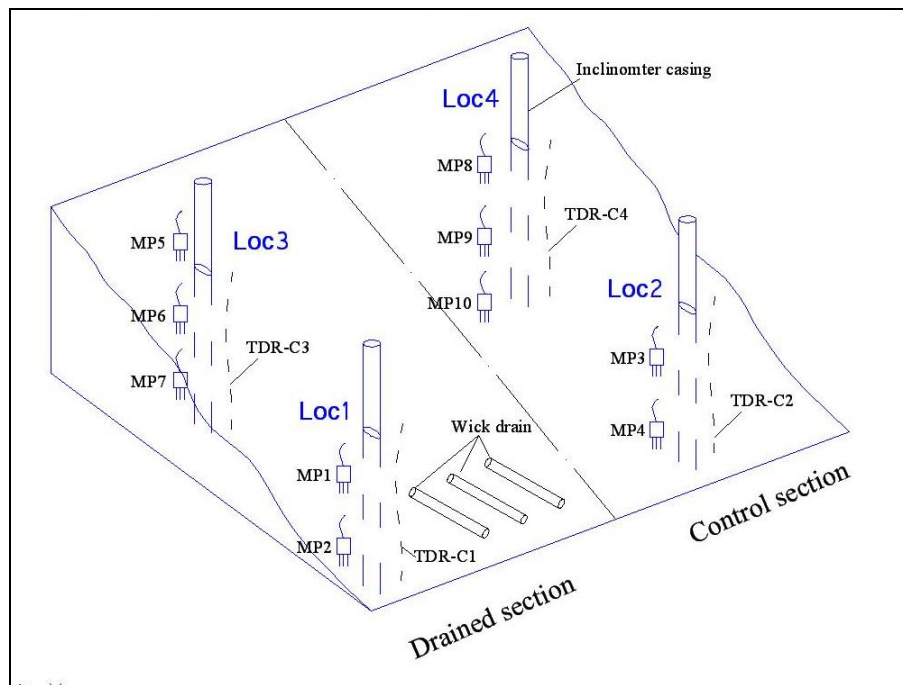


Figure 3-54: 3-D view of the monitoring equipment installed within the slope.

The drains were installed in early December when there was little if any precipitation and the near surface of the slope was frozen. As a result, there no flow was observed from any of the drains. Within two months a manifold system was created to connect each drain to a common discharge location. This system, which terminated at a tipping bucket rain gauge to measure discharge, is illustrated in Figure 3-56.

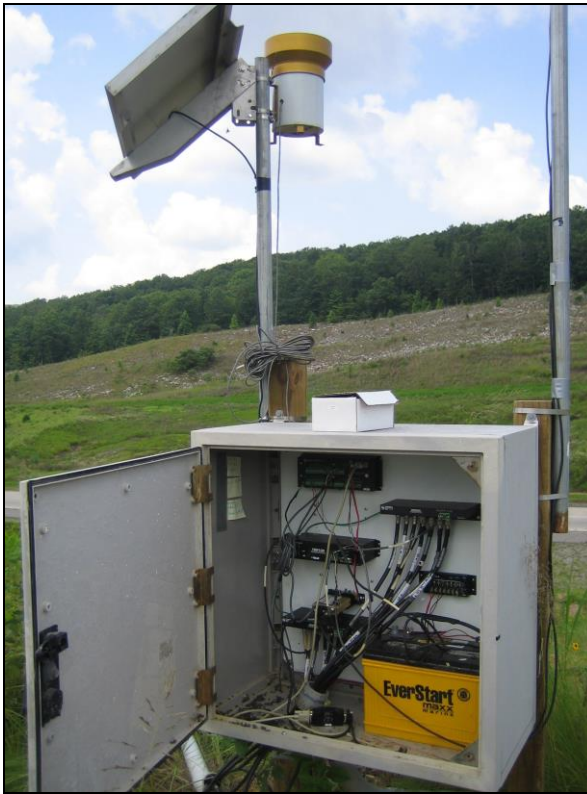


Figure 3-55: The protective enclosure housing the Data acquisition system, telecommunication system, and storage battery.





Figure 3-56: Completed slope monitoring and drainage collection system.

### 3.4.3 Monitoring schedule

When measurements from the TDR100, the thermocouple, and rain gauges were made, these data were then stored inside the memory of the datalogger CR10X, with a storage capacity was 2-megabites. With a large number of data recorded from all of the above devices, the memory capacity of the datalogger could hold them within about two weeks without any overwriting. Thus, the data must be collected no longer than two weeks; otherwise some data will be lost due to overwriting. However, with the help of the cellular modem, the data could be transferred remotely from the site to a PC. Therefore, the data retrieving from the datalogger were made randomly within two weeks.

However, since the inclinometer measurements must be made at the site and the piezometers do not have a remote connection to a computer, their readings must be recorded at the site. Initially, it was decided to collect the data from the piezometers and to make an inclinometer measurement every week so that such a small movement of the

slope could be detected. However, after two months of monitoring, the changes in slope movement were nearly the same. Thus, the inclinometer measurements and data collection from the piezometers were conducted every two weeks later in the study.

## Chapter 4

### RESULTS AND DISCUSSION

#### 4.1 Introduction to Research Results and Data Analysis

After the installation was completed, the drain performance was monitored for approximately seven months, from February to September 2007. The evaluation of the drain performance was based on the results of the data recorded from the measuring devices. The equipment, as described in detail in Chapter 3, included the inclinometer and TDR cables for slope movement monitoring, moisture probes for monitoring the changes in moisture content, piezometers for ground water table (GWT) monitoring, and rain gauges for in situ daily precipitation and flow capacity monitoring. When the data recorded from these measuring devices were collected, they were processed and analyzed to evaluate the performance and effectiveness of the drain system in slope stabilization. The data analysis included the two following parts:

- 1) *Field result analysis.* In this part, the data recorded from the inclinometer, moisture probes, TDR cables, piezometers, and rain gauges were analyzed and the results were performed in many graphic plots, which were made by Microsoft<sup>®</sup> Excel as well as DigiPro<sup>®</sup> and HOBOWare<sup>®</sup> software. These plots will help to compare the differences in slope movement, changes in moisture content, and GWT between the drained section and the control section.
- 2) *Parametric analysis.* The optimum drain configurations in clayey soil including drain length and drain spacing were determined through this

analysis using Plaxflow software. The analysis was also applied to other types of soil with different values of hydraulic conductivity so that the optimum spacing grid of the drain in these soils could also be determined.

Additionally, a cost analysis was also performed to evaluate the cost-effectiveness of this horizontal drainage method. The result of this analysis was performed in total cost per foot of drain installed, and it was compared to the cost of the conventional horizontal drainage method using PVC pipes to determine if it was a cost-effectiveness remediation for slope failure.

## **4.2 Field Results**

There were four locations at the slope site where the measuring devices were installed. Referred to Figure 3-51 in chapter 3, Loc1 and Loc3 are the two positions in the drained section, in which Loc1 was near the slope toe and Loc3 was in the upper part near the crest of the slope. Similarly, Loc2 and Loc4 were in the lower and upper regions of the slope in the control section corresponding to the same levels of Loc1 and Loc3. The results recorded from these measuring devices were analyzed and then performed individually from Location 1 to Location 4 for the data comparison between the drained section and the control section.

### **4.2.1 Slope Movement Monitoring**

The slope movement was monitored by both the inclinometer and the TDR cables. This section presents the results in chronological sequence of the inclinometer plots and TRD cable plots during the time of the experiment.

#### **Inclinometer Plots**

The readings from the inclinometer measurement were processed using the DigiPro<sup>®</sup> software to perform the slope movement at these four locations through many cumulative and incremental displacement plots. As defined in chapter 3, the *Incremental Displacement* is the change in lateral increment of subsequence readings at each interval relative to the baseline reading while the *Cumulative Displacement* is the overall change in lateral displacement of all readings over the length of the casing. The *Cumulative Displacement* plots are usually used by many researchers to perform the overall movement of the slope during the monitoring time while the *Incremental Displacement* plots are very useful to identify the location of the shear zone along the casings, which cannot be done by the *Cumulative Displacement* plots. Therefore, both of these two plotting types were used in this section to display the overall movement of the slope and clearly characterize the development of the shear zone at all locations during the experiment time.

The inclinometer readings were made at every 1 foot interval from the bottom up to the head of the inclinometer casings. Initially, the measurements were made weekly; however, the results showed that there were no significant differences between the readings in a short one-week period at the beginning time of the experiment. Thus, it was decided to make a measurement every two weeks in the later times.

The data collection of the inclinometer measurements was continuously conducted from the beginning of March to the end of June 2007. The last readings were made on June 21<sup>st</sup>, when the measurements at the next time could not be done due to the casing bending. At this time the slope moved a significant distance, resulting to a large bending of the casings. As a result, the inclinometer probe could not be lowered through

the deformed position in the casings to make measurements. Any attempt trying to drop the probe through that position would cause damages to the body of the probe or even lead to a lost of the inclinometer probe, which was relatively expensive. Therefore, the inclinometer surveys were decided to terminate after Jun 21<sup>st</sup>. Although the measurement was ended since then, the results from the inclinometer reading plots were very useful in the comparison of slope movement between the drained section and the control section.

Figure 4-1 and Figure 4-2 display the cumulative displacement of the slope at Loc1 and Loc2. At the beginning time small movements lightly occurred in the drained section, which are expressed by many small deviations staying close together at the value of 0.2 in displacement in Figure 4-1. There was almost no movement increasing in the drained section until the end of April. However, the movement of the slope in the control section was bigger than that in the drained section. A short time after the drain installation the movement in the control section was recorded at 0.6 in., as shown in Figure 4-2, and this value was still increasing over the time. At the end of April the movement at the toe of the slope in the control section was approximately 0.9 in, which was higher than the 0.3-in-movement measured at the slope toe in the drained section. The movements of the slope measured in both the drained section and the control sections at this time were very little; therefore the effectiveness of the drains during this time was insignificant.

However, the difference in slope movement between the drained section and the control section became more remarkable and the effectiveness of the wick drains was most characterized at later time, when many rainfalls were recorded frequently. During the summer, from May to September, many high intensity rainfalls often occurred at the

site, bringing a large amount of water into the slope. This water was the cause of an increase in pore water pressure built up within the slope, resulting to a loss of soil strength and a large displacement at 3.2 in. in the control section, as illustrated in Figure 4-2. As no drainage was applied in the control section, the water inside this area was still remained and the control section continued moving. In contrast, the largest movement measured in the drained section was about 2.2 in, which was less than that of the control section. The smaller movements in the drained section were due to the effect of the wick drains in removing the water out of this section. When the water was drained out, the strength of the soil increased proportionally. As a result, slope movement at the drained section was reduced and its stability was improved correspondingly as the drains were installed into the slope.

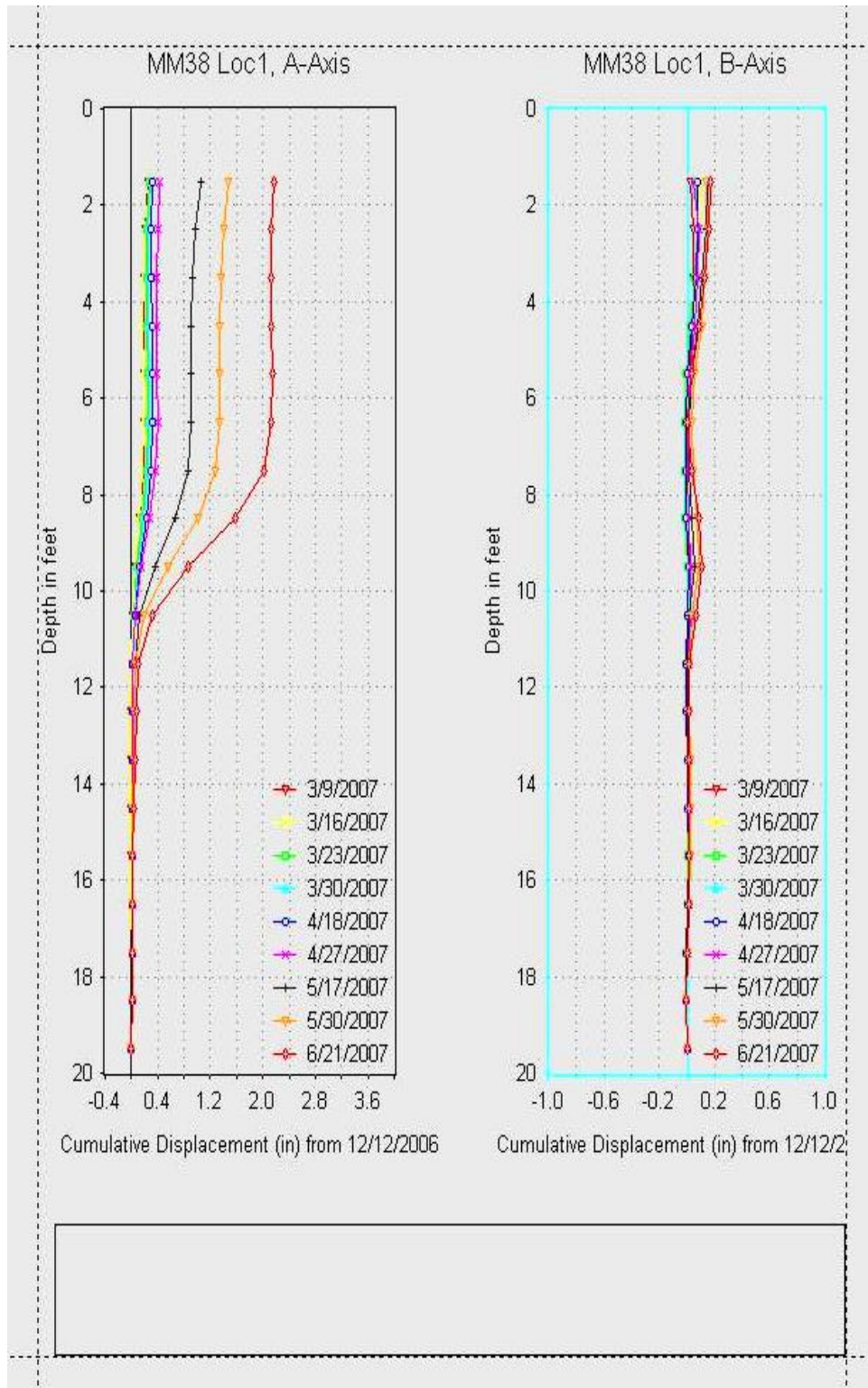


Figure 4-1: Cumulative displacement of Location 1.



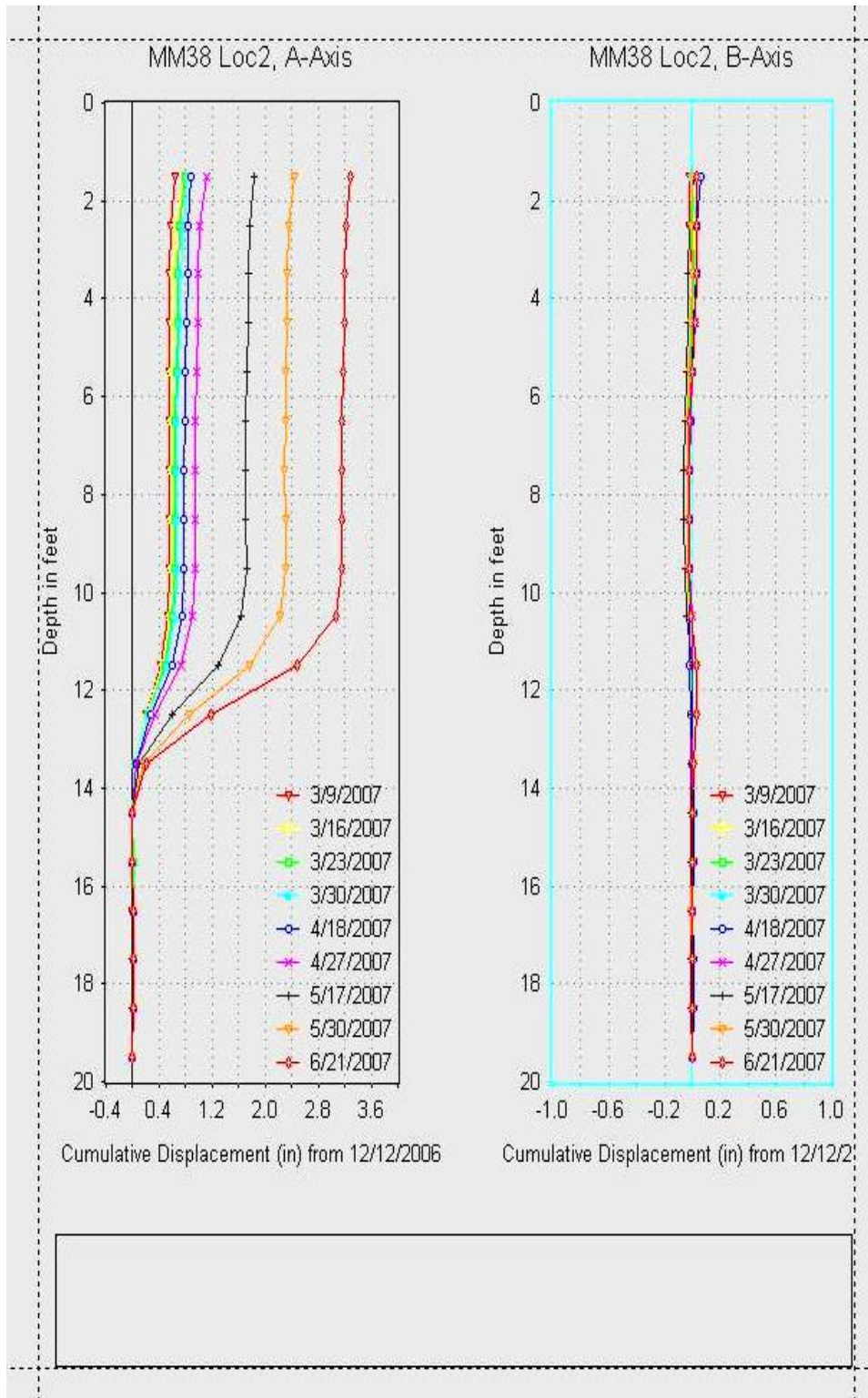


Figure 4-2: Cumulative displacement of Location 2.

The incremental displacement of the slope at Loc1 and Loc2 are respectively displayed in Figure 4-3 and Figure 4-4 below. As can be seen in these figures, the increment of the movement in the drained section was almost nothing at the beginning time of the experiment, and the biggest increment was recorded at 0.7 in. at the later times. However, the slope movement increment in the control section was recorded higher at the first time of the experiment, and the most increment value was measured approximately 1.3 in., which nearly doubled than that at the drained section. This was the result of the free-drainage condition in the control section, which caused a decrease of effective stress and soil strength. Therefore the slope kept moving with a higher magnitude at later times than the previous times. On the other side, the drain system helped to convey the water out of the drained section, making the movement in this slope section reduced.

Figure 4-3 and Figure 4-4 were also very useful to locate the positions of the shear zones along the casings at Loc1 and Loc2. Here, the shear zones were the areas where the slip surface passed through the casings and sheared them, or bended them. As demonstrated in these figures, the shear zones at Loc1 developed at the middle of the casing, about 9 ft below the ground surface, while it was seen approximately 12 ft down from the head of the casing at Loc2. The *Incremental Displacement* plots were also useful to evaluate the compatibility in slope movement monitoring between the results measured by the inclinometer method and the TDR cable method, which will be discussed later in this Chapter.

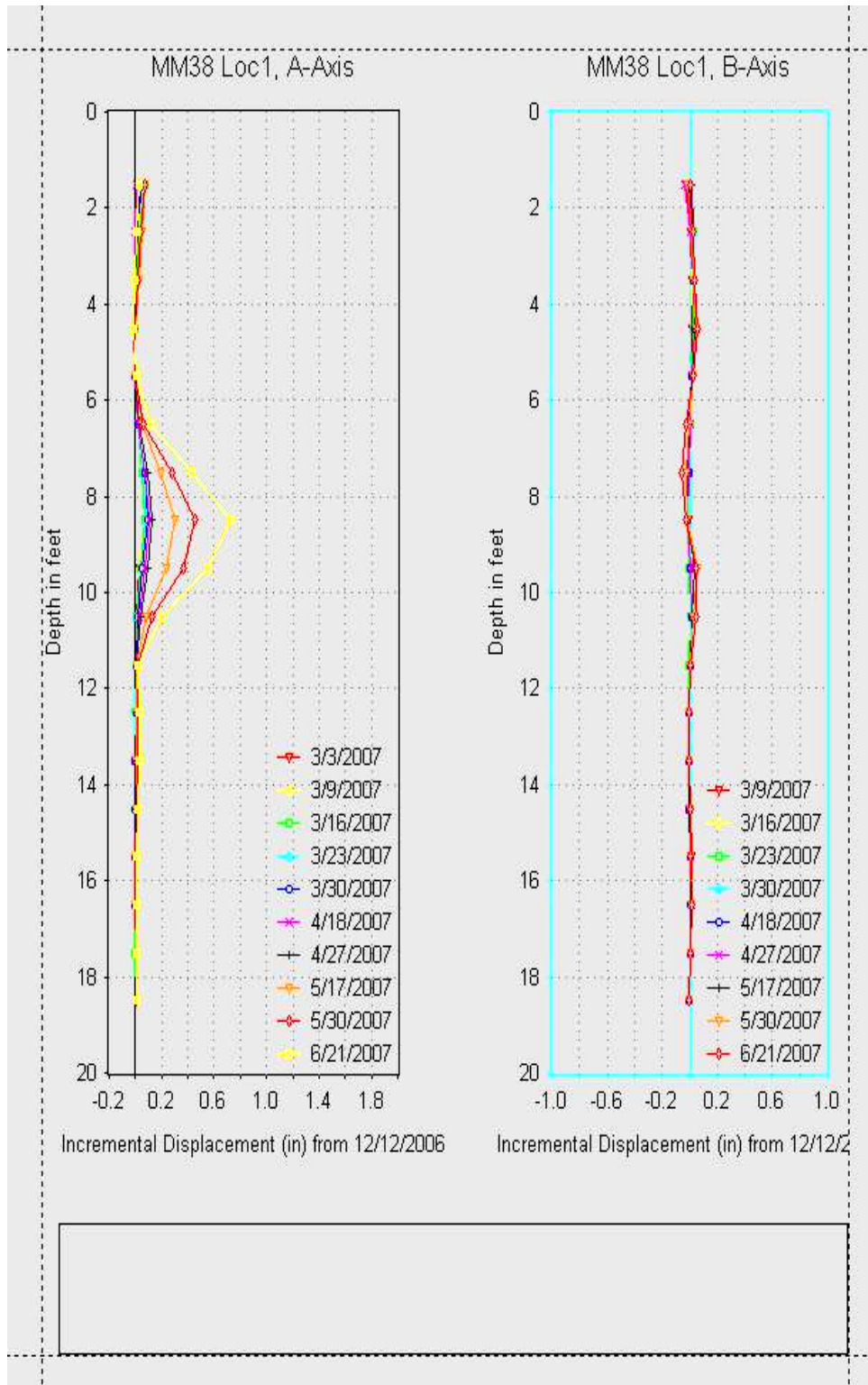


Figure 4-3: Incremental displacement of Location 1.

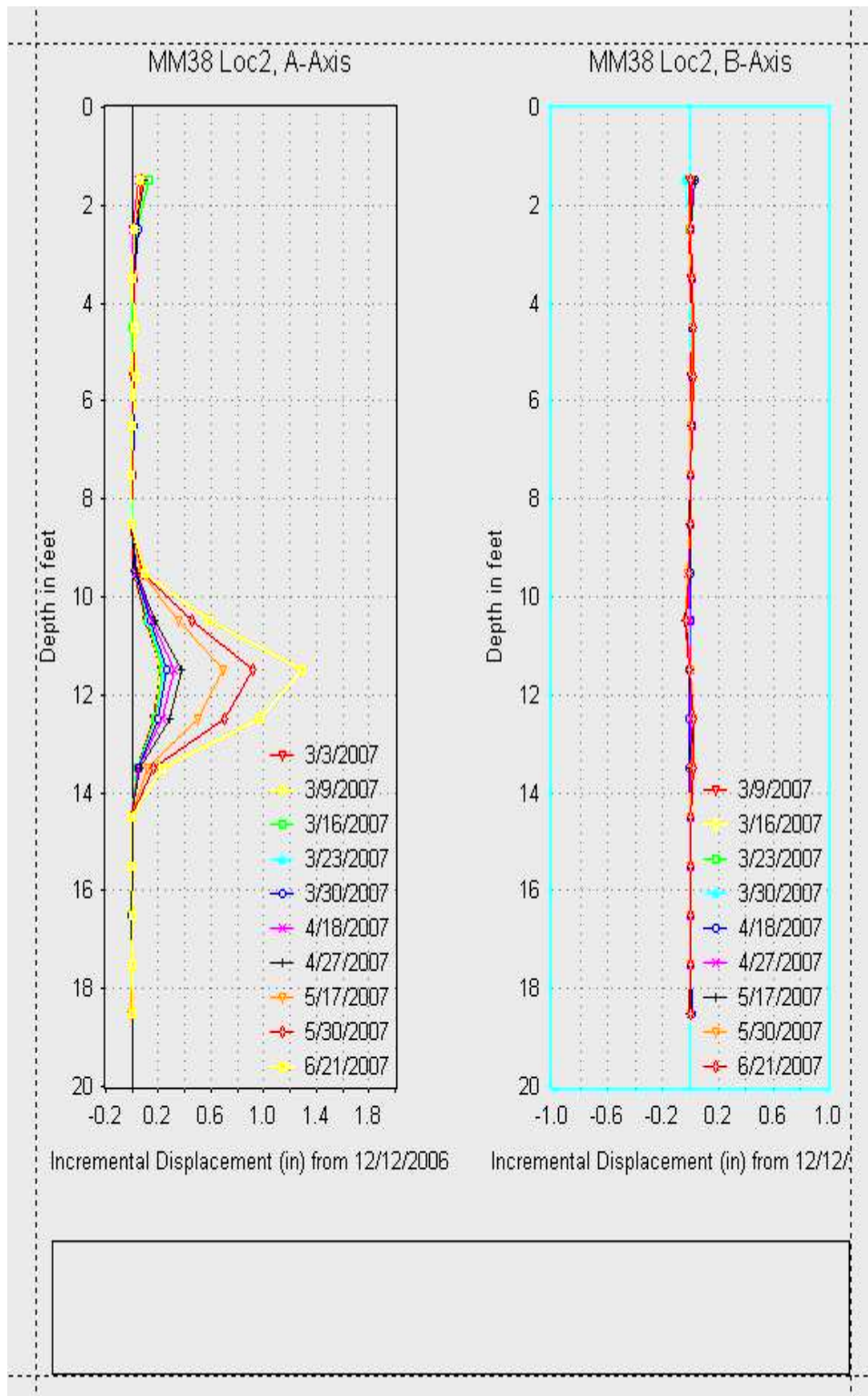


Figure 4-4: Incremental displacement of Location 2.

The cumulative displacement of Loc3 and Loc4 on upper part of the slope are displayed in Figure 4-5 and Figure 4-6 while their incremental displacement are respective expressed in Figure 4-7 Figure 4-8. Again, both the cumulative displacement and the incremental displacement measured at Loc3 were always smaller than those at Loc4, as shown in these figures. The highest movement recorded at Loc3 was only 1.8 in while the slope moved a distance at 2.4 in at Loc4 on the last day of the inclinometer survey. The *Incremental Displacement* plots also pointed out that the progression of the movement occurred faster in the control section than it did in the drained section, when comparing the 0.5-in highest increment at Loc3 to the highest increment of slope movement at Loc4, which was about 1.0 in. As in the lower part of the slope, the movement in the upper region of the slope in the drained section was reduced significantly compared to that in the control section at the later time of the experiment. Similarly this reduction in slope movement proved the functionality and effectiveness of the drains; as a result, more slope stability was gained with the presence of the drains inside the slope.

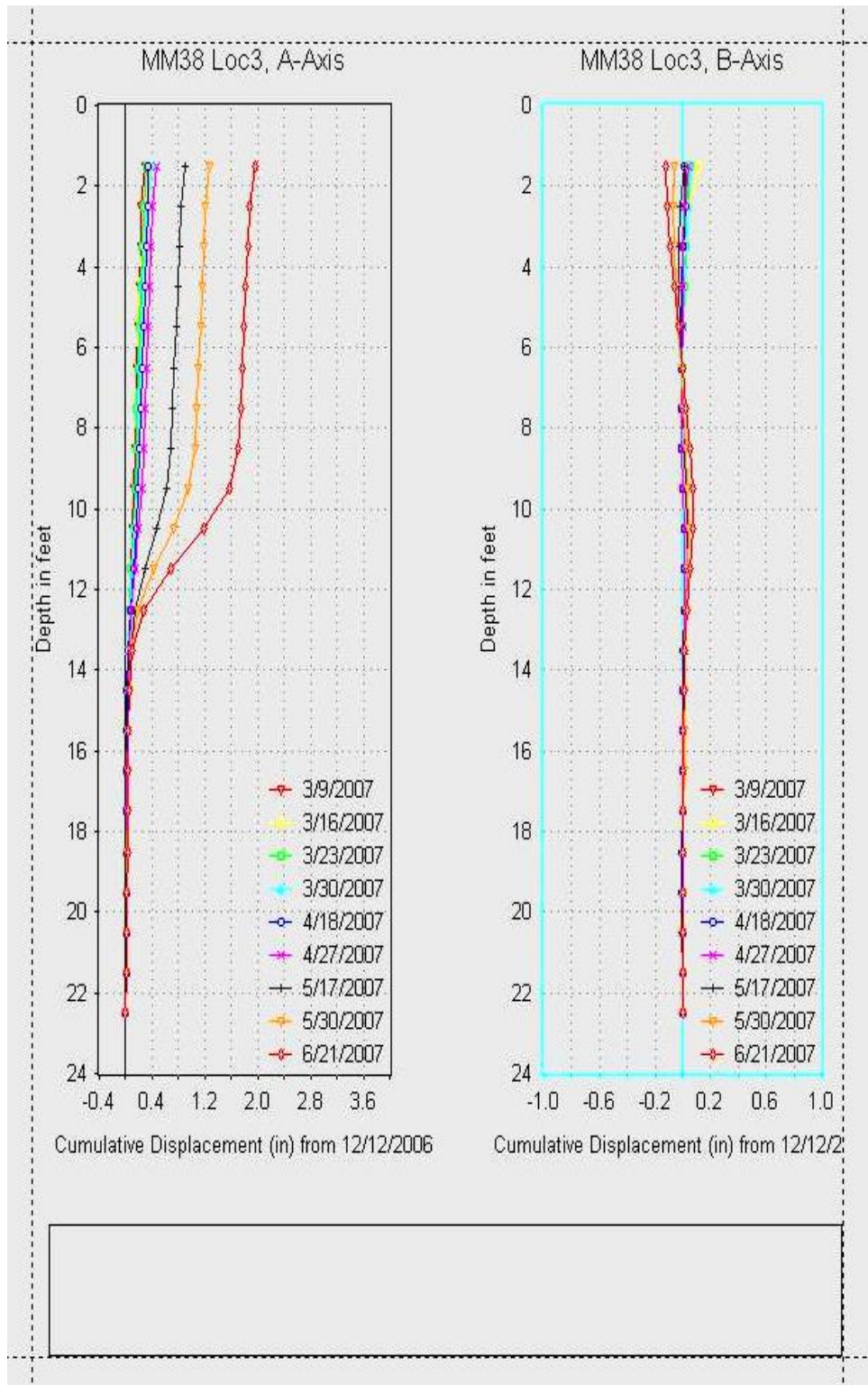


Figure 4-5: Cumulative displacement of Location 3.

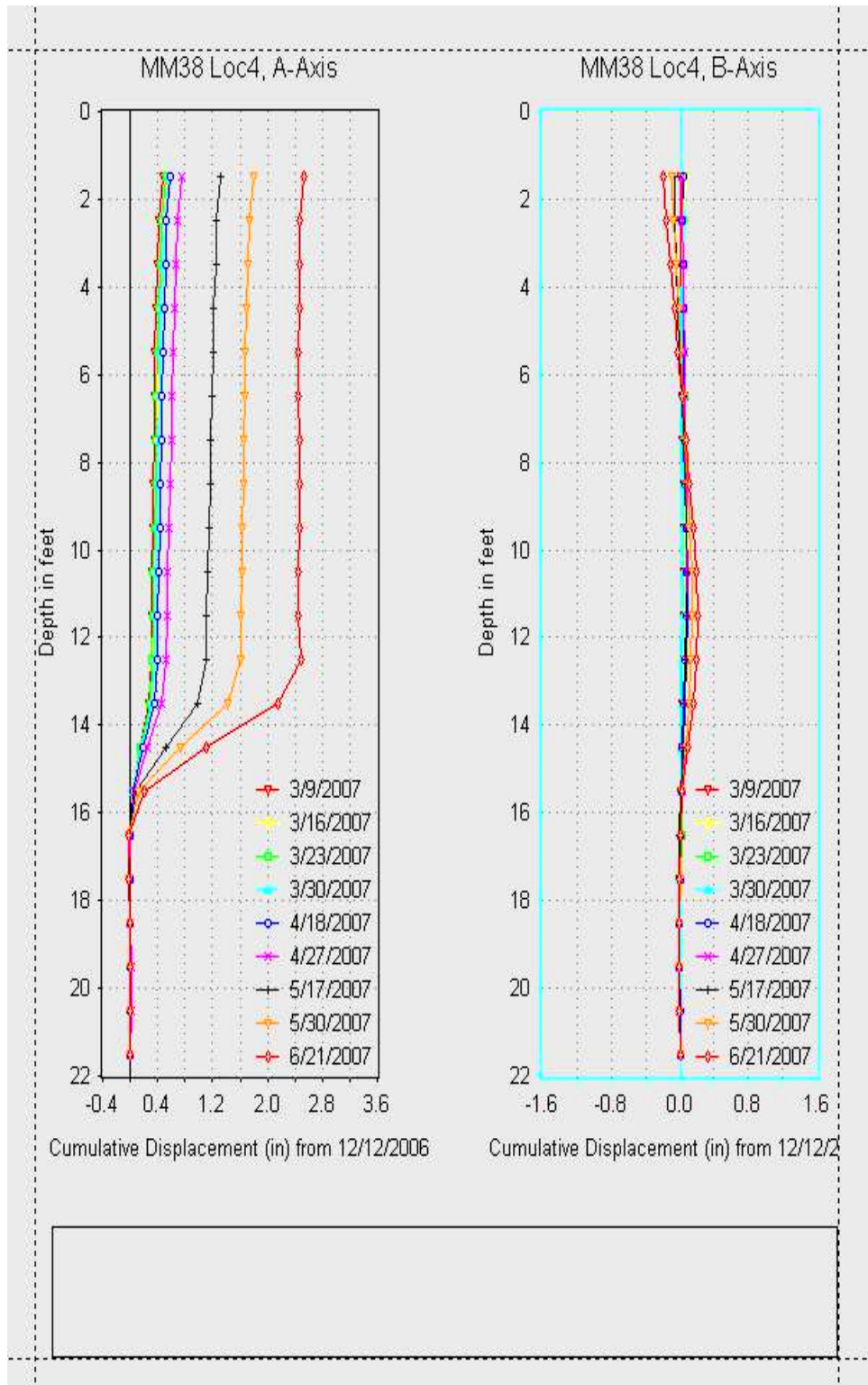


Figure 4-7: Cumulative displacement of Location 4.

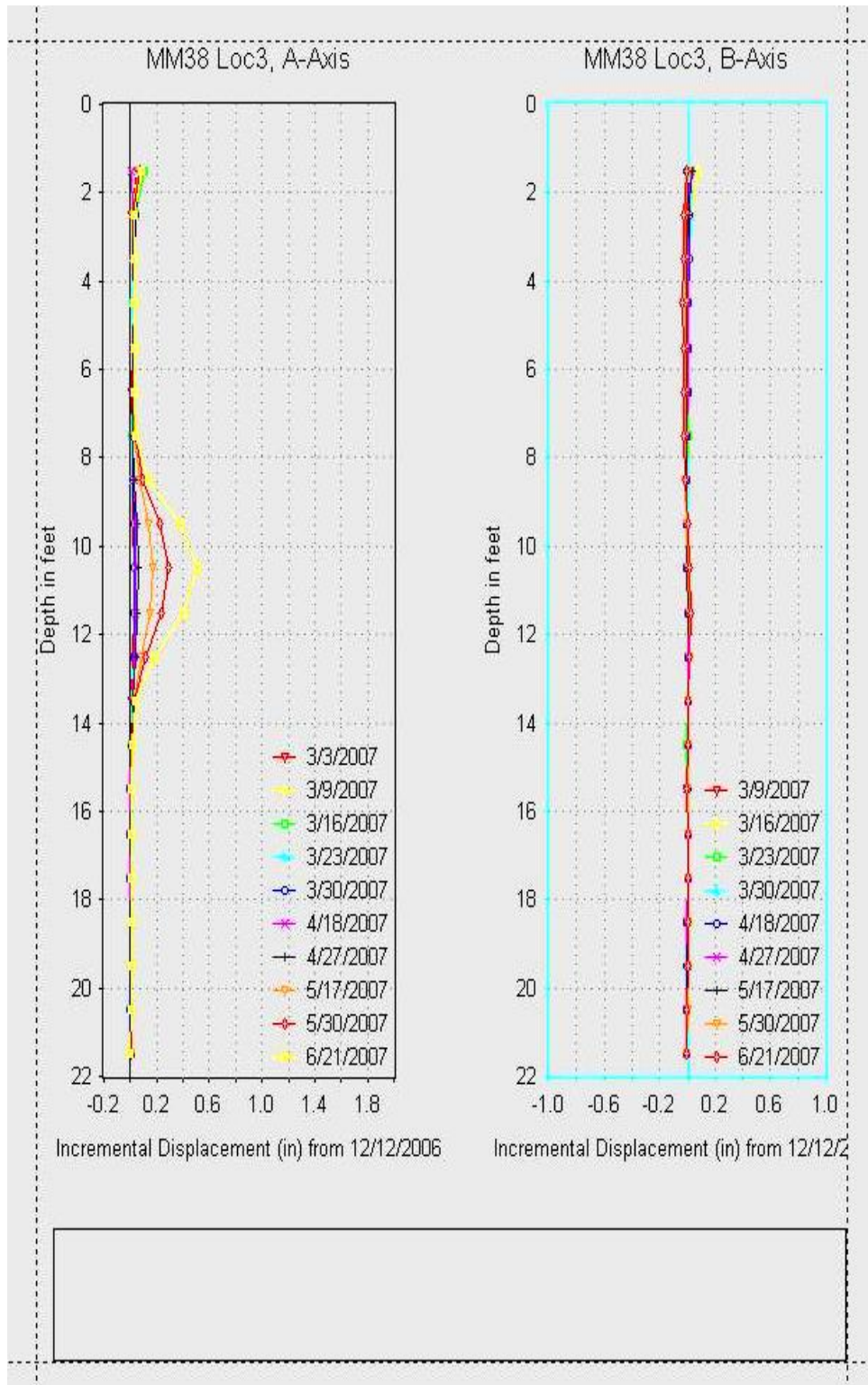


Figure 4-6: Incremental displacement of Location 3.



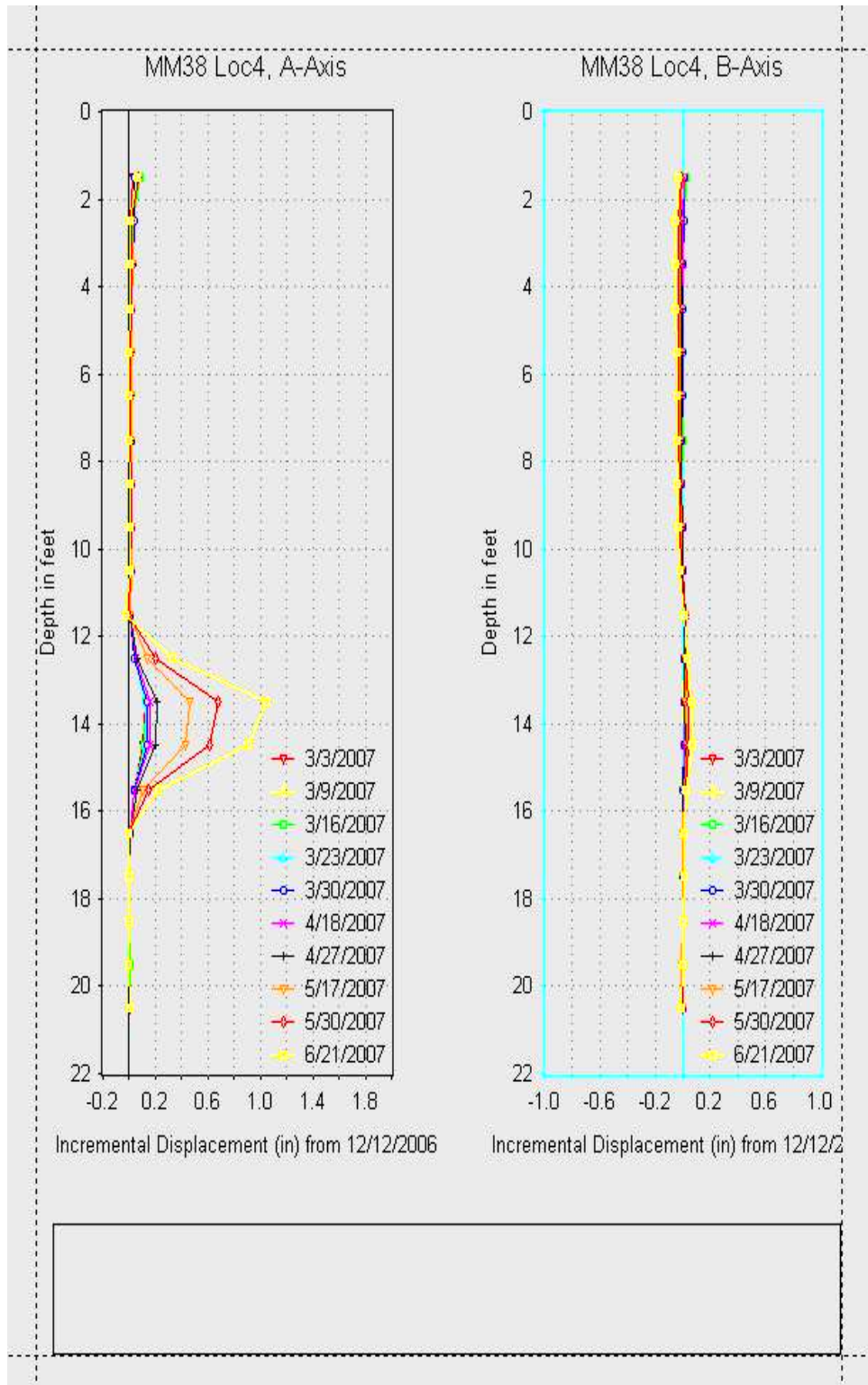


Figure 4-8: Incremental displacement of Location 4.

In order to obtain the overall movement occurring within the slope, the results of the slope displacement were plotted together in one chart for a better comparison. Figure 4-9 displays the increase of the movements measured by the inclinometer at four locations during the experiment. From Figure 4.9, it can be seen that the slope movement progressed in two different periods. Small movements occurred during the first stage of the experiment when the amount of free water within the slope was very little, and the largest movements were recorded during the summer when high intensity rainfalls occurred more frequently. This figure also shows that the movements of the slope in the drained section were always smaller than those in the control section, where no drains were installed. In the second stage of the experiment the movement in the control section the slope at Loc2 progressed very fast while the displacement of the slope in the drained section occurred at a lower rate. The remarkable difference in slope movement between the drained and the control sections clearly clarifies the effect of the wick drains in reducing slope movement. Since the inclinometer surveys were terminated at the end of June, no additional data were obtained for the comparison. However, the results were quite useful to characterize the effectiveness of the drains in reducing slope movement and increasing the stability of the slope. Through this movement profile higher movements in the control section are assumed to be encountered in the future.

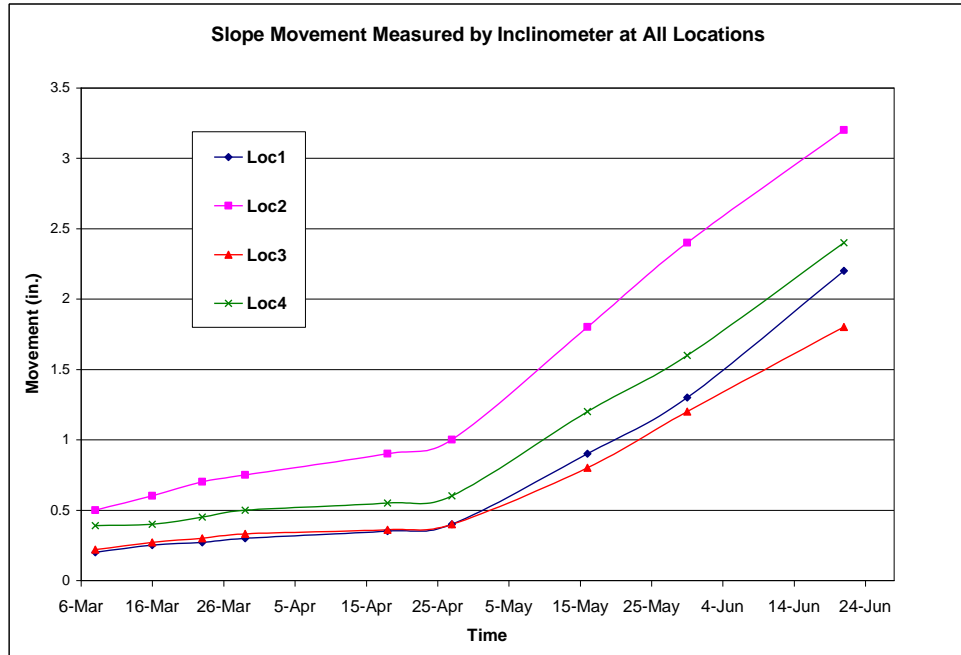


Figure 4-9: Slope movement measured at all locations by the inclinometer.

Since the slope moved such distance of 3.2 in. at Loc2, as measured by the inclinometer, a failure eventually occurred and a crack was found on the slope surface. This crack was observed to happen in the middle of June, after many large rainfalls occurred. The crack was seen on the upper part of the slope and above the inclinometer casings at Loc3 and Loc4, as illustrated in Figure 4-10. It progressed most in the right side of the slope, or in the control section, while a small portion of the crack developed in the drained section. Figure 4-11 and Figure 4-12 illustrate the progress of the crack and its termination in the drained section and in the control section, respectively.



Figure 4-10: Location of the crack on the slope surface.

This crack prolonged with an average width of 4 in. on the drained section while its width measured on the control section was about 6 - 8 in. Especially, a big opening was found on the slope surface as the crack progressed. This opening was on the control section, at the right side of the Loc4. The position of this fissure on the slope surface is specified in Figure 4-11 and its widest opening was measured approximately 14 in., as illustrated in Figure 4-13. With the information of the crack captured from Figure 4-10 to Figure 4-13, a layout of the failure was created in Figure 4-14 to illustrate the progression of the crack on the slope surface. From this figure, it can be seen that the failure mainly occurred on the control section. Although the slope actually failed in both sections, the crack progressed on the drained section might be the consequence of the development of the failure on the control section. The failure was hypothesized to occur on the control section first and it expanded onto the drained section as the crack became larger, resulting

to small slope movements in the drained section, as recorded by the inclinometer. Therefore, only the control section actually failed while the stability of the slope in the drained section was still satisfactorily maintained, which proved the effectiveness of the drain system in controlling slope stability.

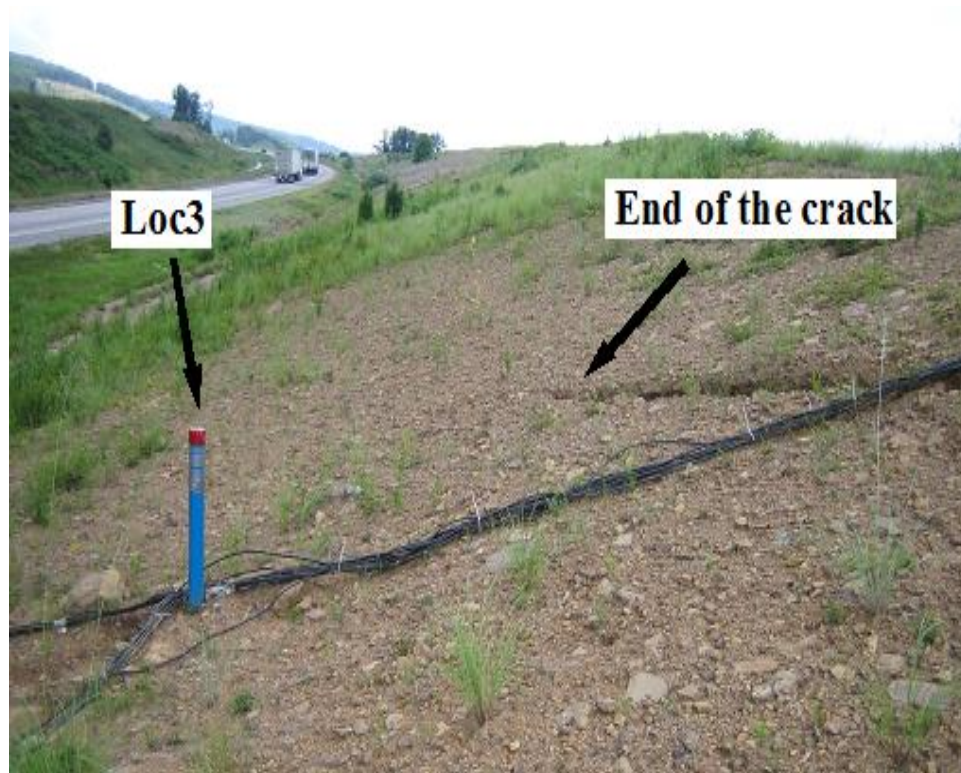


Figure 4-11: The progress of the crack and its termination on the drained section.



Figure 4-12: The progress of the crack and its termination on the drained section.



Figure 4-13: The width of the opening measured by a tape measurement.

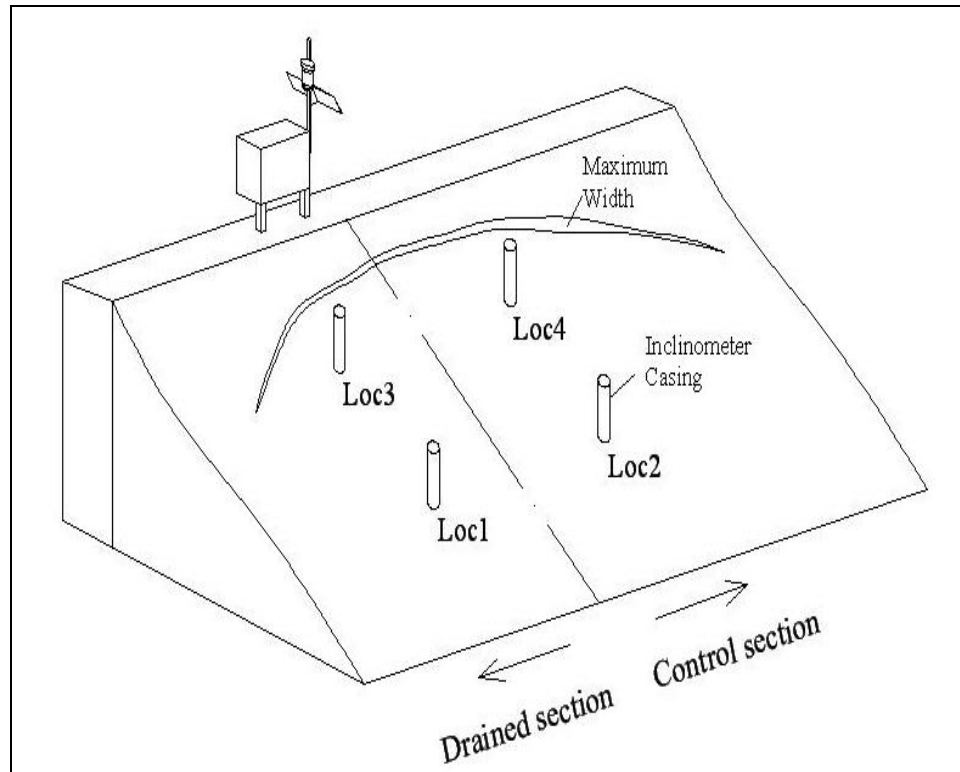


Figure 4-14: The lay out of the failure developed on the slope surface.

### TDR Cable Waveforms

In this study, the slope movement monitoring was also conducted using the TDR cable waveforms. One TDR cable was installed at each location, giving a total number of four cables used in the study. The waveforms were made by the TDR100 and they were collected by the datalogger CR10X. Then these waveforms were plotted in Microsoft® Excel worksheets to monitor the movement developed within the slope during the experiment time.

Figure 4-15 to Figure 4-17 respectively display the waveforms of the TDR cable at Loc1 during the experiment, from February to September, when the experiment terminated. The waveform at the bottom of Figure 4-15 was recorded first when the experiment started, and it served as the baseline signature to compare with the subsequent waveforms collected at later times. By searching on the TDR cable signature, a

movement occurring within the slope was recognized by a deep spike along the waveform, as discussed in Chapter 3. The waveforms displayed in Figure 4-15, and the first waveforms in Figure 4-16 did not show any movement detected at Loc1 since no clearly identified spikes can be seen on these waveforms. The very tiny spikes occurring along these waveforms were actually the signal reflections of the cable when the cable was crimped by many rock fragments during the consolidation process of the soil within the slope, as explained in Chapter 3. This reflection resulted to a series of very small spikes along the TDR cable waveforms. Therefore these tiny spikes did not represent for the actual movement that was recorded by the TDR cables. It can be seen that from February to the middle of June, slope movement at Loc1 was still undetectable by the TDR cable waveforms although the slope moved a small distance at this location, as recorded by the inclinometer. However, there was a small fracture on the TDR waveform collected on Jun 21<sup>st</sup>. This fracture can be visually recognized at the middle of this waveform, indicating that a movement within the slope had been recorded by the TDR cable. At the same time the slope movement measured by the inclinometer was approximately 2.1 in, as shown in Figure 4-1. From that time, the slope movement at Loc1 progressed more over the time and it can be easily seen through the development of the spikes in the subsequent waveforms in Figure 4-16 and Figure 4-17. On these waveforms the spikes continued to expand deeper and deeper so that the slope movement at Loc1 can be clearly identified in the TDR cable signatures.



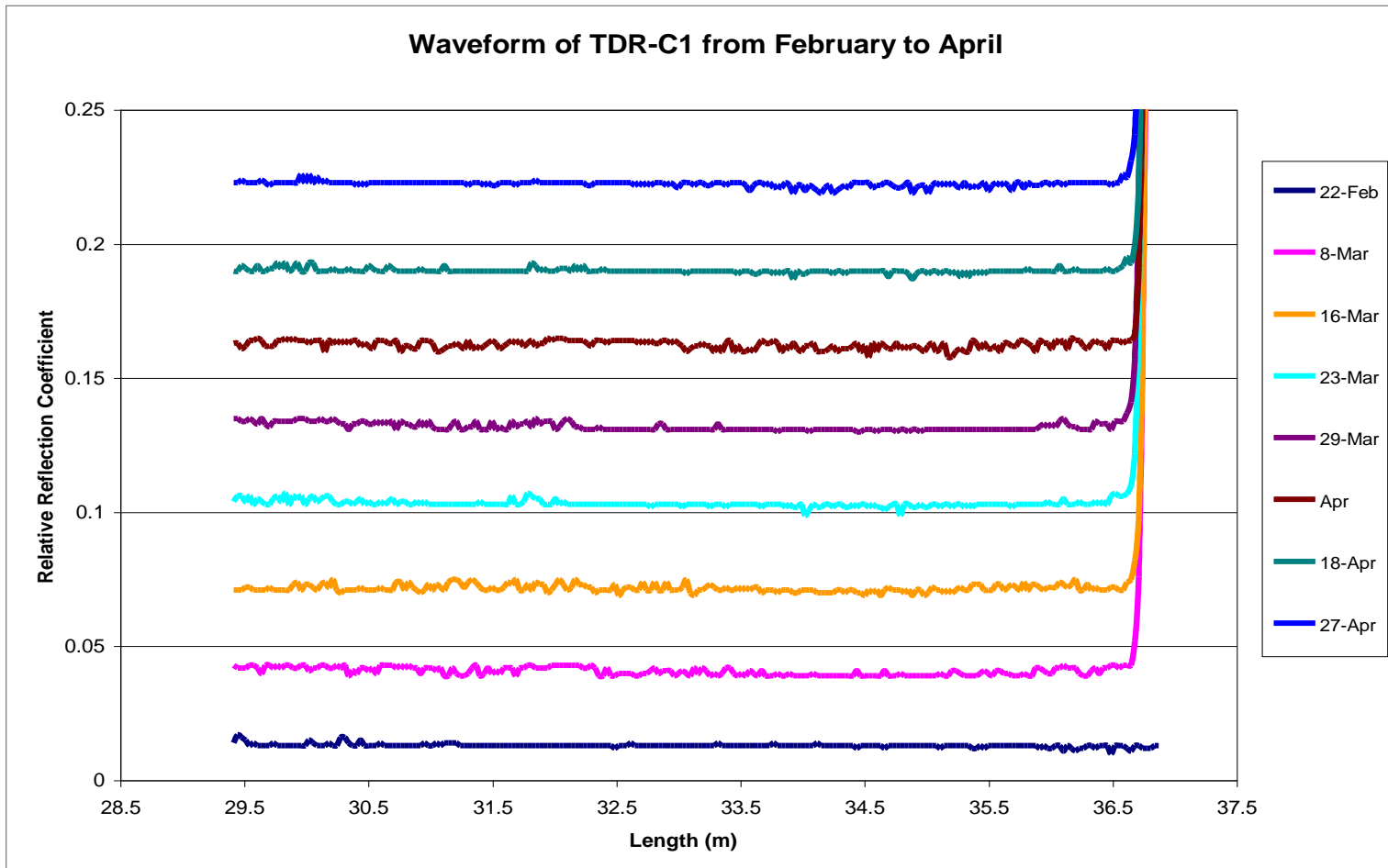


Figure 4-15: TDR cable waveforms at Location 1 from February to April.

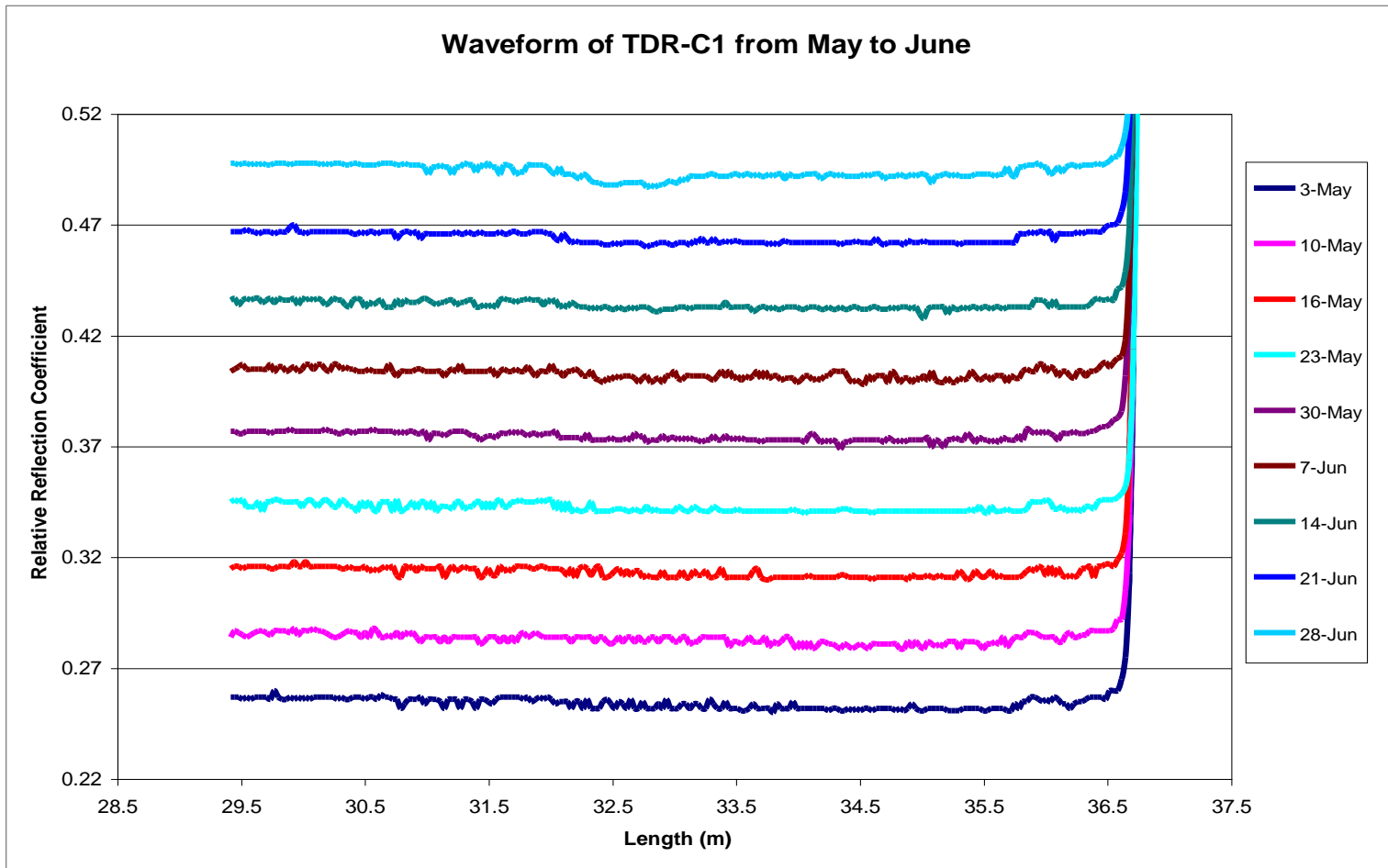


Figure 4-16: TDR cable waveforms at Location 1 from May to June.

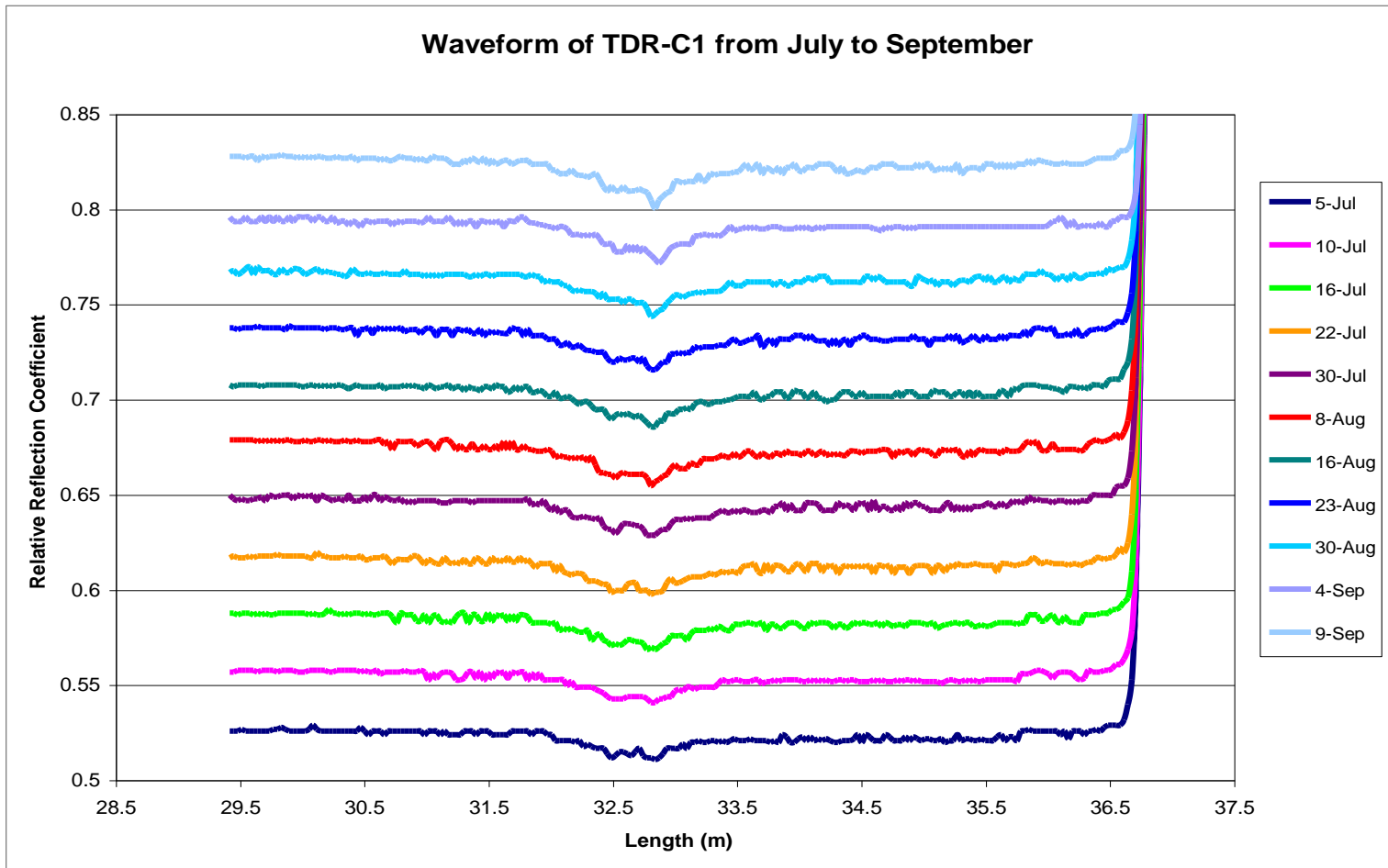


Figure 4-17: TDR cable waveforms at Location 1 from July to September.

From these figures above, it can be seen that the slope movement at Loc1 was detected at the middle of the waveform, and the position where the slip surface passed and sheared the TDR cable was located near the mark of 32.7 m on the waveform. It should be noticed that the length of the waveforms displayed in these figure above was the actual length of the section of the cable that was buried inside the slope. The distance from the starting point of these waveforms to the shear position was approximately 9 ft. By inspecting the location of the shear zone at Loc1 in Figure 4-3, it can be seen that the shear zone occurred at a distance of 8-9 ft. below the slope surface. The difference between these distances was insignificant when compared to the depth of the casing. Therefore, the results obtained from the TDR cable waveforms were compatible with the data recorded by the inclinometer measurement, and both of these methods can be used similarly to locate the position of the shear zone develop inside the slope.

The TDR cable waveforms at Loc2 collected during the experiment are displayed in Figure 4-18 to Figure 4-20. Again, there were no spikes found on the waveforms that clearly showed a movement occurring within the slope during the first time of the experiment, from February to April. The first movement detected at Loc2 was on May 30<sup>th</sup>, when the slope movement at this location experienced a distance of 2.4 in. as measured by the inclinometer.

Similarly, Figure 4-21 to 4-26 expressed the TDR cable waveforms at Loc3 and Loc4 collected by the TDR system during the experiment. As can be seen in these figures, the slope movements at Loc3 and Loc4 could be recognized by the TDR waveforms only after Jun 28<sup>th</sup> since no spikes that indicated slope movements were found on these cable before that time. At the same time, the movements measured by the

inclinometer were actually progressed a distance of 1.8 in at Loc3 and 2.4 in. at Loc4. From the results recorded by both the inclinometer method and TDR cable method, it can be seen that no movements were detectable by the TDR waveforms if their results from the inclinometer measurement were less than 2 in. As a result, it was concluded that the TDR cable method could only be applicable to measure such failures whose movement progressed more than 2 in. while the inclinometer was more appropriate to measure smaller movements.

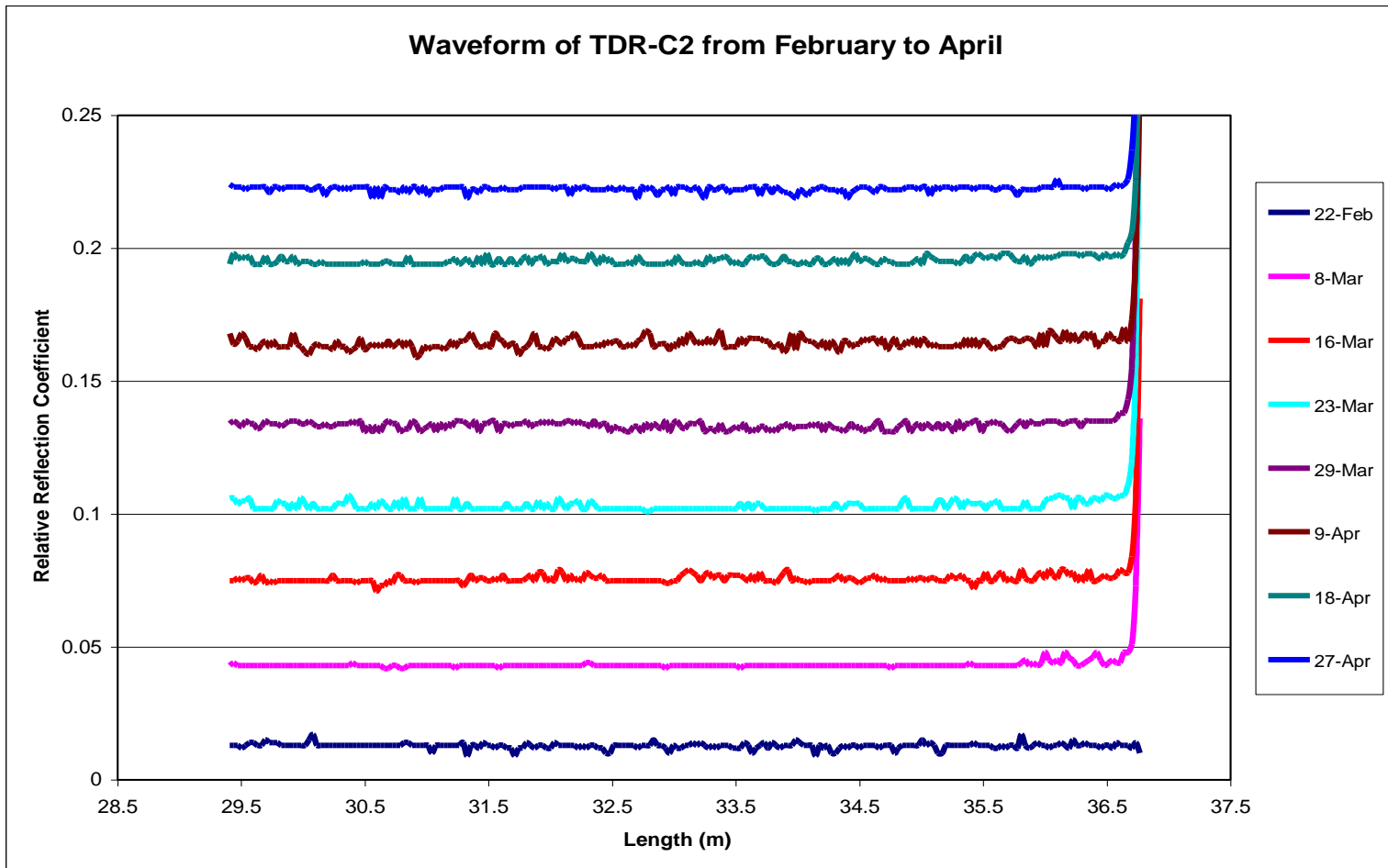


Figure 4-18: TDR cable waveforms at Location 2 from February to April.

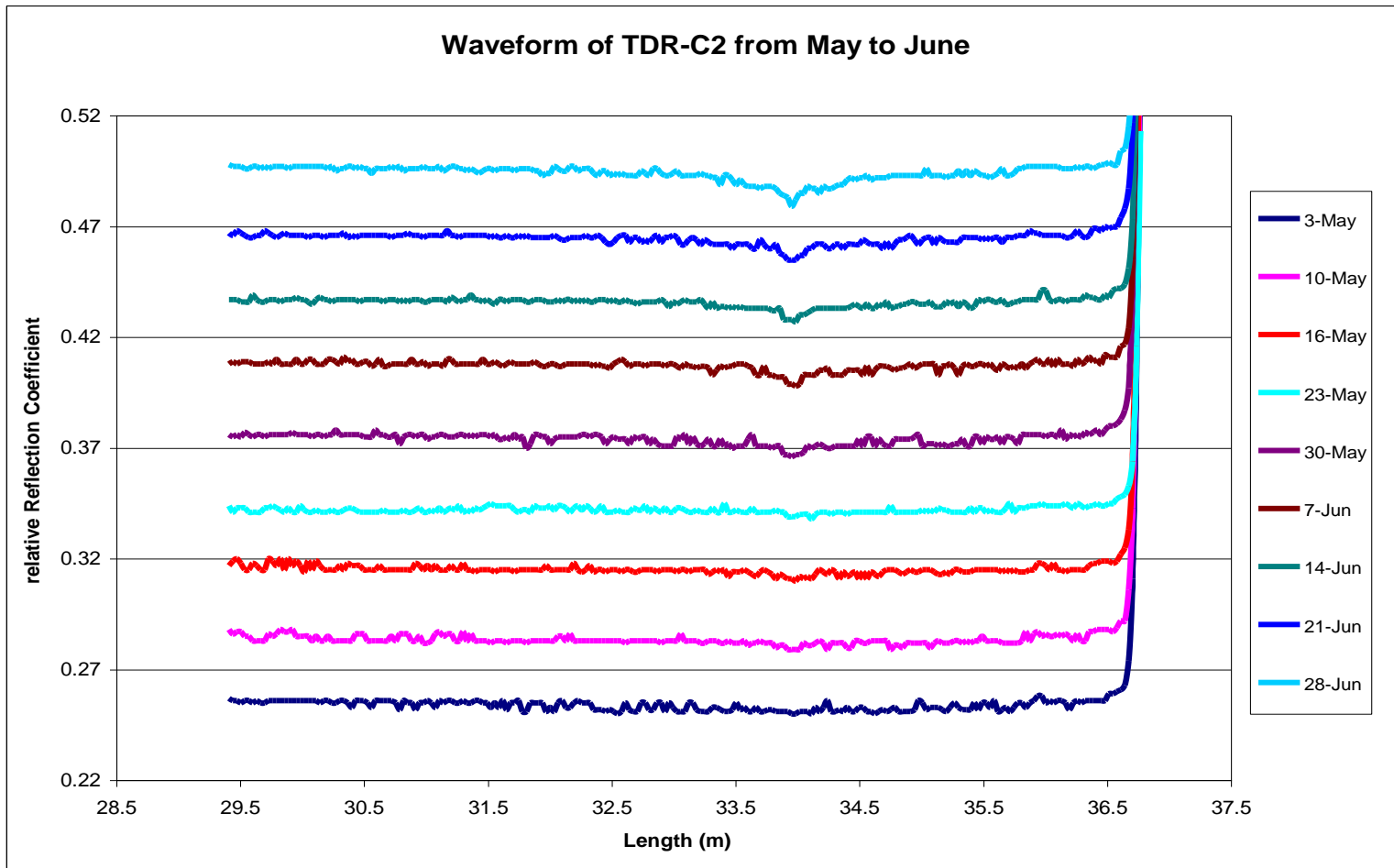


Figure 4-19: TDR cable waveforms at Location 2 from May to June.

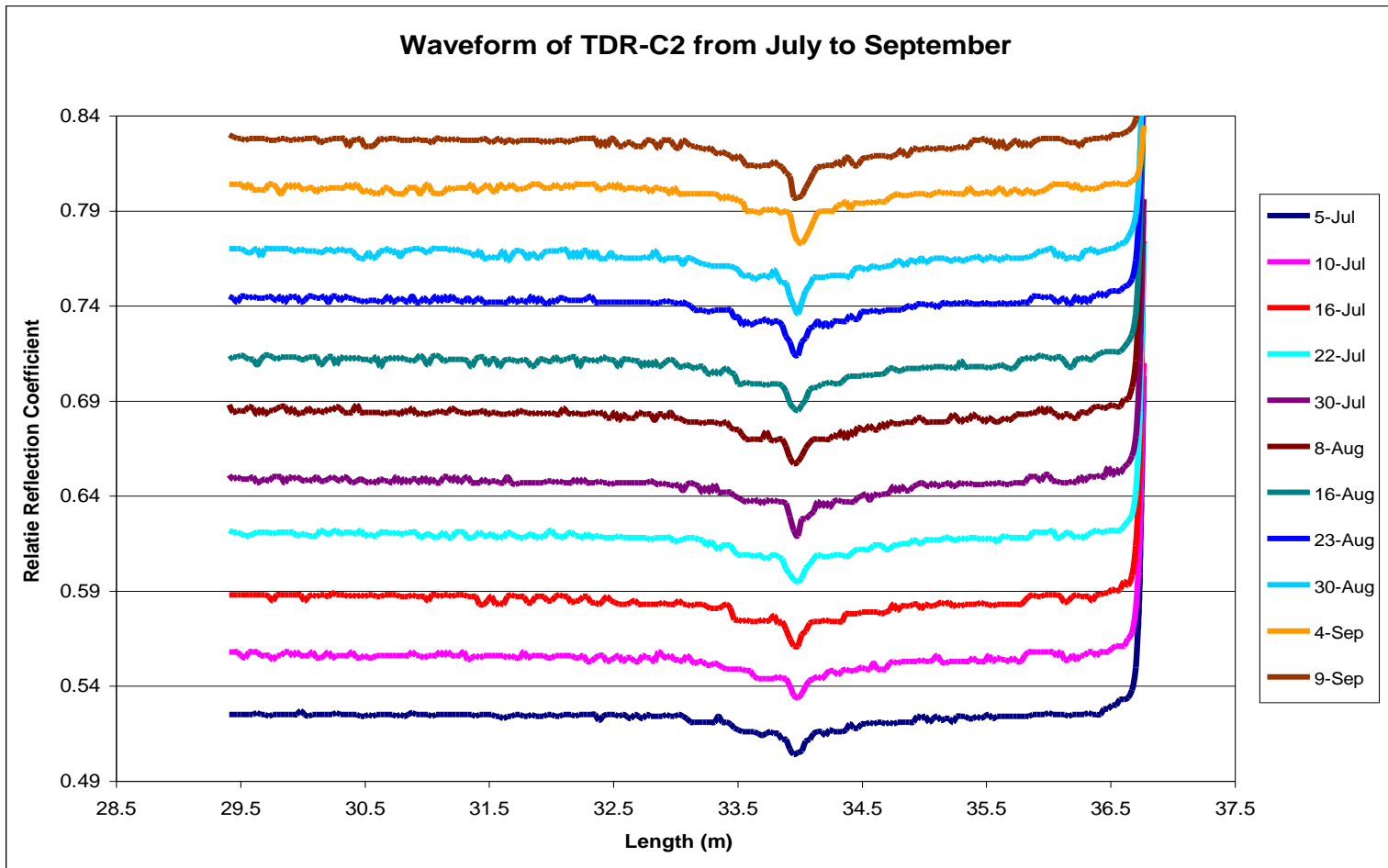


Figure 4-20: TDR cable waveforms at Location 2 from July to September.



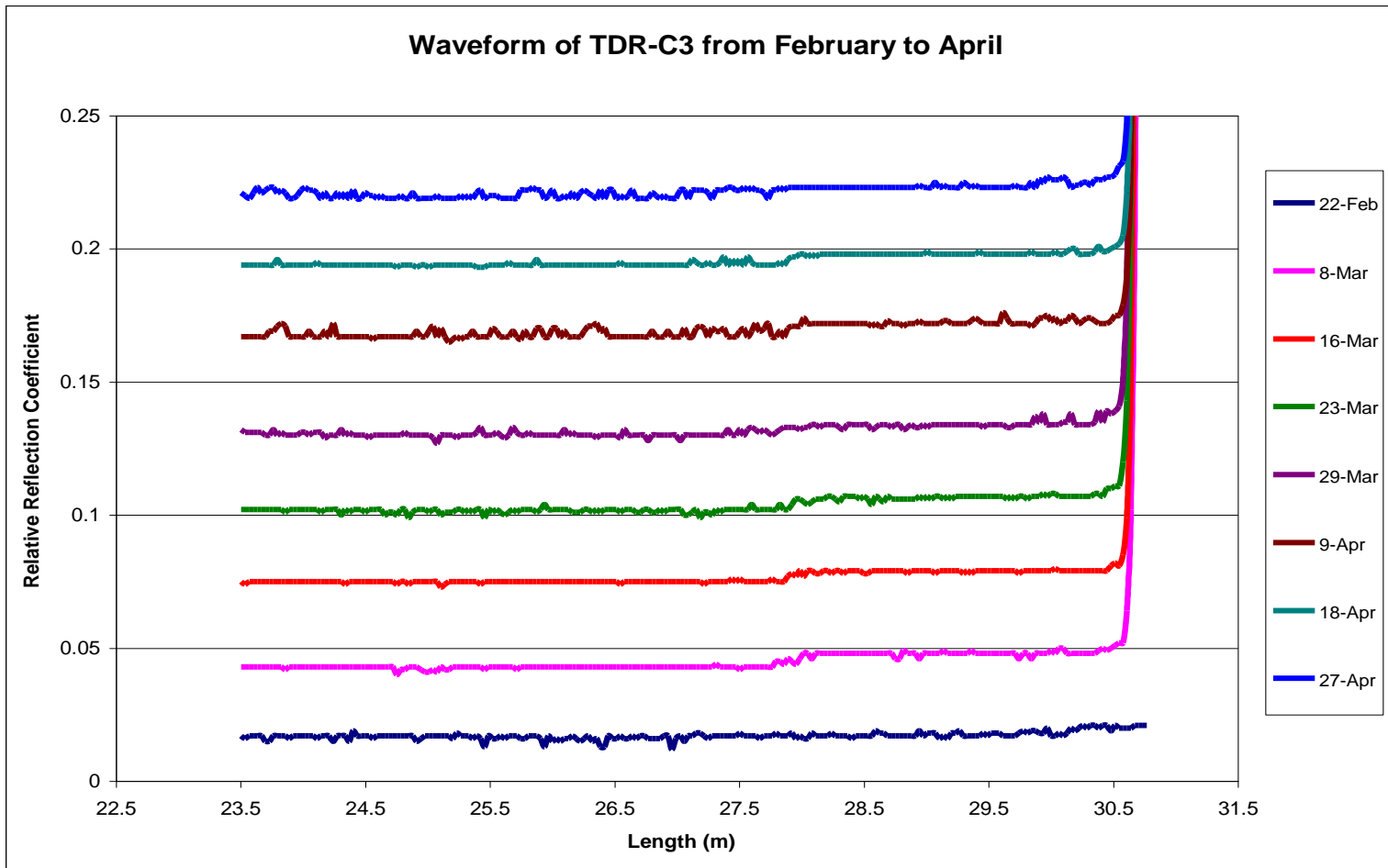


Figure 4-21: TDR cable waveforms at Location 3 from February to April.

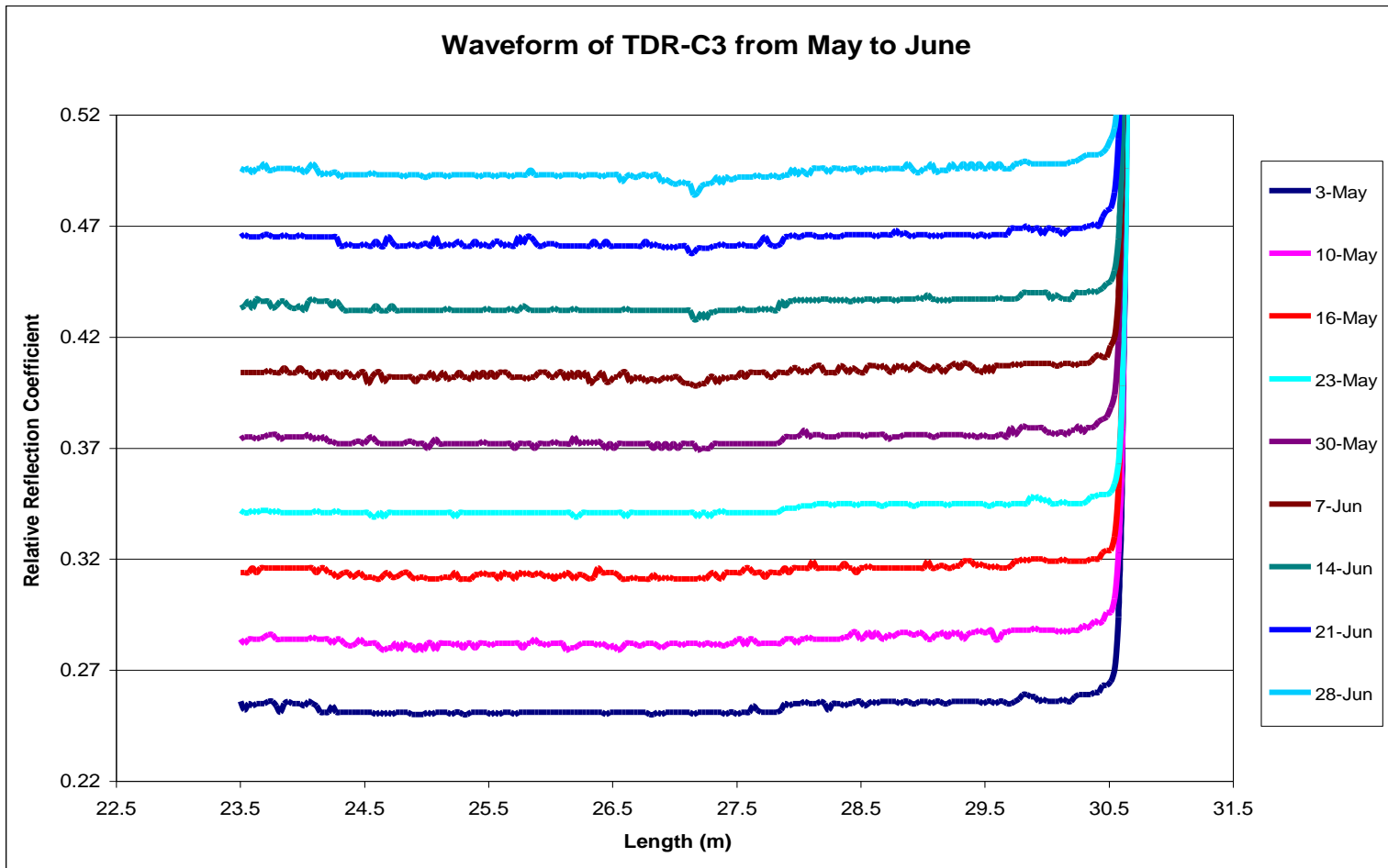


Figure 4-22: TDR cable waveforms at Location 2 from May to June.

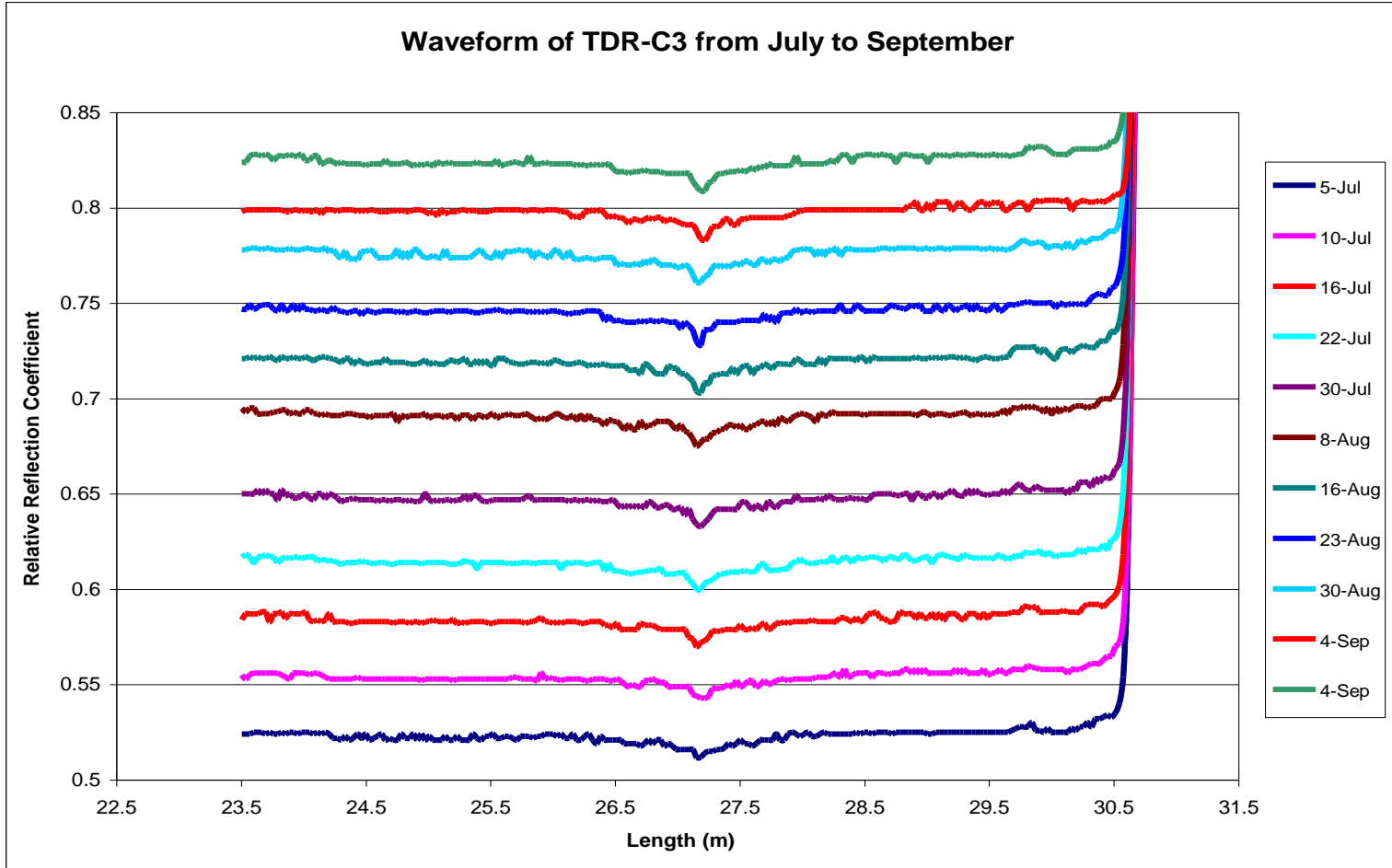


Figure 4-23: TDR cable waveforms at Location 3 July to September.

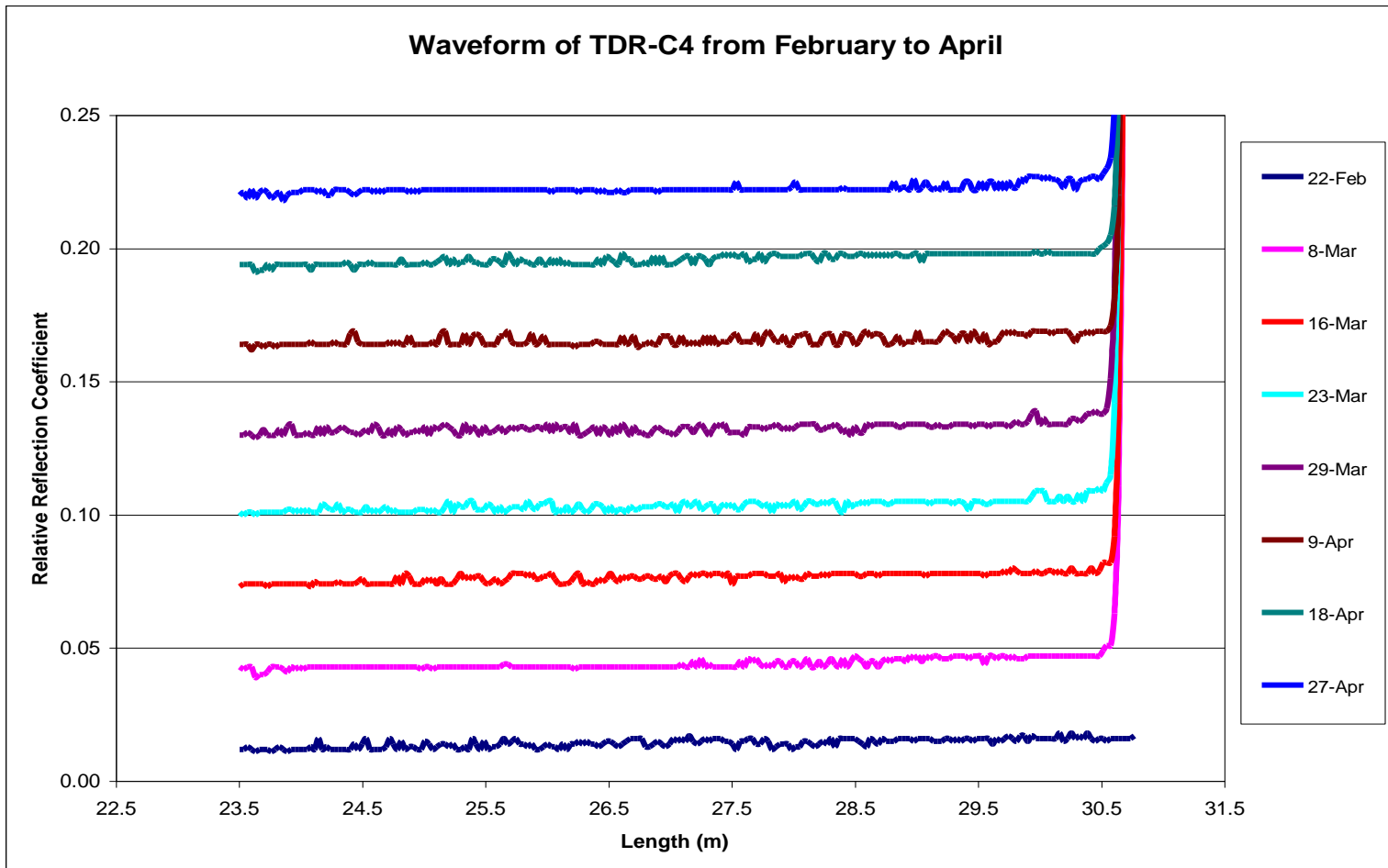


Figure 4-24: TDR cable waveforms at Location 4 from February to April.

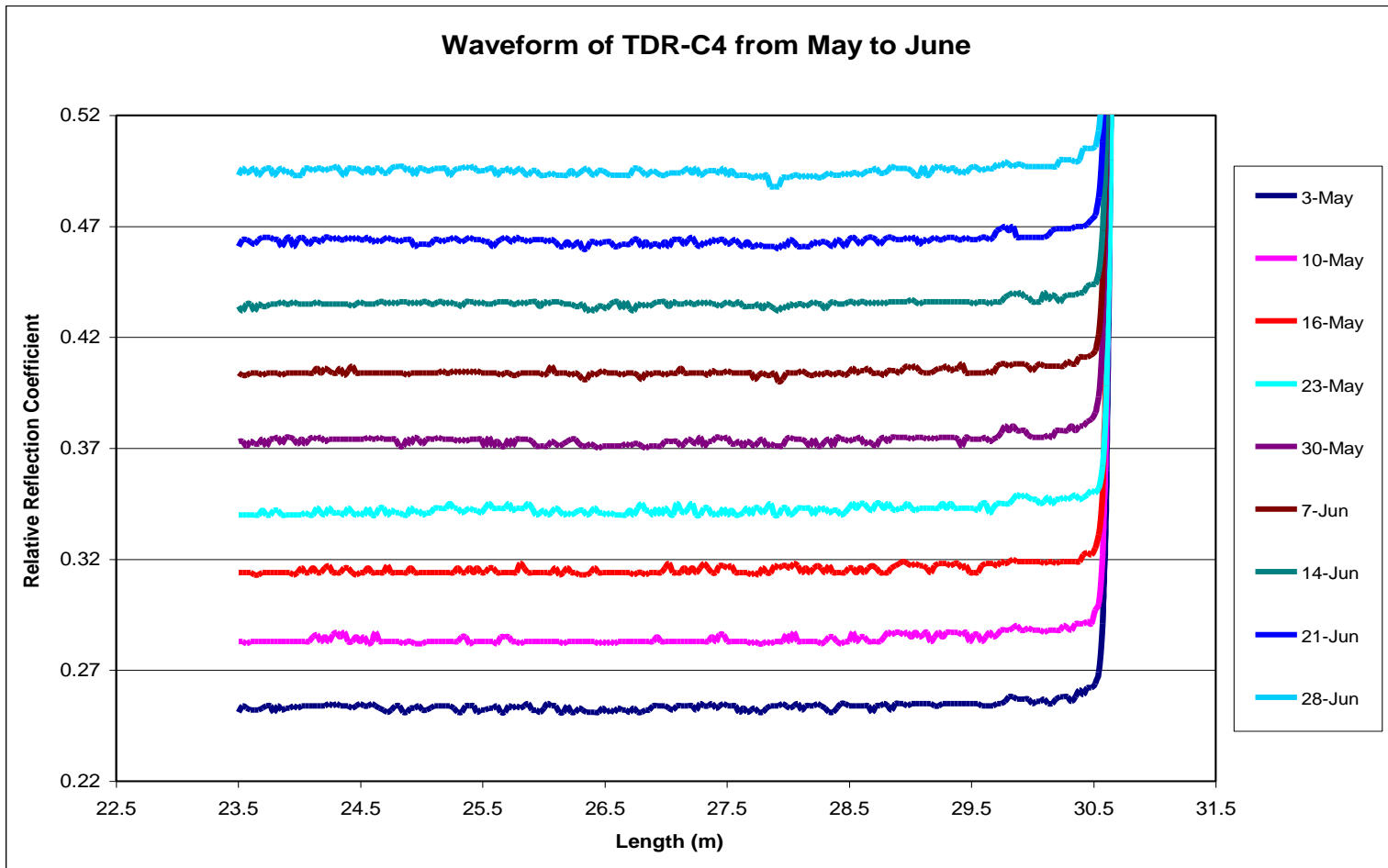


Figure 4-25: TDR cable waveforms at Location 4 from May to June.

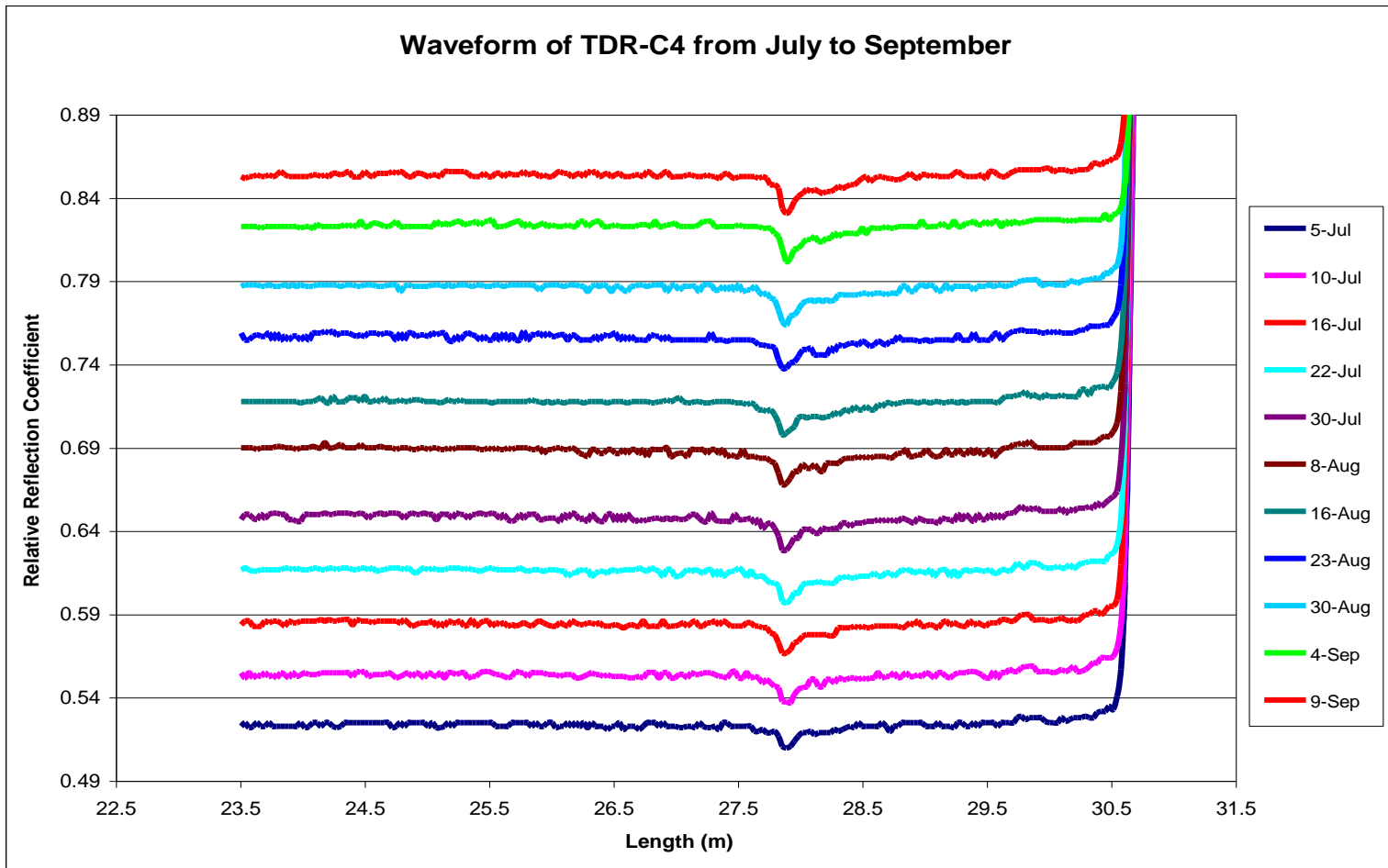


Figure 4-26: TDR cable waveforms at Location 4 from July to September.

By inspecting on the TDR cable waveforms in the above figures, it can be easily seen that the spikes which indicated the occurring movements enlarged more and more as the movements measured by the inclinometer became larger. It is due to the fact that the more the slope displaced the more the cables were bended, resulting to higher reflection coefficients at the bending position. Therefore, it was hypothesized that the increasing of cable deformation was linearly proportional with the increase of slope movement measured by the inclinometer. A comparison was made to investigate the compatibility between these methods. In this comparison only the waveforms collected at the same time of making the inclinometer measurements were selected so that the data were consistent. Then the reflection coefficients of the waveform at the bending positions were extracted and compared to the slope displacement measured by the inclinometer. Figure 4-27 to Figure 4-30 demonstrate the relationship between the data measured by the inclinometer and TDR cable method at Loc1 to Loc4. A linear trendline was added in each figure for an attempt to display the linear relationship between these methods. From these figures it can be seen that the data stayed very close near the trendlines at small movements and they scattered a small distance around the trendlines as the movements became larger. The scatter of the data might be due to the noise and inaccuracy of the TDR measurements since many tiny noises, or very small spikes, frequently occurred along the TDR waveforms during the data collection. However, these data couples seemed to increase in a linear fashion because the distances from the data plotted to the trendlines were not large and a trend of linear relationship between these data couples can be seen in these figures. Especially the data plotted in Figure 4-28 almost stayed in the trendline, showing a linear relationship between them. Also, the last three data couples

plotted in Figure 4-30 increased linearly together. These figures were the plots of the data recorded at Loc2 and Loc4, where large movements were encountered. The movement measured at the other locations in the drained section were not large, therefore the linearly relationship between these method was not clearly determined as in the control section. However, the data comparison in these figures was quite satisfactory to express the linear relationship between the data recorded by inclinometer and TDR cable method for slope movement monitoring. Also, more studies on slope movement monitoring using both of these methods needed to be done so that the above conclusion could be more clarified.

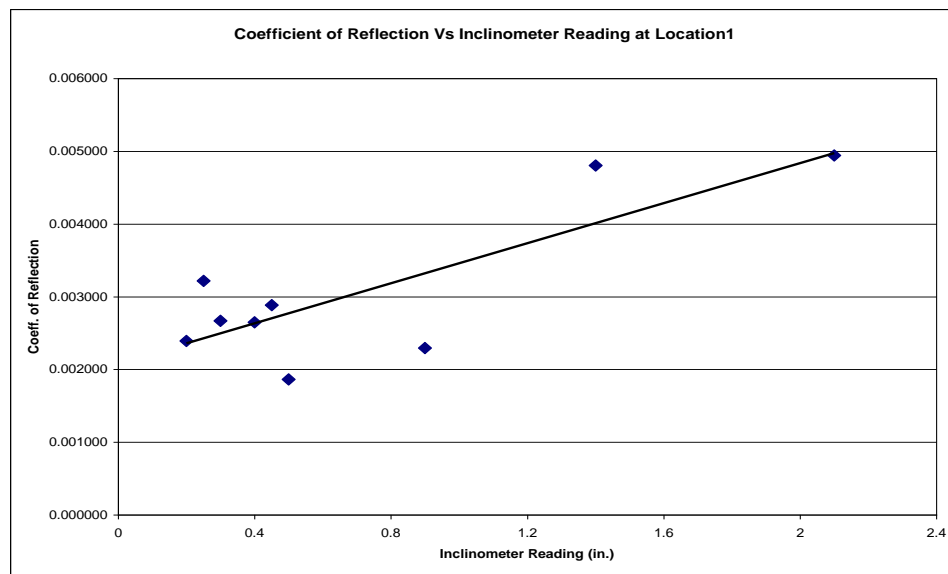


Figure 4-27: Relationship between the slope movements measured by inclinometer and TDR cable methods at Loc1.



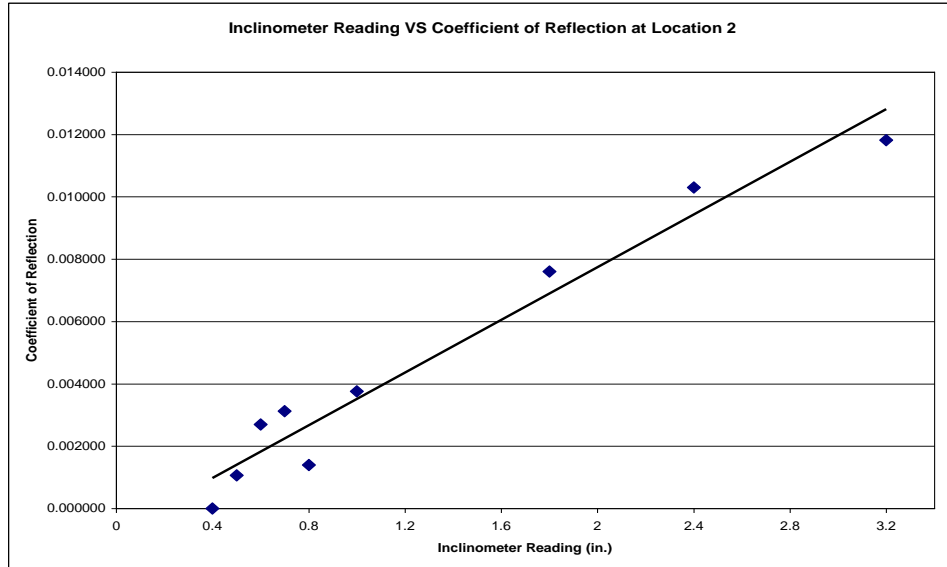


Figure 4-28: Relationship between the slope movements measured by inclinometer and TDR cable methods at Loc2.

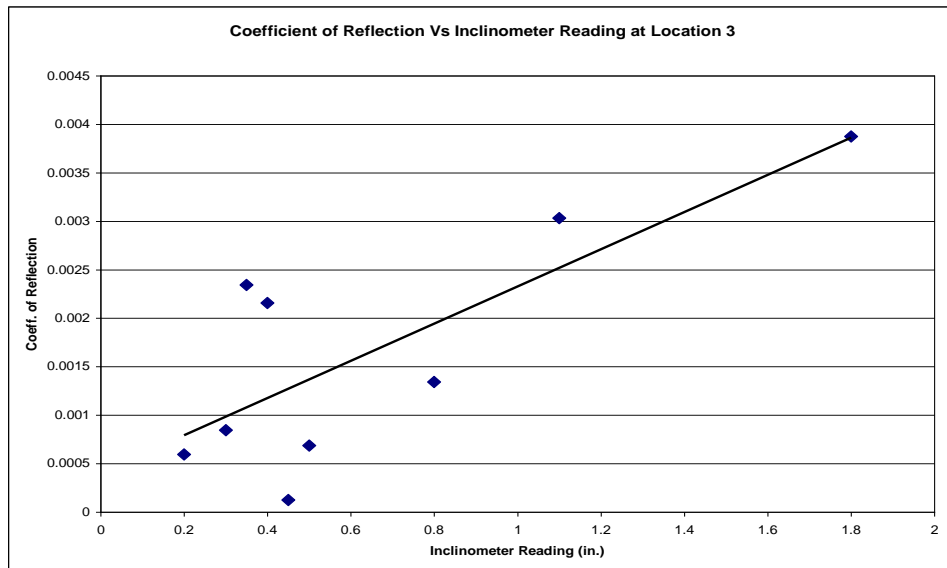


Figure 4-29: Relationship between the slope movements measured by inclinometer and TDR cable methods at Loc3.

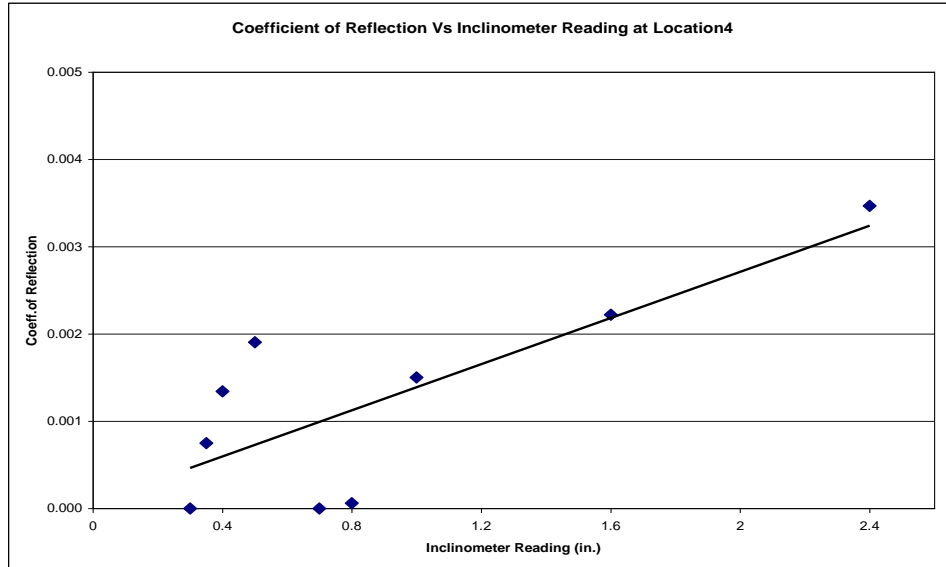


Figure 4-30: Relationship between the slope movements measured by inclinometer and TDR cable methods at Loc4.

#### 4.2.2 Moisture Content Monitoring

Moisture content is a familiar parameter in geotechnical engineering and it is directly related to the amount of water within a soil medium. When the moisture content of the soil within a slope increases, the pore water pressure also increases, resulting to a decrease of soil strength and slope instability. Thus, moisture content is an important indicator for slope stability and reducing moisture content within a slope is very necessary to increase the stability of that slope.

In this study, ten moisture probes were installed to measure the changes in moisture content within the slope. Five moisture probes were installed in each slope section, two of them in the lower part (Loc1 and Loc2) and other three in the upper region of the slope (Loc3 and Loc4), as illustrated in Figure 3-51 in Chapter 3. These moisture probes recorded the volumetric moisture content of the slope during the experiment. Then the results of volumetric moisture content were converted to

gravimetric moisture content, which is more familiar with geotechnical engineering, for the comparison analysis.

Figure 4-31 and Figure4-32 respectively express the changes of moisture content measured at the top and the bottom positions between the drained section, Loc1, and the control section, Loc2. As can be seen in these figures, the moisture content in the drained section was always lower than that compared to the control section. This difference was not significant at the top of the slope since the moisture contents recorded at this level were nearly the same, which was about 35%-38%. However, the moisture content recorded at the bottom of Loc1 was remarkably lower than that at Loc2. During the experiment, the moisture content at the bottom at Loc2 was almost stable at 36% while the moisture content at the bottom at Loc1 was less than 25%. This is due to the fact that the moisture probe at the bottom of Loc1 was installed at a lower level than the location of the drains. When free water was present, it was collected at the toe of the slope where the drains were installed, leaving less water flowing down below the drains. Therefore, the moisture content at the bottom of the drained section was kept lower since an amount of water was removed out of the slope by the drains. In contrast, the water was remained in the control section since no drainage was applied in this area, resulting to a consistently high moisture content profile in the control section. As a result, the moisture content within the drained section was remained low within the drained section as the drains were installed into this area.

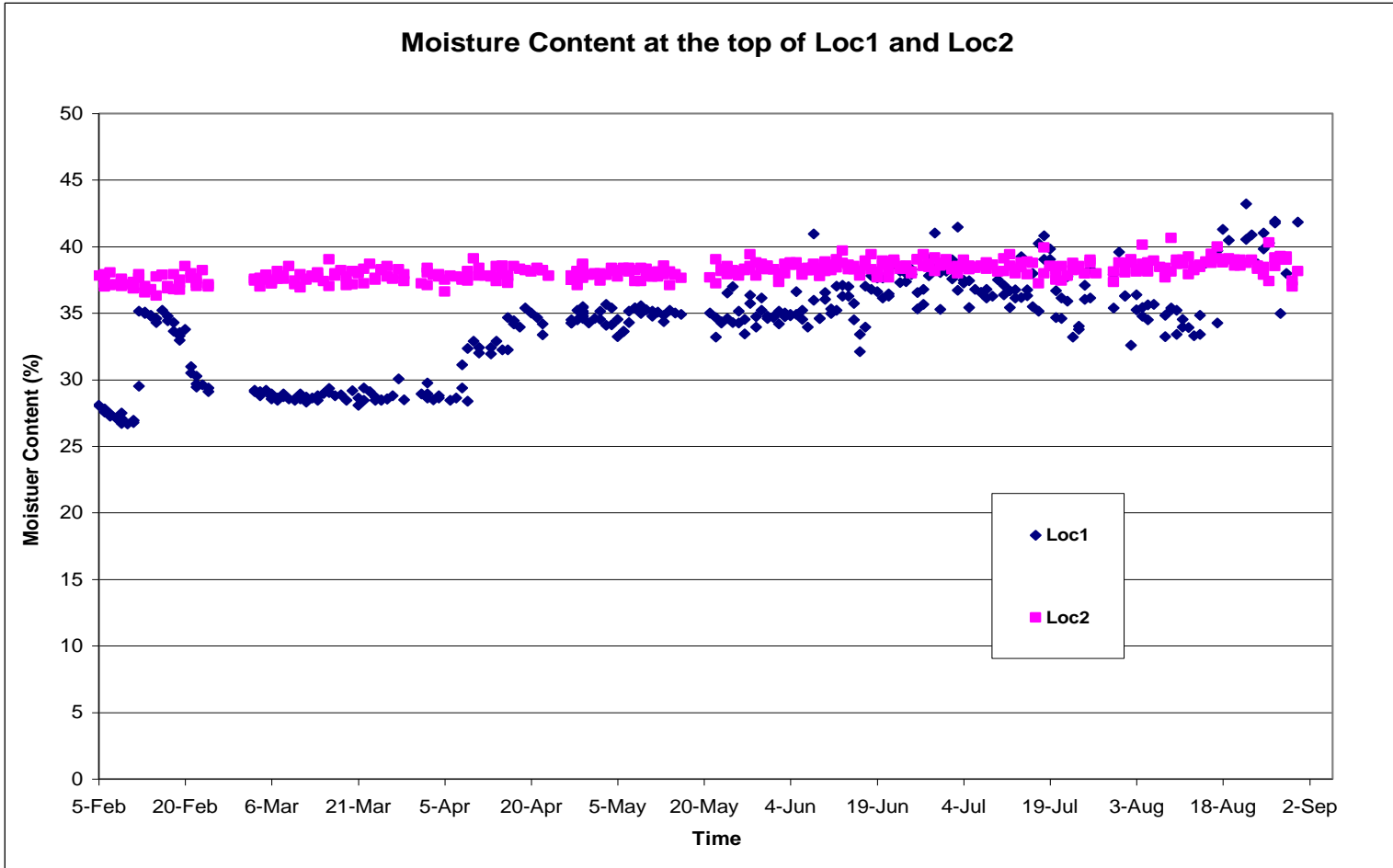


Figure 4-31: Moisture content profile at the top of Loc1 and Loc2.

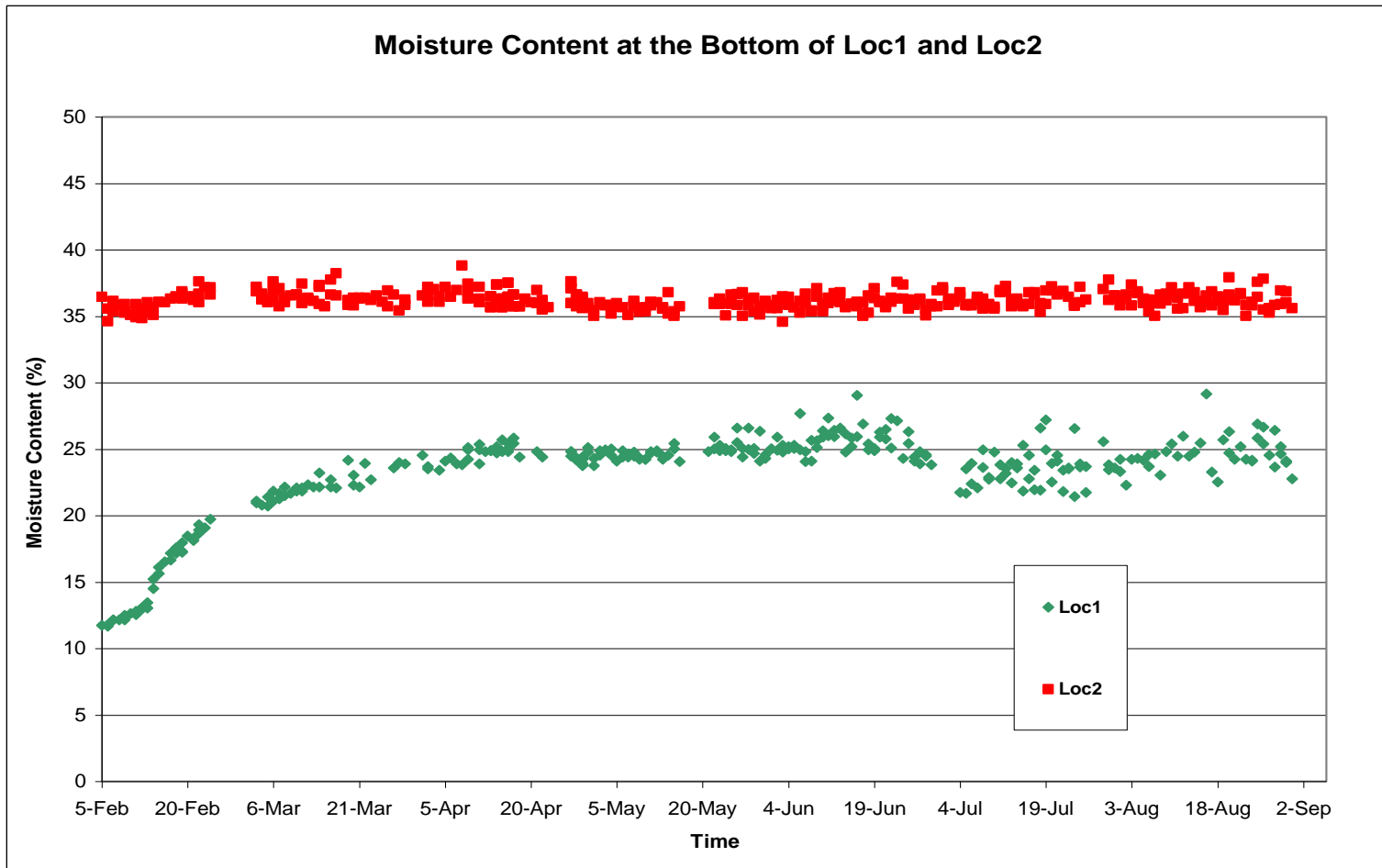


Figure 4-32: Moisture content profile at the bottom of Loc1 and Loc2.

The results of the moisture content monitoring within the upper part of the slope, Loc3 and Loc4, are expressed in Figure 4-33, Figure 4-34, and Figure 4-35. These figures respectively display the fluctuation of the moisture contents measured at the top, the middle, and the bottom at Loc3 and Loc4. Among these positions the maximum moisture content was measured the top of Loc4, which was more than 75% as illustrated in Figure 4-33. Since no drainage was applied in the control section and the hydraulic conductivity of the clay was very low, the water coming from many large rainfalls during the summer was accumulated within the soil medium and made the soil saturated. Therefore the moisture content near the slope surface under un-drained condition remained very high. However, the data measured at the top of Loc3 showed much lower moisture content results, which were merely about 40%. The large difference of moisture content results between these positions can be explained by the fact that an amount of water was removed out of the drained section, resulting to less water retained inside this slope section. Therefore, the moisture content of the soil near the ground surface in the drained section was lower than that in the control section as a volume of water in that position was removed out of the slope by the drains.

Unlikely as in the top position, the difference in moisture content at the middle position between Loc3 and Loc4 was less remarkable. The moisture content at Loc 3 was stable around 37% while that value recorded at Loc4 was in range of 40% to 50%, as illustrated in Figure 3-34. This might be because the amount of free water near the surface at Loc4 was more than that at the middle of this location, resulting to a higher water concentration and larger moisture content. However, the moisture content data at

the middle of Loc3 were always smaller than those recorded at Loc4, indicating a higher value of slope stability in the drained section compared to the control section.

The effectiveness of the drains was most characterized in the comparison of the moisture content between the bottom of Loc3 and the bottom of Loc4. As illustrated in Figure 4-35, the moisture content in the control section at this position was relatively high, about 38%, which was the result of the un-drained condition in this slope portion. In contrast, the moisture content recorded at the bottom of Loc3 was almost three times lower than at Loc4, which was around 13% as in Figure 4-35. It also showed that the soil at this position was almost dry and no water infiltrated to this area. It can be easily explained by the effect of the drains in this situation. The drains were installed at a distance above the bottom of Loc3; therefore they collected most of the water and drained it out of the slope, leaving no water flowing downward. Thus the soil in this position was kept dry over the time and the moisture content within remained very low, resulting to an improvement in slope stability.

As a conclusion, the moisture content within the control section was always higher than that in the side of the slope. This was the result of free-drainage condition in that slope section, which maintained a high level of water concentration inside the slope and led to more instabilities and slope failures. On the other side, the moisture content at the drained section was remained less than in the control section during the experiment, especially at the bottom position. This lower moisture content indicated a reduction of the free water and less movement recorded within the drained section, proving the effectiveness of the drains in removing water out to increase the stability of the slope.

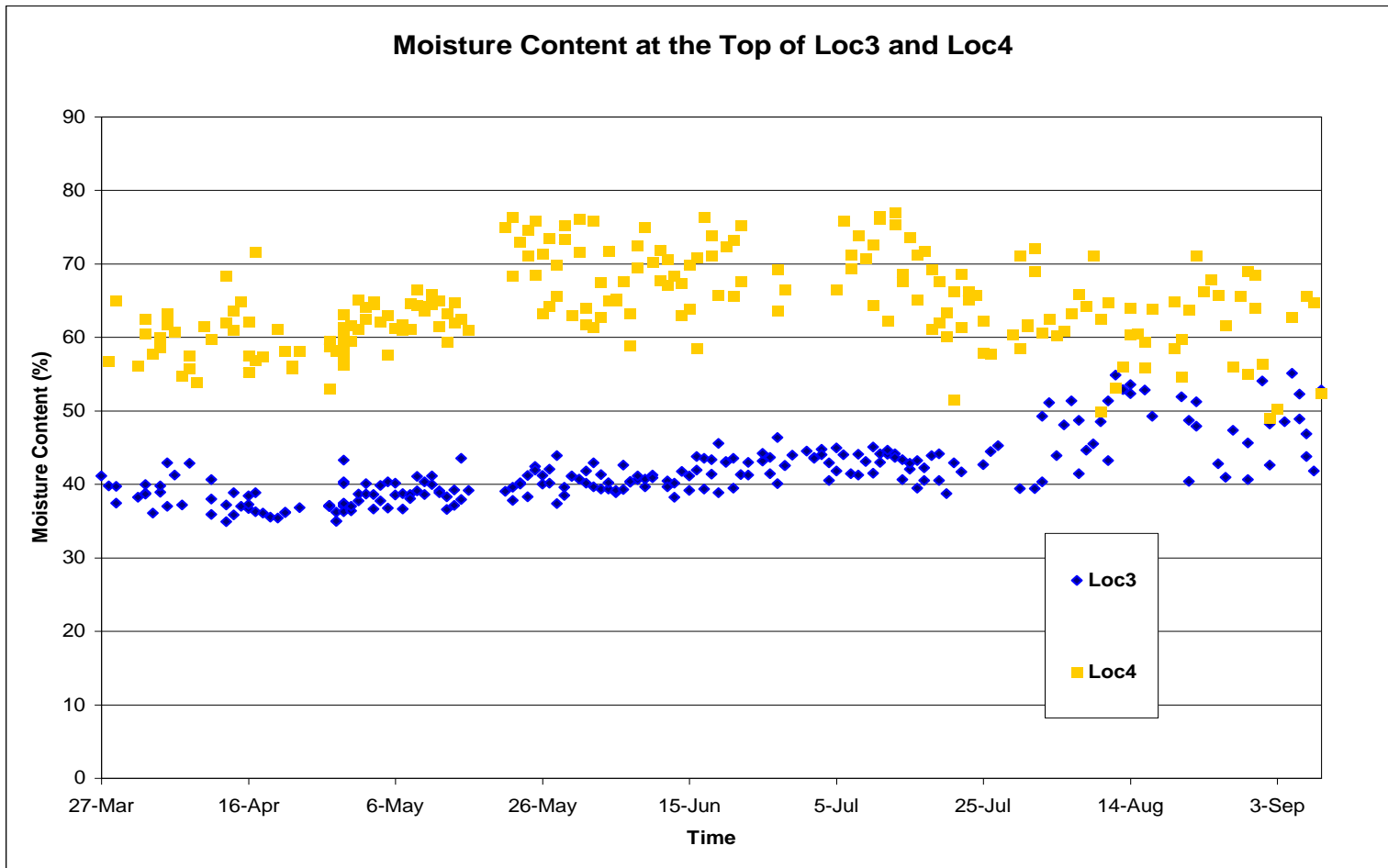


Figure 4-33: Moisture content profile at the top of Loc3 and Loc4.



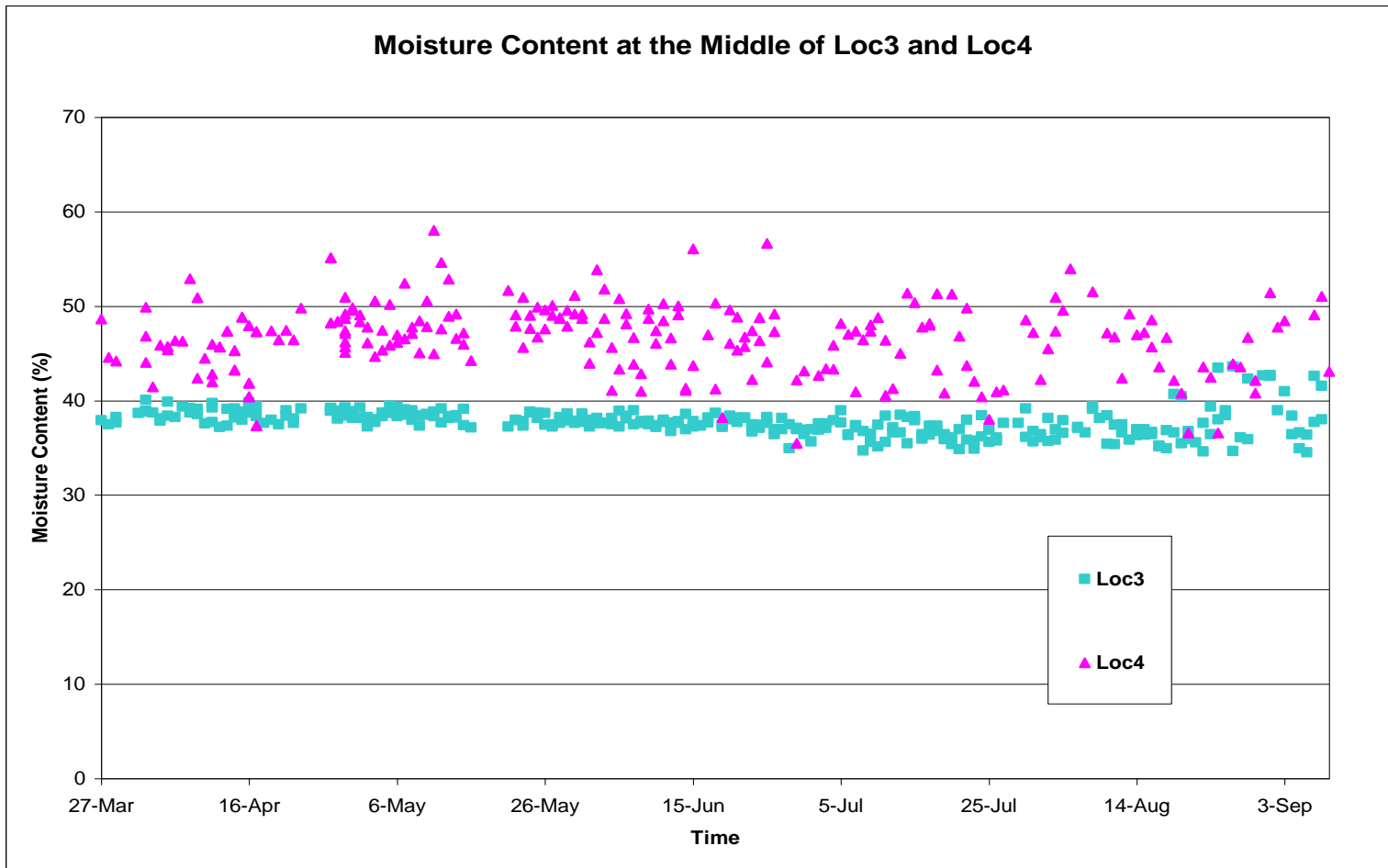


Figure 4-34: Moisture content profile at the middle of Loc3 and Loc4.

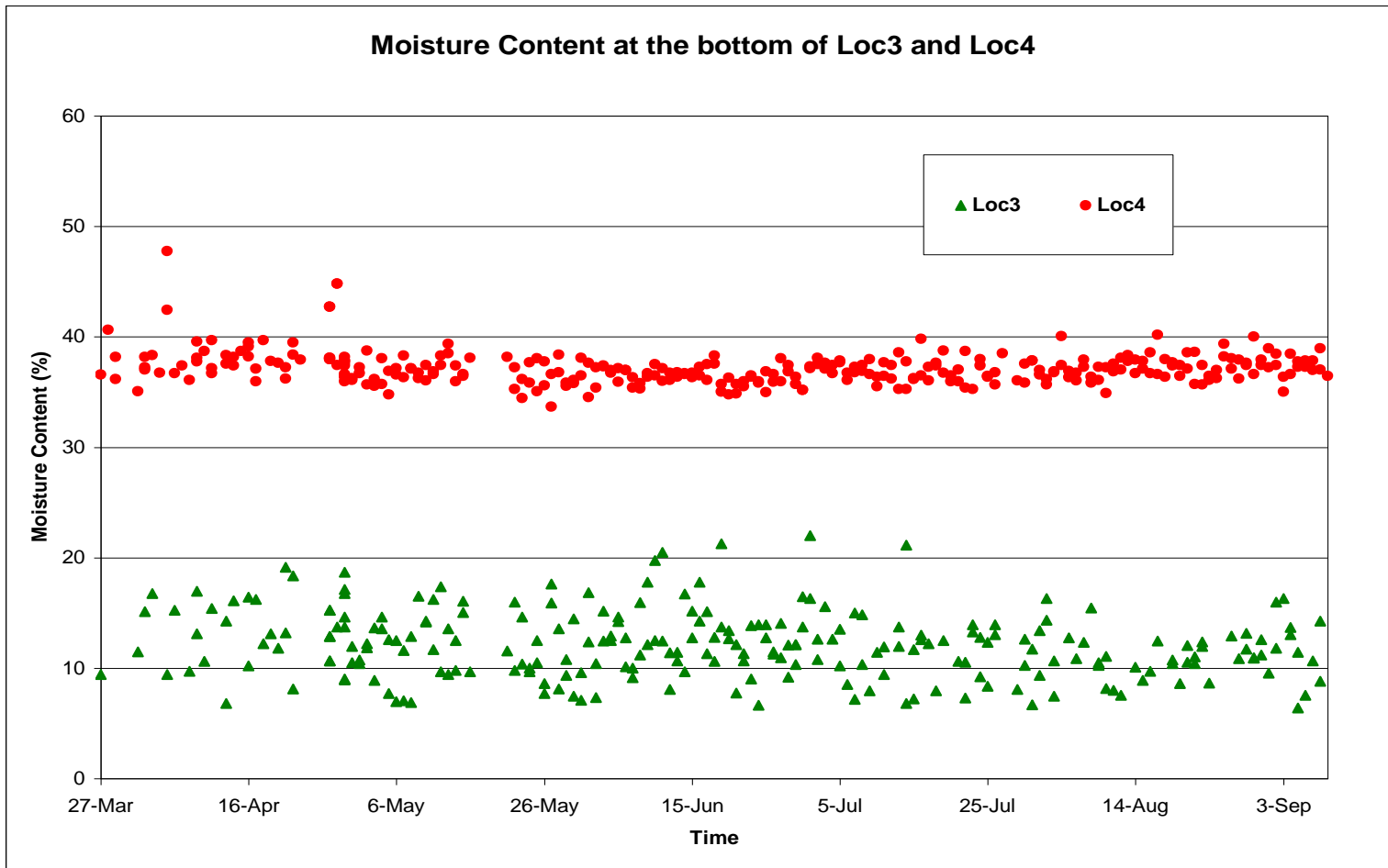


Figure 4-35: Moisture content profile at the bottom of Loc3 and Loc4.

### **4.2.3 Flow Capacity and Daily Precipitation Monitoring**

In this study, a total number of 18 drains with 234m (767ft) length were installed near the toe of the drained section. Among them, 16 drains were evenly spaced at 1m parallel spacing. The installation of these 16 drains was stopped when a layer of bedrock was encountered after they were advanced a distance of 12m (40ft) into the slope. The length of these drains was about two-third of the distance from the toe to the crest of the slope. The other two drains were installed into the slope with a cutover angle, resulting to a deeper penetration. The maximum installation depth of these two drains reached about 21m (70ft) and their installation was also terminated at the bedrock layer.

A trip to the site was made two months after the drain installation to investigate the functionality of the drains after they were installed into the slope. At this time the pipe system was not installed and the drains were exposed out at the slope toe. Several of them were found moist while the others were still dry, and there was no out flow observed from the drains. It was because the free water inside the slope that mainly came from small snow melts during the winter was insignificant. Therefore the drains were inactive at the initial time of the experiment. However, the drains were still functional since some of them were found in moist condition, which meant that an amount of water was conveyed inside the drains.

Later a PVC pipe system was created to collect the water and a rain gauge was set up to measure the out flow coming from the drains. At the same time another rain gauge was installed to record the daily precipitation at the site. The results of daily precipitation and out flow measurement are displayed in Figure 4-36. In this figure, it can be seen that no rainfalls occurred at the site until the end of April and nearly no out flow was

accordingly measured during this time. A large rainfall was recorded on April 23<sup>rd</sup> and many rainfalls occurred more often since then. In this figure, there was a short time between the time of the rainfall event and the time that the out flow started to be recorded. This delaying time was due to the fact that it took a while for the water to travel from the slope surface down to the drains within the low permeable clay. Since a large amount of the water was drained out, the movement of this slope section was reduced significantly as illustrated in the slope movement comparison discussed above.

The data of the daily precipitation and out flow measurement from Jun16<sup>th</sup> to July 22<sup>th</sup> were extracted and plotted in Figure 4-37 to characterize the response of the drains in removing the water that came to the slope from outer sources. As illustrated in this figure, the rains almost occurred daily during this time, and the out flow was seen to increase proportionally as the water accumulated more and more into the soil from these continuous rainfalls. When the rains occurred less often at the later time, the out flow respectively decreased. Therefore, the drains effectively responded to remove the water coming into the slope so that the slope movement was reduced.

During the experiment the highest recorded outflow was approximately 100 lit/day, as expressed in Figure 4-37. Distributing this value for total 18 drains installed, the maximum discharge capacity of a single drain was about  $5.6 \times 10^{-3} \text{ m}^3/\text{day}$  or  $9 \times 10^{-4} \text{ gal/min}$ . Comparing this value to the discharge rate obtained from the wick drain manufacturer, which was about 1.6 gal/min, it can be seen that the actual discharge capacity of the drain at the site was much lower than the design value. This low result of the actual drain discharge capacity was mainly because of the low hydraulic conductivity of the clay. Since the hydraulic conductivity of this soil was very low, the seepage flow

inside the slope was very slow and it took a long time for the water to travel down to the drains. Therefore the discharge capacity of the drains could not reach the standard value as desired.

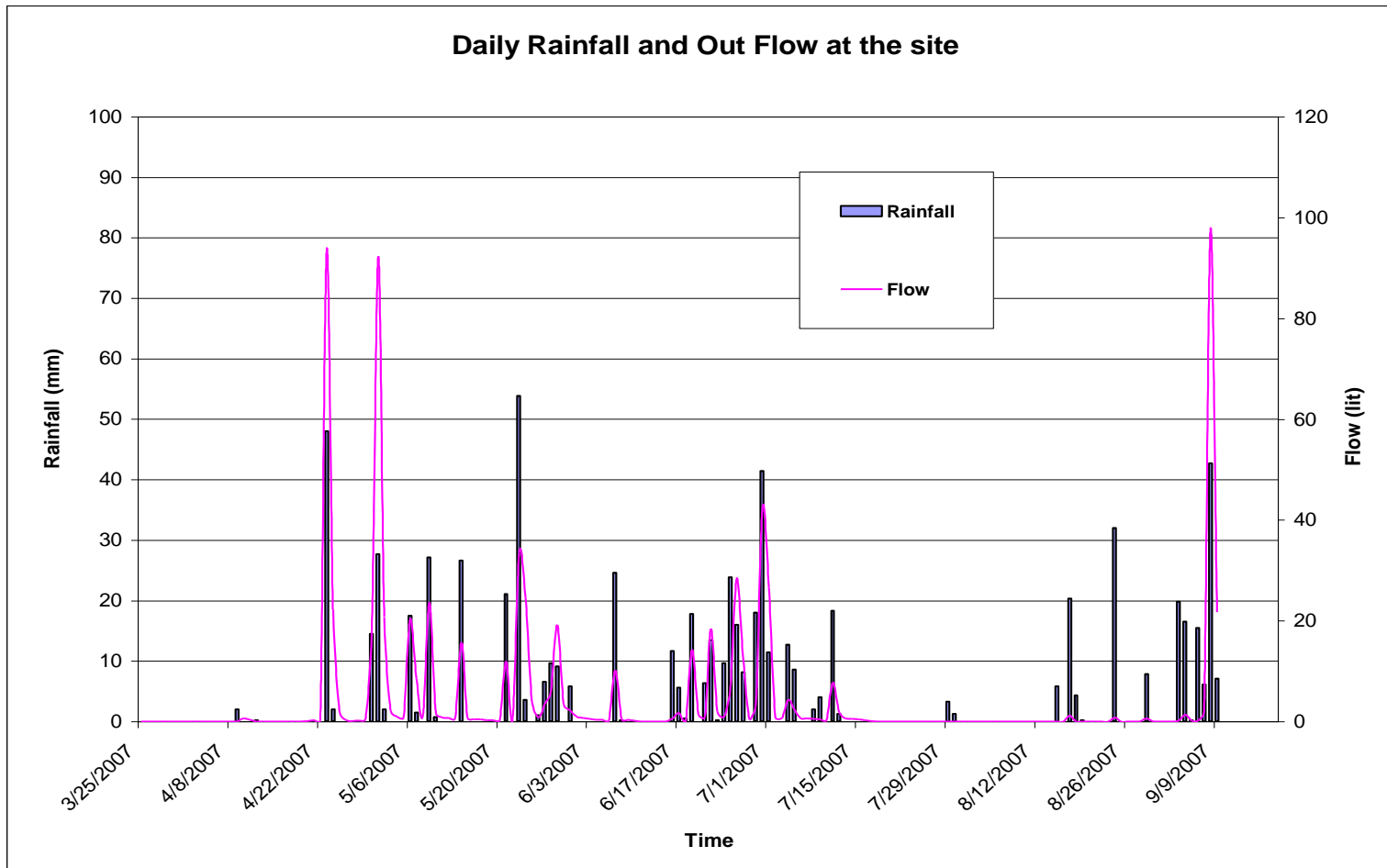


Figure 4-36: Daily precipitation and flow capacity of the drains.

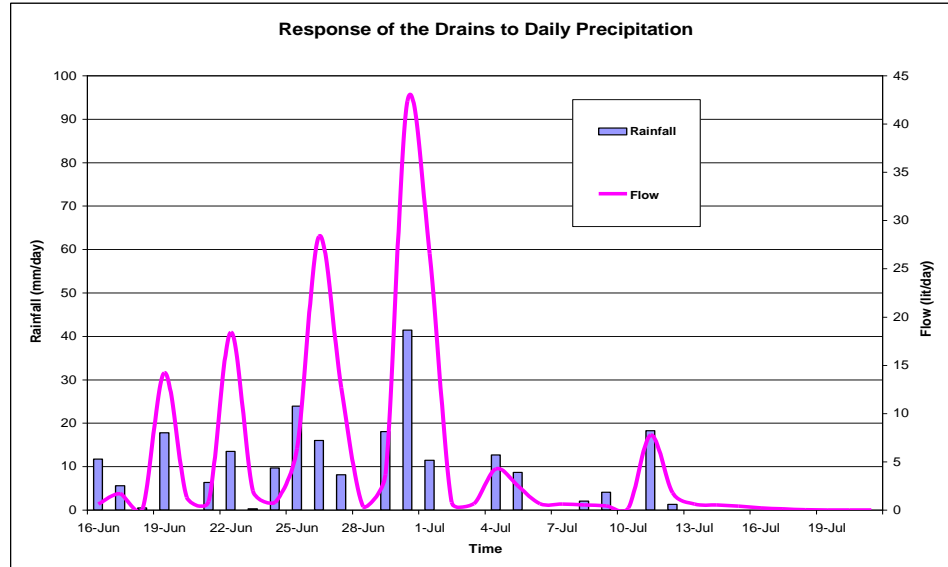


Figure 4-37: Response of out flow from the drain system to daily precipitation at the site.

Although their actual discharge capacity was not high, the drains were still removing water from the slope and lower the moisture content within the slope. The reduction of moisture content can be seen again in Figure 4-38 and Figure 4-39, which respectively illustrate the changes of moisture content profile at Loc1/Loc2 and Loc3/Loc4 corresponding to the out flow. It can be seen that the moisture content within the control section was always higher than compared to the drained section, especially at the bottom positions. As can be seen in these figures, the moisture content at the bottom of Loc1 and Loc3 gradually decreased as the out flow started to be recorded. In contrast, the moisture content at the top of Loc4 in the control section increased during the time that many rainfalls often occurred. As a result, the drain system worked to remove water out of the slope, proving its effectiveness in lowering the moisture content and increasing slope stability.

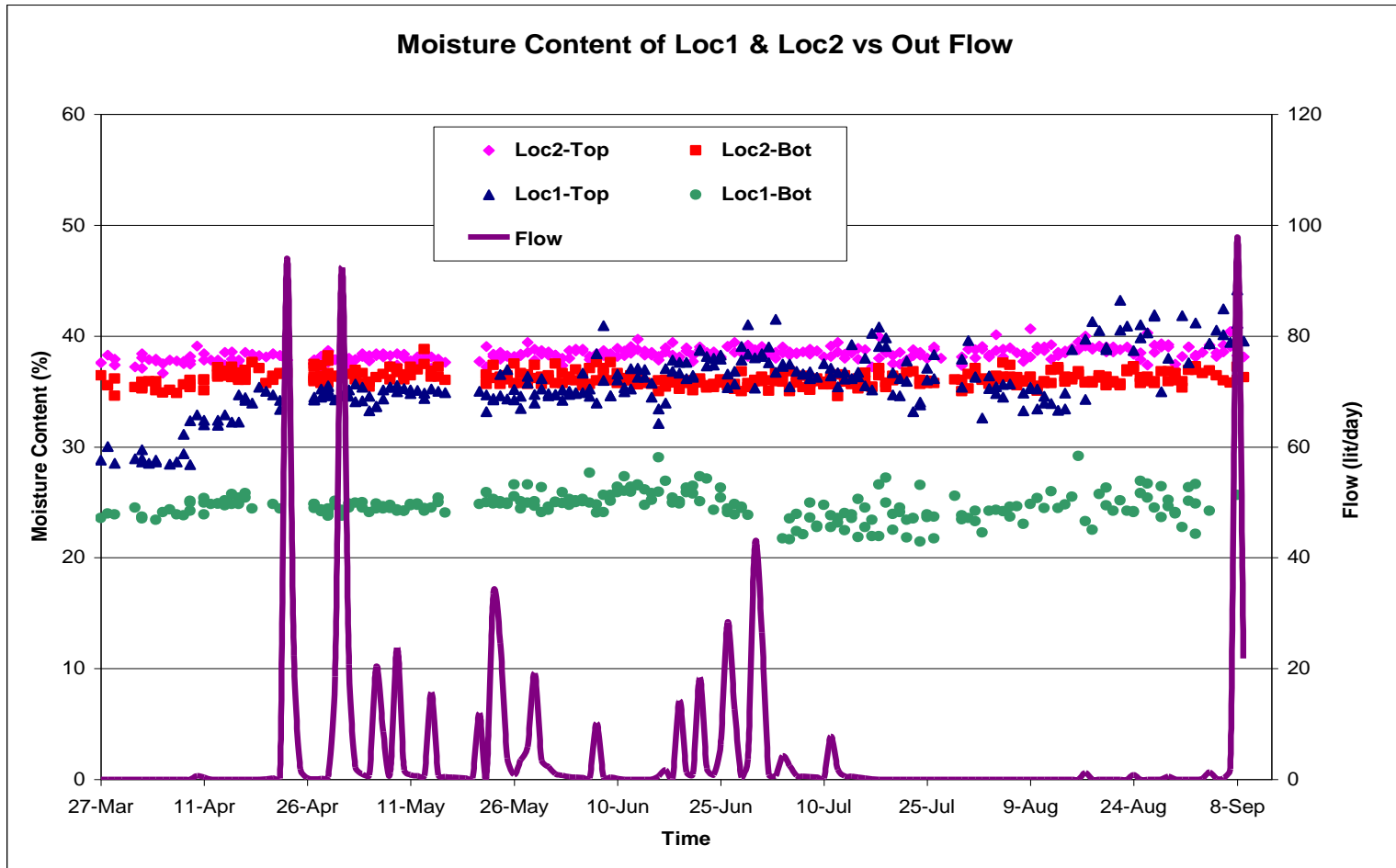


Figure 4-38: Moisture content profile at Loc1 and Loc2 and out flow capacity of the drains.



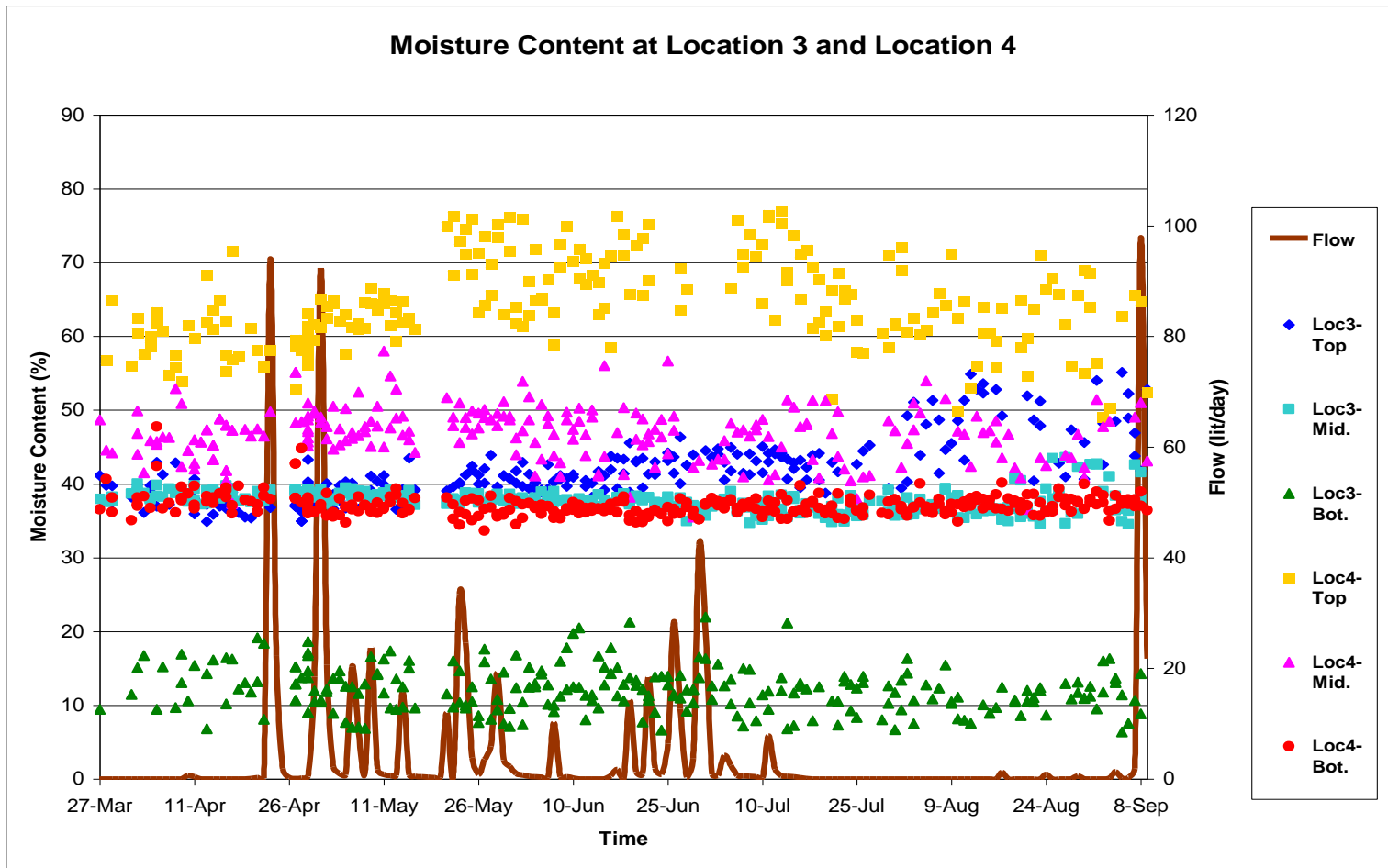


Figure 4-38: Moisture content profile at Loc3 and Loc4 and out flow capacity of the drains

#### **4.2.4 Ground Water Table Monitoring**

In this study, the ground water table (GWT) within the slope was measured by four piezometers and the data were plotted by the HOBOTM Ware software for the duration of the monitoring. These piezometers were located at the bottom of the casings to record the changes of water level at all locations. The results of the GWT monitoring at four locations were displayed in Figure 4-40 below. Since the piezometers were placed at the bottom of the casings at all locations, the depths of the GWT reported from the bottom of these locations. As can be seen in this figure, the highest GWT was measured at Loc4 while the piezometer at Loc3 recorded the lowest value of GWT. However, all of these GWT results were recorded far below the slope surface, and the highest GWT recorded was about 5 ft above the bottom of the casings. Since the depths of the casings buried at Loc/Loc2 and Loc3/Loc4 were respectively about 15 ft and 19 ft below the slope surface, it can be said that the GWT did not come up to the slope during the experiment. Therefore, the location of the GWT recorded by these piezometers indicates that the GWT did not impact slope instability at the location of the respective boreholes.



Figure 4-40: Ground water table profile at all locations.

### 4.3 Parametric Analysis

#### 4.3.1 Optimum Drain Length Determination

Together with the evaluation of the workability of the drains, another scope of this study is to determine their optimum configuration in clayey soils, including the length and the spacing of the drain system. Also, the configuration determination was conducted in other types of soil having different values of hydraulic conductivity. This analysis was done by using the seepage FEM Plaxflow software, as described before in Chapter 3.

A 20ft-height slope model was created with the inclination of 3:1 (H:V) to represent the actual geometry of the slope at the site. There was a site exploratory investigation conducted three years before the experiment started. Based on the soil profile obtained from this exploratory, the slope consists of two layers of soil, the clay

layer overlying a layer of shale. The clay layer covered the whole body of the slope while the shale layer was encountered about 2 ft below the slope toe. To simulate the actual condition of the slope, the slope model created in Plaxflow also consisted of two layers of soil, in which the clay soil lied above the shale layer. The properties of the clay soil obtained in Chapter 3 were assigned to the soil profile definition in Plaxflow. Since there was no sample of the shale obtained from the exploratory, it was assumed that the shale had the same properties with the clay soil except the lower hydraulic conductivity, which was about  $1 \times 10^{-9}$  cm/s. The slope model created in Plaxflow is shown in Figure 4-41 below. Since no addition benefit could be gained when the drains are installed in the upper parts of the slope, the drains were only modeled near the toe of the slope in this parametric analysis.

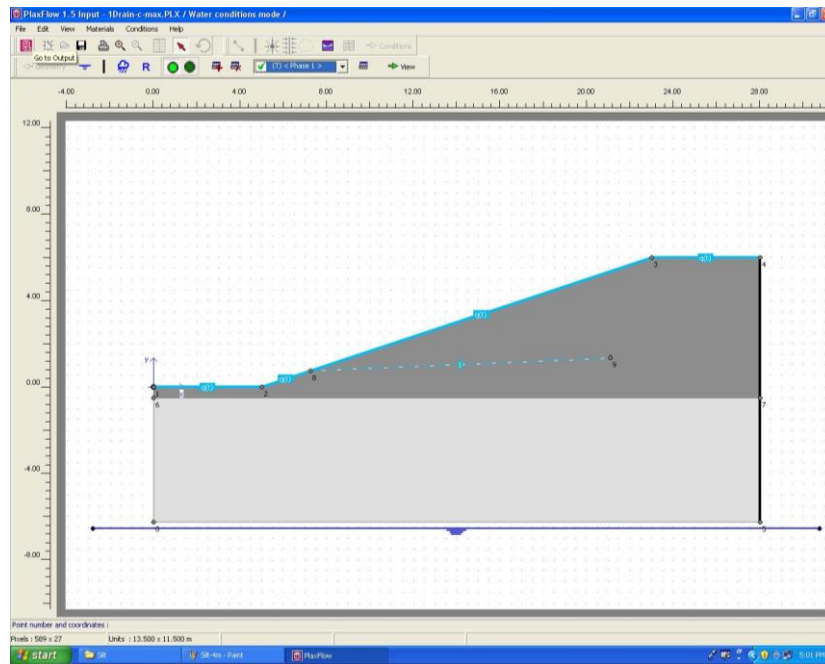


Figure 4-41: Slope model in the parametric analysis.

Four scenarios with different drain configurations were created in this analysis.

No drainage was set up in the first scenario. In the second scenario, a short drain was

model to the middle of the slope. A longer drain was created in the next scenario and its length nearly reached the crest of the slope. The longest drain in the last case passed through the slope crest a short distance. The configurations of the drain in these scenarios are shown in Figure 4-42 (a) to (d). Based on the precipitation data obtained from the rainfall measurement, a rainfall event was created to stimulate the precipitation for the slope model. From the field results, the highest intensity of a rainfall recorded during the experiment was 54 mm/day, and this value was assigned in the precipitation model in the analysis. This rainfall was assigned at the first day of the time phase and no rainfall was made at later time. The drain performance was analyzed in a 15-day period. Before the analyses were conducted, the boundary conditions were assumed as following:

- The soils were homogenous and isotropic within the slope.
- The hydraulic conductivities of the soils were equal in vertical and lateral directions.
- Closed boundary condition was assigned to the vertical right line of the model.
- The GWT was far below the toe of the slope.

From this analysis, the effect of drain length can be compared based on the *Active Pore Pressure* (APP) results, which are expressed on the legend on the right side of the output windows. A series of Figure 4-42 (a) to (d) shows the Active Pore Pressure corresponding to these scenarios. Here, Plaxflow defines pressure outputs as negative values, thus the APP is the inverse of the pore water pressure, which is more familiar to geotechnical engineering. When the APP within a soil medium increases, the pore water pressure built up decreases, leading to an increase of the effective stress as well as soil

strength. From these figures, it can be seen that the APP builds up inside the slope increases as the drain penetrates deeper into the slope; however, it decreases when the drain goes farther over the slope crest. In the un-drain scenario, the APP obtained is the lowest one while the APP results in other scenarios are always higher. The difference in APP between the un-drained case and the other drained cases is due to the effect of the drains inside the slope. When the drains are installed, they help to convey the water out and lower the GWT within the slope, thus reducing the pore water pressure and increasing the slope strength. But the effect of the drains does not always proportionally increase as their length extends deeper into the slope. In the third scenario, the highest APP was obtained at  $59.85 \text{ KN/m}^2$  as the drain was installed close to the slope crest, as illustrated in Figure 4-42 (c). An increase in the drain length did not result to a higher value of APP but it made the APP value decreased instead, as in Figure 4-42 (d). This point is in agreement with the conclusions of Cai, Ugai, Wakai, and Li (1998) and Lau and Kenney (1983) which stated that no additional benefit would be gained if the drains extend beyond the critical length, i.e. “the distance between the slope toe and the slope shoulder” (Cai, Ugai, Wakai, and Li, 1998). The highest APP was obtained when the drain was modeled approximately three-fourth of the distance between the slope toe and the slope crest, as in Figure 4-42 (c). The length of the drain in this scenario was then considered as the critical drain length since the APP did not gain higher when the drain extended farther than the critical length. As a result, the length of the drain modeled in Figure 4-42 (c) was determined as the optimum length in this analysis.

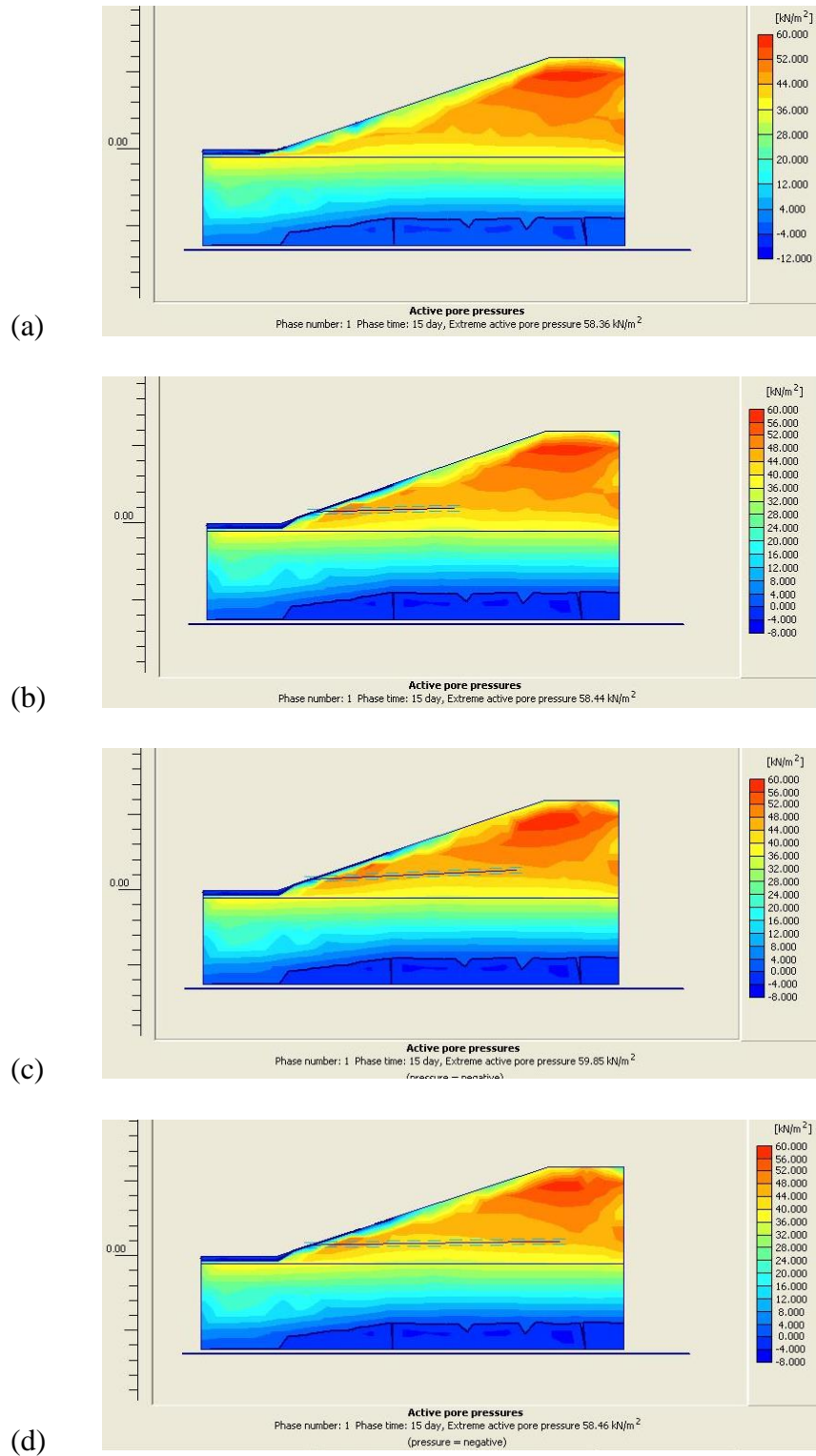


Figure 4-42: Active Pore Pressure results of the drain length analysis.

Additionally, the drain performance can be evaluated through the Degree of Saturation (DoS) results. The DoS results of this analysis corresponding to different drain scenarios are displayed in Figure 4-43 (a) to (d) below. From these figures, it can be seen that the areas with low value of DoS expands with the presence of the drain inside the slope. The areas having low DoS stand for the places where lesser volume of water is met, which means that the pore water pressure at these areas is low, resulting to higher effective stresses and soil strength. Thus the stability of the slope will increase as the DoS inside the slope decreases. As can be seen in Figure 4-43 (a) the areas of low DoS only concentrates on the top of the slope, where no drain was installed, and they expand more and more to the slope toe as the drain went deeper into the slope. These areas were seen most in Figure 4-43 (c), the third scenario, when the drain was modeled with the length that was determined earlier as the optimum value. In this figure, the areas having low DoS expanded most of the body of the slope. Similarly to the APP expression, the DoS profile inside the slope in the longest drain was not as good as in the previous condition although the drain length was increased. As a result, the drain length displayed in Figure 4-42 (c) and Figure 4-43 (c) was the optimum length which improved the stability condition of the slope most. From the above results, the drain length determination analysis showed that increasing the length of the drain over a critical length did not give any additional benefit for slope stability, and the length of the drain specified above was concluded to be the optimum length to be applied in this drainage method.



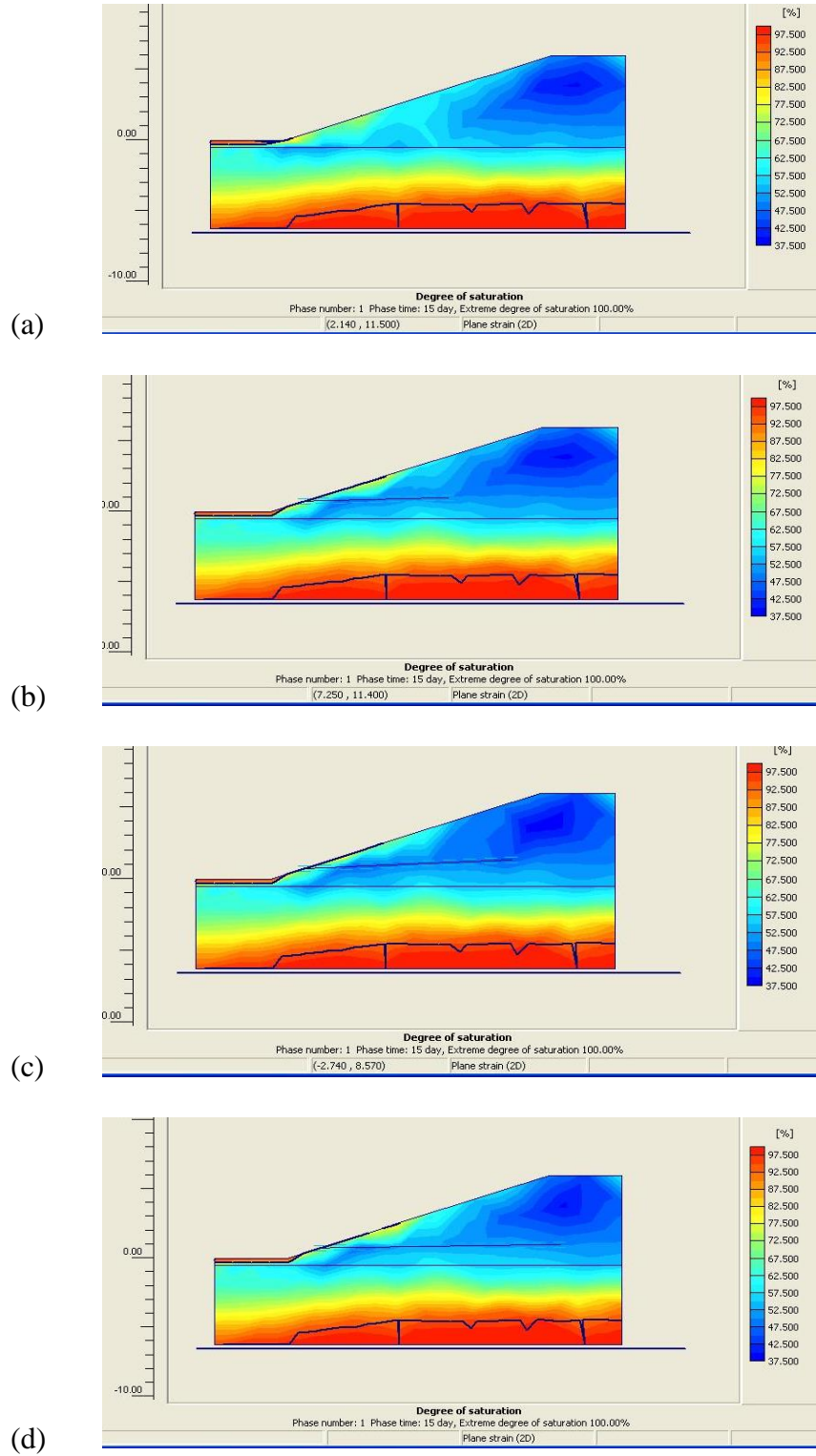


Figure 4-43: Degree of Saturation results of the drain length analysis

### 4.3.2 Optimum Drain Spacing Determination

#### Clayey soil

In this drain spacing determination, a cross section at the middle of the slope was modeled as in Figure 4-43. The same assumptions, soil properties, boundary conditions, time phases and precipitation profile from the previous analysis were applied to this analysis so that the results could be consistent. However, the model for the drains was different from that compared to the drain length analysis. In the previous analysis the drain was model as series of line elements that has zero phreatic pressures ( $p=0$ ), and the water within the slope was drained out due to gravitational flow from the inside to the outer slope surface. However, it was impossible to model the drain with the same manner in this situation since there was no slope surface defined in the 2-D cross section modeling and the gravitational flow in this situation was actually the downward seepage flow from the clay to the shale layer, not the outward drainage flow as expected. Therefore, it was decided to model the drain by a well in this situation since they have the same function to remove the water out of the slope. Figure 4-43 also expresses a series of wells that were used to model for the drains in the spacing grid determination. The main difference between a natural drain and a well is that the drain collects the water by gravitational flow while the well contracts the water through pumping. Moreover, the well always sucks water with the amount equal to its discharge rate during its operation while the drain only conveys water when free water is present. Therefore the matric suction or the active pore pressure within the soil medium is very high when using a well to model for a drain. As a result, the comparison in this analysis cannot be made by the

APP results, and the DoS values are used instead to determine the optimum drain spacing.

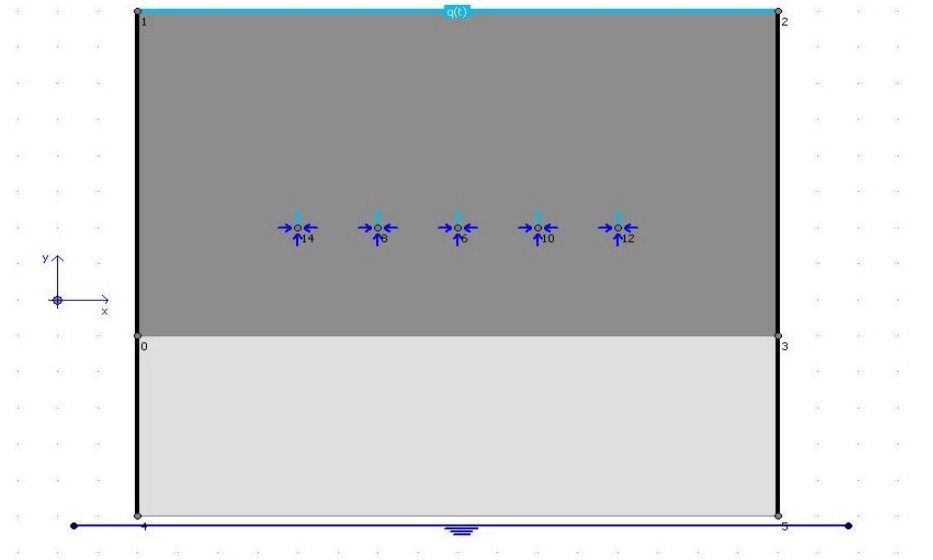


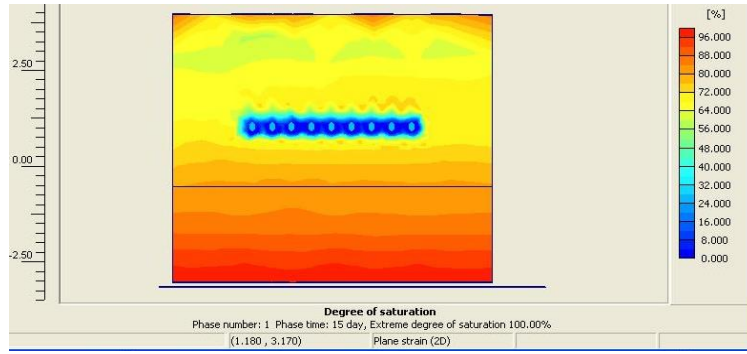
Figure 4-44: A cross section model in the drain spacing determination.

Many scenarios were created in the optimum drain spacing analysis. In each scenario many drains were evenly spaced at a distance on a horizontal line as illustrated in the figure above. The position of this horizontal line represented for the position of the drain to be installed within the slope. The actual discharge capacity of the drain system obtained from field results was set as the discharge rate of the wells to simulate the drain workability correspondingly to the actual condition. As mention earlier the maximum out flow was recorded approximately 100,000 ml/day or 100 l/day. This value was divided by 18 total drains installed, giving a number of  $5.6 \times 10^3$  ml/day or  $5.6 \times 10^{-3}$  m<sup>3</sup>/day for a single drain discharge capacity. This value of discharge capacity was then assigned for each drain modeled in this analysis. Since the hydraulic conductivity of this clay soil was very small, the influence zone of a drain, the area in which water was collected only by that drain, in this type of soil was also assumed to be small. Therefore, the value of drain

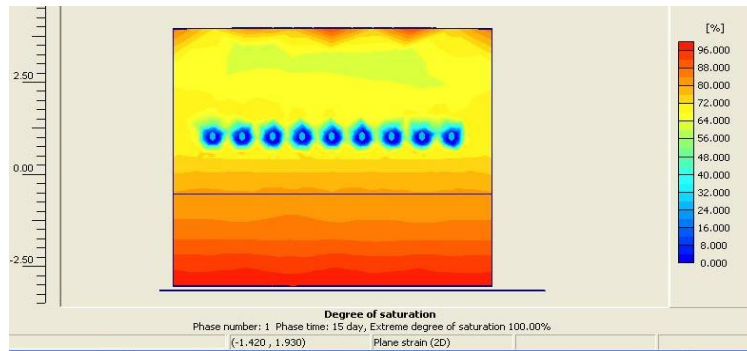
spacing in clayey soil in each scenario was set increasingly from 0.5 m, 0.75 m, 1 m, and 2 m. The results of the DoS corresponding to the values of drain spacing assigned above are displayed in Figure 4-45 (a) to (d).

In these figures the degree of saturation around the drains was lower than that in the other areas, which was the result of the drain effect. Here, the water in the vicinity of the drains was removed out, resulting to lower DoS in that area while other parts of the slope remained high DoS. Also, the DoS was lowest at center of each drain and it gradually increased, or the effect of the drains was less and less, as the distance from the core of the drain increased. This contour area around each drain indicating its DoS level was the influence zone of a drain. The influence zone of a drain varies in different types of soil depending on the hydraulic conductivities of those soils. The higher value of hydraulic conductivity of the soil, the larger area the influence zone can reach, and vice versa. It can be seen that the influence zone of the drain in the clay soil was small, approximately less than 1m in diameter. In the 0.5-m drain spacing, there was an overlap of the influence zones around the drains. This overlap indicated that the drains were influencing over each other, the spacing was not optimum as well as wider distances were applicable. As the spacing increased to 0.75m, there was no overlap between these influence zones as they stayed close to each other, leaving no areas having high DoS between them. When the spacing of the drains was increased to 1m and wider, their influence zones started to be far apart to each other and the areas between them remained high DoS. Based on the results from these figure, it was assumed that the effect of the drains would be lesser as the drain spacing was more than 2m. As a result, the spacing ranging from 0.75m to 1m was considered as the optimum drain spacing in clay soil.

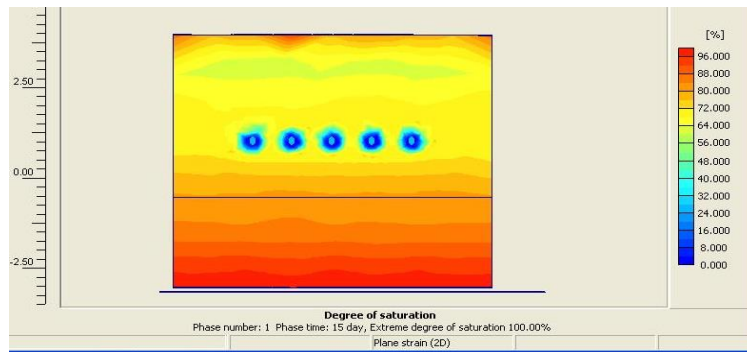
(a) 0.5-m spacing



(b) 0.75-m spacing



(c) 1-m spacing



(d) 2-m spacing

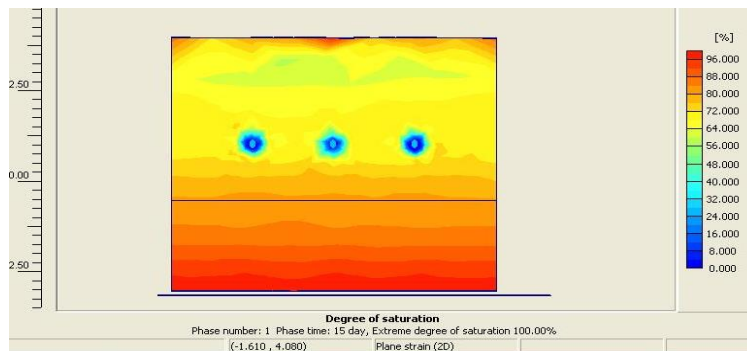


Figure 4-45: Degree of saturation results with different spacing in clay soil.

## Other types of soil

The optimum drain spacing determination analysis was also conducted in many other types of soil having different values of hydraulic conductivity. The other soils chosen were the silty clay and silt soil whose hydraulic conductivities are higher than that of the clayey soil. The selection of other soil types was restricted to the sandy soils since these soils usually have high hydraulic conductivities and no drainage methods are necessary for these types of soils. Therefore, only clayey soil, silty clay and silt soil were modeled in the parametric analysis to obtain the optimum drain spacing.

Since the values of the hydraulic conductivity of these soils are higher than that of the clayey soil and there was no information about the actual discharge flow rate of the drains in these soils, the values of the discharge rate of the drains modeled in these soils must be adjusted. The changes in discharge capacity of the drains in these soils were made based on Darcy's law, which states that the increase of the discharge capacity is linearly proportional with the increase of the hydraulic conductivity of the soil, as expressed in the following equation:

$$q = k * i * A \quad (\text{Eq. 4-1})$$

Where        q: discharge rate (m<sup>3</sup>/s)

              k: hydraulic conductivity of the soil (m/s)

              i: hydraulic gradient

              A: cross section in which the discharge passes through (m<sup>2</sup>)

Based on that assumption, the discharge capacities of the drains in silty clay and silt soil were adjusted to be higher than that of the clayey soil since the hydraulic conductivity of the clayey soil was lower. Table 4-1 expresses the estimated values of the

hydraulic conductivities and the adjusted discharge rates of the drains in silty clay and silt soil.

Table 4-1: Estimated hydraulic conductivities of the silty clay and silt soil and the discharge capacity of the drains in these soils.

Soil type	Hydraulic Conductivity (cm/s)	Discharge capacity (m <sup>3</sup> /day)
Clay	$3.5 \times 10^{-7}$ (actual)	0.0056 (actual)
Silty clay	$1 \times 10^{-6}$ (estimated)	0.02 (estimated)
Silt	$1 \times 10^{-5}$ (estimated)	0.2 (estimated)

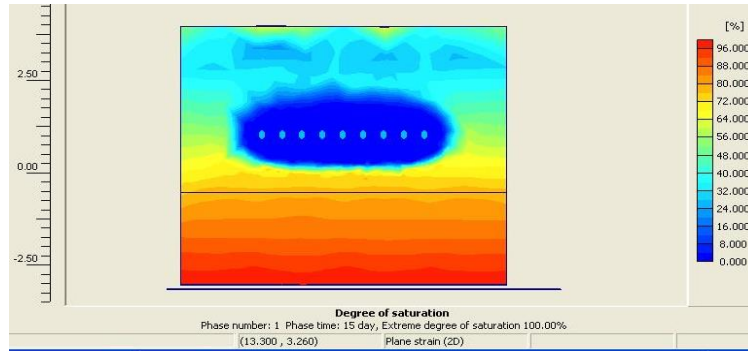
The values displayed on the above table were assigned to the model, and the same assumptions, precipitation profile and the boundary conditions were applied to this analysis so that the results are consistent. Since the hydraulic conductivities and drain discharge capacities of new the soils were higher than those of the clay soil, the spacing between the drains were assigned in larger distances.

Figure 4-46 (a) to (d) respectively express the DoS results of the drain spacing analysis in silty clay corresponding with the spacing of 0.5m, 1m, 1.5m and 2m. As can be seen in these figures, the influence zone of the drains was larger than that in the clay soil, which was due to the higher values of soil hydraulic conductivity and drain discharge capacity. In these figures the influence zone of the drains in the silty soil began to be far apart when the spacing was 1.5m or higher while an overlap of the influence zone between the drains was encountered in the 1m spacing grid. Therefore, the distance

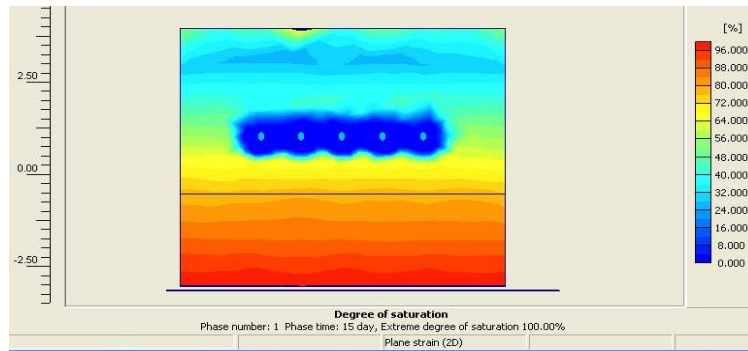
from 1.5m to 2m obtained from this analysis is considered the optimum drain spacing for the silty clay.



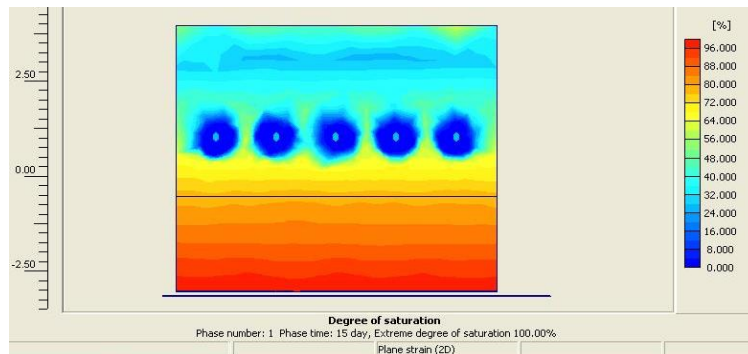
(a) 0.5-m spacing



(b) 1-m spacing



(c) 1.5-m spacing



(d) 2-m spacing

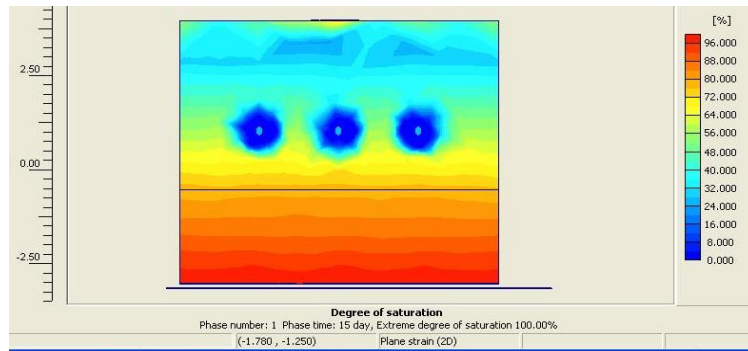
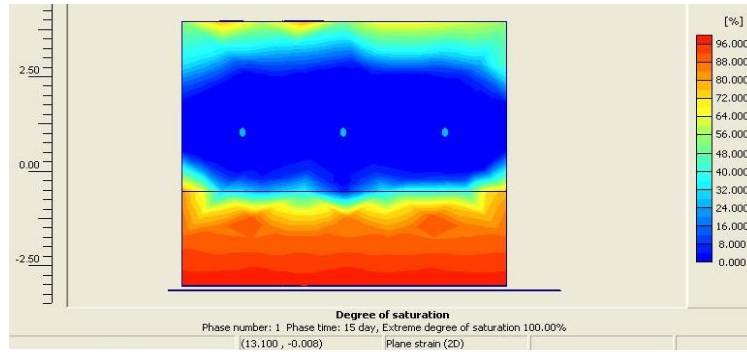


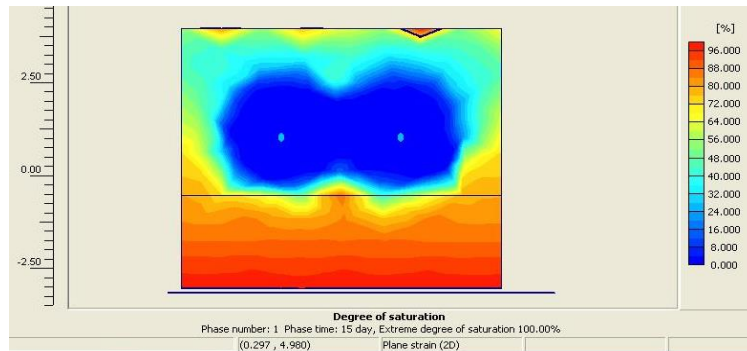
Figure 4-46: Degree of saturation results with different spacing in silty clay.

The results of the grid spacing analysis in silt soil are illustrated in Figure 4-47 (a) to (d). In this analysis, the spacing was setup to be in range of 2.5m, 3m, 3.5m, and 4m. The results show that the influence zone of the drains in this type of soil was much larger than that in the analysis of other soils and they almost covered the area of the upper soil layer. This is because the silt soil had the highest hydraulic conductivity among the soils in the parametric analysis and the discharge capacity of the drains in this soil was modeled proportionally higher. As can be seen in these figures, there was an overlap between the influence zones of the drains when the grid spacing was 3m or finer. These influence zones stayed very close together with the 3.5-m spacing grid and a small gap of higher DoS began to appear as the spacing was wider at 4m. No larger drain spacing were modeled since it was certainly that the gap between the drains would expand bigger as the spacing increased more. Thus the optimum drain spacing for the silt soil obtained from this analysis was about 3.5m to 4m.

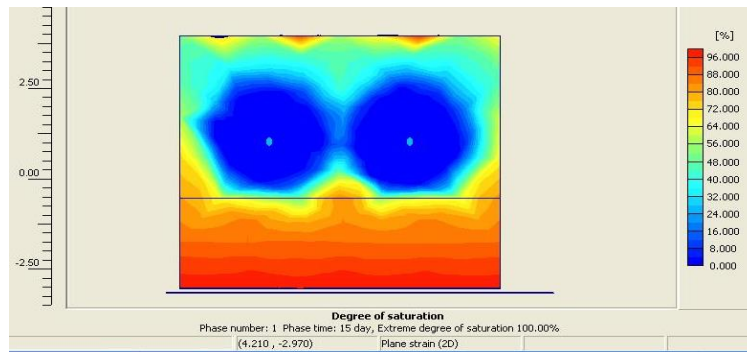
(a) 2.5-m spacing



(b) 3.0-m spacing



(c) 3.5-m spacing



(d) 4-m spacing

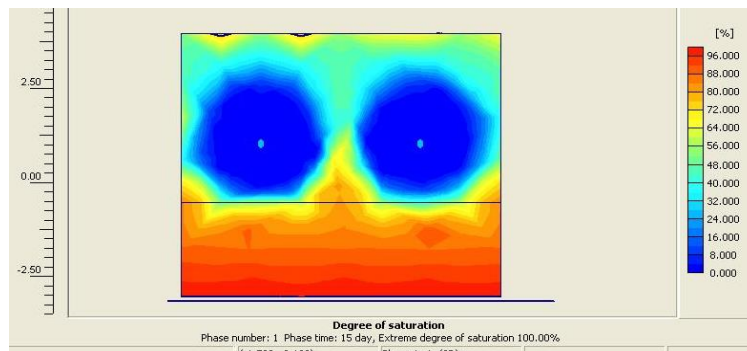


Figure 4-47: Degree of saturation results with different spacing in silt soil.

Based on the results obtained from the drain spacing analysis, it was concluded that the optimum spacing for the drains to be installed varies with different types of soil, with smaller spacing required for soils that have low values of hydraulic conductivity. The optimum drain spacing obtained from these analyses is displayed in Table 4-2 below, and they can be used as references for the design of horizontal drainage in the soils that have similar properties and hydraulic conductivities.

Table 4-2: Many types of soil with their estimated hydraulic conductivities and optimum drain spacing.

<b>Soil type</b>	<b>Hydraulic conductivity</b> (cm/s)	<b>Optimum drain spacing</b> (m)
Clay	$3.5 \times 10^{-7}$	0.75 – 1
Silty clay	$1 \times 10^{-6}$	1.5 – 2
Silt	$1 \times 10^{-5}$	3.5 – 4

#### **4.4 Cost-Effectiveness Analysis**

One of the scopes of this study was to evaluate cost of the installation procedure in order to determine if this horizontal drainage method is an effective and economic method as desired. The evaluation was done based on considering the cost of the installation as well as the cost of the drain material over the total length of drains installed. The cost of the drain material was obtained from the manufacturer with the price of \$0.25/ft. However, it was only the price of the flat wick drains. Therefore, the final price of the rolled-and-tighten wick drains, which was the drains used in this study, was estimated approximately \$0.45/ft. including the labor and material costs for rolling

and tightening the drains. In this study one trackhoe and one bulldozer were used to install the drains into the slope, as described in Chapter 3 before. The costs of the machinery and their operators for the drain installation are displayed in Table 4-3.

Table4-3: Costs of the machinery and operators for the drain installation.

Trackhoe	Machinery	\$2500/week
	Operator	\$40/hr.
Bulldozer	Machinery	\$1000/week
	Operator	\$40/hr.

Beside the machinery and operator costs listed above, the cost of the labors that assisted the drain installation must be counted into the total cost. As described in Chapter 3, the drain installation procedure was quite simple and easy, and it did not require well-trained labors as well as a big number of labors. Therefore, it was estimated that only two labors were needed to assist the drain installation. The cost of the labor usually ranges about \$18/hr, and it was added to the other costs to obtain the total cost of the drain installation.

A number of 18 drains with approximately 770 ft. were installed into the slope during Dec 11<sup>th</sup> and Dec 12<sup>th</sup> 2006, giving a total time of 16 hours exerted for the drain installation. It should be noted that the working time was defined as 8 hrs./day and 5 days/week, and the cost of the machinery listed above was for one week of operation. Combining all of the costs mentioned above, the total cost for the installation as well as the total cost for one foot of installed drain was derived. The total cost of the installation

procedure and the total cost for one foot of drain installed are calculated in Table 4-4 below.

Table 4-4: Total cost of the installation procedure and the total cost for one foot installed drain.

Types		Cost	
		\$/week	\$/hr
Machinery	Trackhoe	2500	62.5
	Bulldozer	1000	25
Operator	x 2		80
Labor	x 2		36
Installation cost per one hour			\$203.50
<b>Total cost for 16 hours of installation</b>			<b>\$3,256</b>
Total length of installed drains			770 ft
<b>Installation cost for 1 foot of drain</b>			<b>\$4.23</b>
<b>Material cost (per foot)</b>			<b>\$0.45</b>
<b>Final cost for 1 foot of drain installed</b>			<b>\$4.68</b>

As can be seen in the above table, the installation cost was about \$4.25 for a linear foot of drain installed. Including the cost of drain material, the total cost for the installation of this drainage method was less than \$5/ft. It should be noted that this total cost was calculated based on the labor cost and machinery cost obtained from the standard wages of the State of Arkansas. Therefore the total cost is anticipated to vary depending on the region in which this horizontal drainage method is applied, and the cost for this method was assumed to be in range of \$4 to \$6 per linear foot of drain installed.

Comparing to the cost of the conventional PVC horizontal drainage method listed by Santi (2001), the cost of the horizontal wick drain method was cheaper, mainly due to the lower cost of the installation. According to Santi (2001), the installation cost of the

drilling method was expensive, at approximately \$20 to \$36 per linear meter or about \$6 to \$12 per foot of drain. Including the cost of the PVC pipes, the total cost for the conventional PVC pipe method would be higher and is not as economical as the horizontal drainage method using wick drains. Additionally, it is anticipated that the cost of drain installation would be reduced as the labors became familiar with the installation technique. In conclusion, the cost of this horizontal wick drain method was more competitive and encouraging than the conventional drainage methods using PVC pipes.

## **CHAPTER 5**

### **CONCLUSIONS**

#### **5.1 Summary of Work**

An extensive literature review was completed to document the history and development of the horizontal drainage method for slope stabilization. The important factors that affect the performance of the drains were also documented for the implementation of the new drain material to be used in this drainage method. Laboratory tests were conducted to determine the properties of the soil at the site. These properties served as the inputs for the parametric analysis completed later. The measuring devices that were used in the research included the TDR cable and inclinometer for slope movement monitoring, moisture probes for moisture content fluctuation monitoring, piezometers for GWT monitoring, and rain gauges for precipitation and flow capacity monitoring. A calibration program was developed to insure the accuracy of these devices so that the results were reliable for the drain performance evaluation. A control program was created for the data acquisition for the measuring equipment so that the data collection could be done remotely. A total number of 18 drains were installed at the selected site in a period of 2 days in Dec of 2007, with the total length of installation of 770 ft (234 m). After the installation, the drain performance was monitored for seven months, from February to September 2007, for the evaluation.



## 5.2 Conclusions

- As evidenced by the drainage collection system, the horizontal wick drains responded almost immediately to precipitation events in removing water from the slope.
- Wick drains are effective in lowering the moisture content in the slope. The moisture content in the drained section of the slope was always lower than the moisture content in the control section.
- Movement in the drained section for the site was not completely prevented. However, recorded movement in the drained section of the slope was always lower than the movement in the control section of the slope.
- There was general agreement between the inclinometer and TDR equipment in determining the location and the magnitude of the movement along a sliding surface.
- The inclinometer was far more accurate in determining the magnitude of movement. The TDR cable could only detect movements that had progressed more than 50 mm.
- Slope movement could be monitored by the TDR cable long after the inclinometer probe could no longer traverse the inclinometer casing
- Optimal drain spacing decreases as the hydraulic conductivity of the material in the slope decreases.
- Despite overcoming a learning curve for installation and using untrained labor, this horizontal drainage method using driven wick drains proved to be more cost-effective than conventional PVC or galvanized pipe methods.

### **5.3 Recommendations**

There is a strong belief that the failure, or excessive movement, of the control section was responsible for the movement observed in the drained section of the test site. In an attempt to minimize the physical differences between the two test sections and to minimize the amount of data acquisition equipment required to monitor the site, the drained and control sections were located too close to one another. Future studies should insure a separation between control and test locations that would eliminate the possibility of movements in one site triggering movements in the other site.

While the installation of the drains worked, there were many learning hurdles to overcome. The original “pusher” device was too cumbersome and heavy to deal with and a much simpler device was developed to advance the carrier pipe with a tracked excavator and paving breaker. Unfortunately, the drains could not be installed to the desired penetration in the slope. It is felt that the drive head (splitting wedge) was too small and did not create an annulus space between the carrier pipe and the surrounding soil. The resulting friction between the carrier pipe and the soil generated a resisting force that exceeded the push capacity of the excavator, even when coupled with the dynamic action of the paving breaker. Future studies should investigate a variety of sacrificial drive heads that will develop a larger annulus in the soil and one that will allow a more positive connection to the wick drain material.

The most time consuming part of the installation process was the treading of the rolled wick drain material through the drill rod, which served as the carrier pipe. If a pipe with a larger diameter were used the drain could be inserted after the pipe had

been driven. This would avoid the necessity of splicing the drain material and threading it through each section of pipe as it is pushed or driven into the slope. It is recommended that four pipe be used in the future. There is an obvious tradeoff between pipe diameter and wall thickness with ease of drain insertion and the equipment's ability to push or drive the carrier into the slope. Future studies could define the sweet spot for drive head and drive pipe configurations.

Due to the rental of equipment and the brutally cold weather in December, the number of drains installed at the site was not the optimum. There should have been more drains installed if the optimum spacing indicated by the analytical study were adhered to. It is recommended that drain installation be accomplished in more moderate weather and that equipment resources of the district be utilized so that time and cost (while monitored) do not become the determining factor for the number of drains to be installed. Rather, the recommended drain spacing established for the given soil type in the parametric analysis of this study be followed.

## Appendix A: Operating Principles of the Slope Inclinometer

Inclinometer, referred as slope inclinometer, probe inclinometer, or slope indicator, is a device used to measure the magnitude of ground movement (Wong, 2004). The inclinometer probe measures the lateral movement of the ground through measuring the deformation or deviation of a specially grooved inclinometer casing. This casing was previously grouted and passed through the suspected crack zone of the slope. When the slope moves it also bends the casing, and then the inclinometer probe is inserted into the casing to measure the casing deformation.

The main functions of a slope inclinometer list by Dunnicliff (1988) as followings:

- Detect the location of the shear plan of a slope.
- Monitor the magnitude of lateral movement of embankments, slopes, excavations, and tunnels.
- Observe the deflection of bulkheads, piles, and retaining walls.
- Monitor the settlement of embankments, oil tanks, and other structures by using special probes that operate in a horizontal casing.

The body of an inclinometer probe is usually made of stainless steel to prevent it from any damaging when it is immersed in a corrosive environment. Attach on the body of the probe are two wheel couples which are also made of stainless steel. These wheel sets function as sensors to measure the differences in geometry of the casing. The front head of the probe is rubber-covered to prevent any damaging during the measuring process and the end head is connected to a control cable. Figure 3-27 expresses a layout of a typical inclinometer probe. In the sequence of monitoring slope movement, the

casing is firstly grouted into the slope, and the length of the casing must pass the suspected shear zone of the slope. This casing has four cross grooves to orient the direction of the inclinometer probe. To identify the direction of the movement, the direction of the groove which faces to the toe of the slope is marked as the  $A0^\circ$  direction, and the opposite direction is marked as the  $A180^\circ$  direction. The other directions which are perpendicular to the  $A0^\circ$  and the  $A180^\circ$  directions are marked as  $B0^\circ$  and  $B180^\circ$  directions. Figure 3.28 illustrates a cross section of an inclinometer probe inserted into a casing with the wheels orienting in the A-direction. In this figure the  $B0^\circ$  and  $B180^\circ$  directions are discretely marked because they are not the interested directions. But in case that slope movement is also monitored in the B-direction, the B-direction grooves are also marked with the same manner like the A-direction.

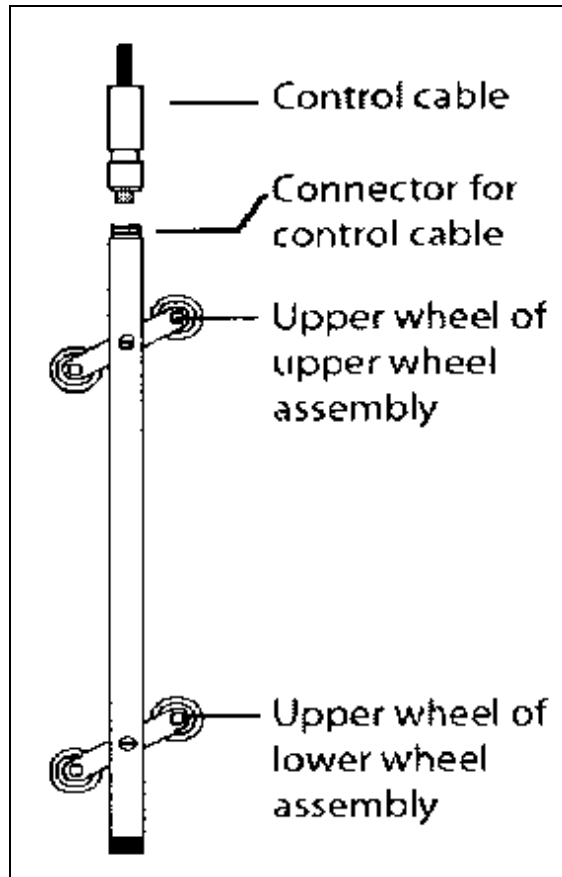


Figure 3-27: Layout of an inclinometer probe (Wong, 2004).

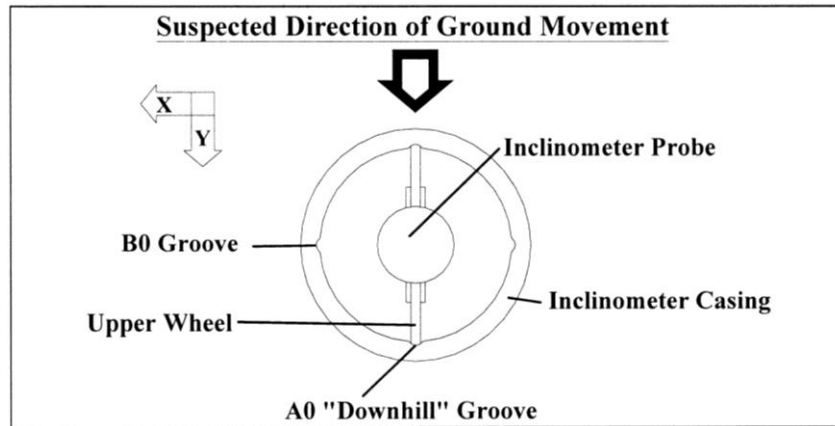


Figure 3-28: Directions of the grooves of the inclinometer casing (Wong, 2004).

Firstly the inclinometer probe is inserted into the casing with the upper wheel of both of wheel couples facing in the downhill direction or the  $A0^{\circ}$  direction. Then it is slowly lowered down to the bottom of the casing through the control cable. When the probe is lowered all the way and reaches the end of the casing, the first reading is made. Then the probe is raised up every 1 ft mark interval to get the readings along the casing. The reading achievement is stopped as the probe is raised up to the top of the casing. Next the probe is turned into the invert direction and inserted into the casing with the upper wheel of both of the wheel couples facing in the  $A180^{\circ}$  direction. Then the readout process is repeated for the  $A180^{\circ}$  direction. The procedure described above will provide two reading sets in the A-direction with the first set known as the " $0^{\circ}$  reading" and the other as the " $180^{\circ}$ " one. This procedure is also applicable to obtain the readings for the B-direction. The first measurement is required immediately after the casing was grouted into the slope, and these reading sets obtained from this survey are considered as the baseline for slope movement monitoring. The subsequent reading sets will be compared

to the baseline to detect the location of the shear plan and the magnitude of the movement of the slope.

The tilt measurement methodology of the casing at any level is obtained by using the sine function (Wong, 2004). The lateral deviation of the casing is computed from its tilt angle ( $\theta^\circ$ ) and the hypotenuse of a right triangle as shown in Figure -29. In this figure the hypotenuse of the right triangle is the distance L between the centers of the two sensor-wheel couples. The deviation of the casing is computed based on the following formula (Wong, 2004):

$$\text{Opposite side (Deviation)} = \text{sine}\theta * \text{Hypotenuse} \quad (\text{Eq.3-9})$$

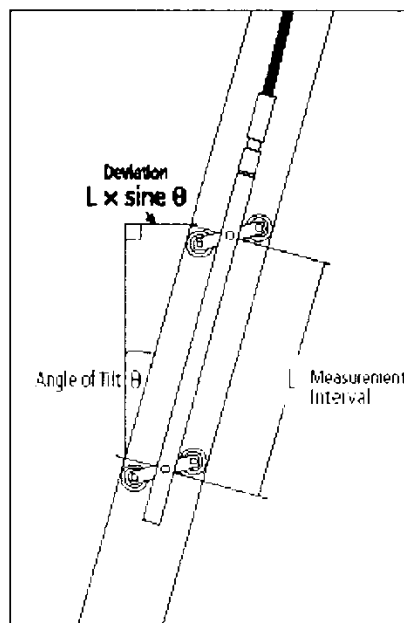


Figure 3-29: The tile measurement methodology of the inclinometer probe (After Slope Indicator, 2000).

The hypotenuse or the parameter L in Equation 3-9 is usually 2 ft (60cm). The above equation helps to convert the measured tilt angle into a lateral movement and it is the basic calculation of slope movement measurement. Here, the readout unit does not directly show the angle of the tile,  $\text{sine}\theta$ , at a specific interval, but it displays an adjusted

output value called the “reading unit” instead (Wong, 2004). According to Wong (2004), the “reading unit” is defined as below:

$$\text{Reading unit} = \text{sine}\theta * C \quad (\text{Eq.3-10})$$

Where: C: instrument constant

English unit: C = 20,000

Metric unit: C = 25,000

With the reading unit obtained from the readout unit and constant C above, the tilt angle is then computed through the equation below:

$$\text{sine}\theta = \frac{\text{ReadingUnit}}{C} \quad (\text{Eq.3-11})$$

Since there are two readings made at each interval, one with 0° direction and the other with 180° direction, the average of them is usually used through the following equation:

$$\text{Average Reading} = \frac{0^\circ \text{ Reading} - (180^\circ \text{ Reading})}{2} \quad (\text{Eq.3-12})$$

By combining Equation 3-11 with Equation 3-12, the value of the tilt angle is computed as following:

$$\text{Sine}\theta = \frac{0^\circ \text{ Reading} - (-180^\circ \text{ Reading})}{2 \times C} \quad (\text{Eq.3-13})$$

With the value sineθ calculated from the above equation and the pre-known distance L, the lateral deformation of the slope is then computed as below:

$$\text{LateralDeviation} = L \times \frac{0^\circ \text{ Reading} - (-180^\circ \text{ Reading})}{2 \times C} \quad (\text{Eq.3-14})$$

For instance, the following parameters are recorded in the A direction at a random position along the casing as follow:



- $A0^\circ$  reading = 579
- $A180^\circ$  reading = -563
- Interval L = 60 cm
- Constant C = 25,000

Then the lateral deviation is computed as below:

$$LateralDeviation = 60cm \times \left( \frac{579 - (-563)}{2 \times 25,000} \right) = 0.6852cm$$

The lateral deviation is calculated at each interval along the casing, and all of these values are plotted in a graph to form the diagram of the movement of the slope at a specific time of measurement. Then the measurements at many different times are plotted together for the comparison to determine the shear zone and the magnitude of the movement of the slope.

## Appendix B Calibration of TDR Cables and Probes

### B.1 Propagation velocity of TDR cables determination

As mentioned earlier in this report, knowing the correct propagation velocity,  $V_p$ , of the cable connected to the TDR100 is very important to obtain the accurate and reliable results from the TDR 100 measurements. Besides using the value of  $V_p$ , which is usually provided by the manufacturer, another method using apparent and real length can be used to determine the correct propagation velocity of a cable. According to the TDR100 manual, the relationship between the real length and the apparent length is expressed as following:

$$\text{Apparent length} = (\text{Actual length}) \times (\text{Selected } V_p / \text{Actual } V_p) \quad (\text{Eq.B-1})$$

The apparent length of the cable is the length of the waveform displayed on the window screen of the PCTDR software when a value of  $V_p$  equal to (1.00) is entered in the *Cable Propagation Velocity* box (TDR100 manual). Using this feature, when the *Selected*  $V_p$  is set equal to (1.00), ( $V_p = 1.00$ ), Equation B-1 can be rearranged to get the Actual  $V_p$  as following:

$$\text{Actual } V_p = (\text{Actual length}) / (\text{Apparent length}) \quad (\text{Eq.B-2})$$

By using the TDR100 and PCTDR software, the apparent length of a cable is then determined. With the physical length, or the actual length, which is already known, the actual propagation velocity of a cable can then be easily obtained.

The above methodology was applied to determine the actual  $V_p$  of the four TDR cables used for slope movement monitoring in the experiment. One TDR cable was directly connected to the TDR100 for each test, and the propagation velocity determination was conducted respectively for all of the cables. The physical lengths, or

the actual lengths, of these cable were measured at 30.5 (100 ft) and 36.6 m (120 ft) for each two TDR cables. When the selected propagation velocity  $V_p$  was set at (1.00), the waveforms of these cables were captured by using the TDR100 and the PCTDR software, as shown in Figure B-1, and their apparent lengths were then determined. With the known values of the actual lengths, the actual propagation velocity of the cables was calculated through Eq.3-16 and the results of the  $V_p$  determination are shown in Table B-1.

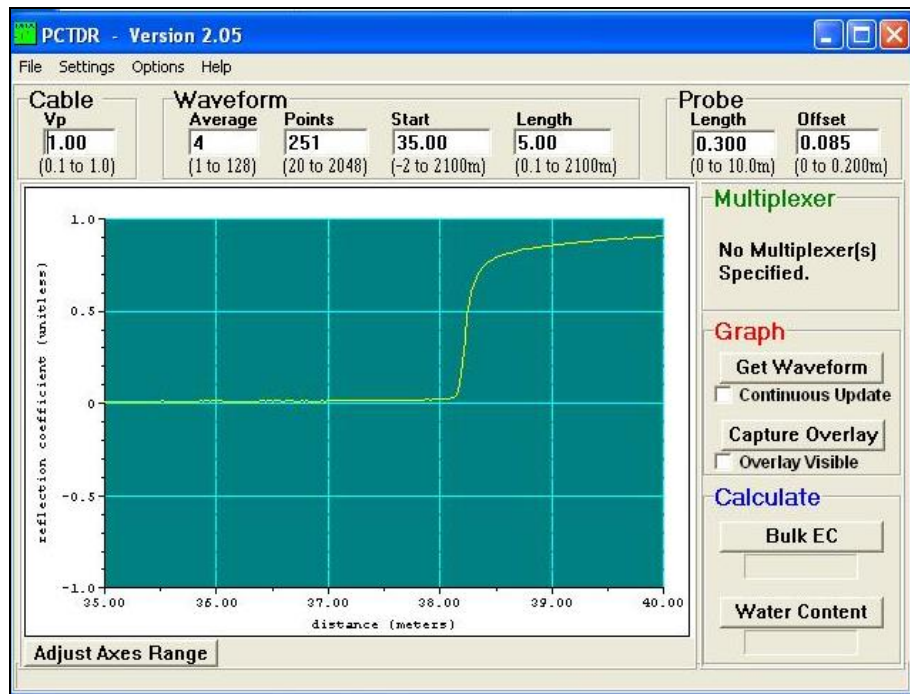


Figure B-1: A waveform captured by PCTDR for  $V_p$  determination.

Table B-1: The calculated propagation velocity of TDR cables.

Cable	Cable length (actual length) (m)	Apparent length (m)	Actual $V_p$	Actual $V_p$ (Averaged)
TDR-C1	36.6	45.7	0.801	

TDR-C2	36.6	45.6	0.803	0.80
TDR-C3	30.5	38.1	0.801	
TDR-C4	30.5	38.15	0.800	

## B.2 Site specific calibration

When the TDR100 makes a moisture content measurement, the recorded result is performed in volumetric moisture content, which is not as familiar in geotechnical engineering as the gravimetric moisture content. Therefore, there is a need to express the relationship between the volumetric moisture content and the gravimetric moisture content of the soil at the site. This work was carried on through the site specific calibration by using the TDR100 and PCTDR software.

A large amount of the soil at the site was taken to the soil lab in University of Arkansas. It was dried in natural condition at room temperature, about 22°C. Then the soil was put in to a 150mm x 300mm (6" x 12") plastic cylinder mold. A moisture probe CS610, which was previously connected to the TDR100, was inserted into the mold to measure the volumetric moisture content of the soil. Figure B-2 shows a moisture probe inserted into a cylindrical mold during the site calibration procedure. By using PCTDR software, the waveform of the signal was captured and the volumetric moisture content of the soil was measured. This value is shown at the bottom left corner in the PCTDR window screen as in Figure B-3. Then a soil sample from the mold was taken out to measure its gravimetric moisture content. With a value of volumetric moisture content

measured by TDR100, there was a corresponding gravimetric moisture content measured by the oven-dried method. These data were plotted in a graph to perform the relationship between the two parameters of the soil moisture content.

The above procedure was repeated many times with an increment in water content for each trial. Initially, the first measurement was made at the naturally dried condition of the soil. Then water was added to the soil to make about 3% moisture content increment for each trial. It was assumed to complete the calibration at gravimetric moisture content up to 40%. But the calibration terminated after the 10<sup>th</sup> trial at about 30% to 33% of moisture content because the soil started to form many big clods, which was difficult to mix the soil thoroughly and hard to insert the moisture probe into the mold.



Figure B-2: The plastic cylinder mold for site specific calibration.

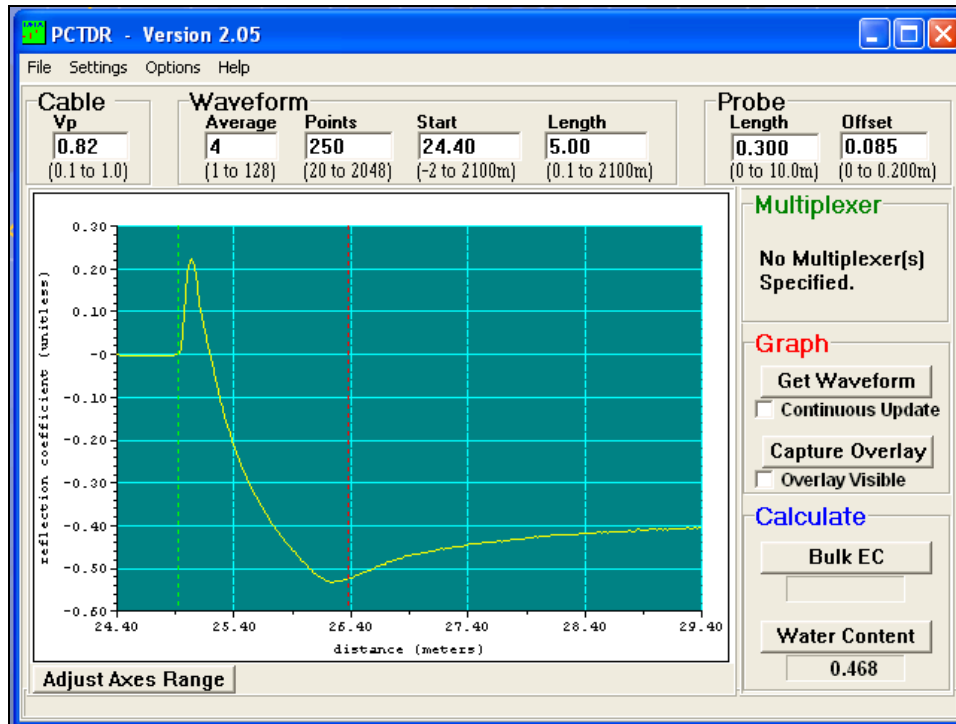


Figure B-3: A waveform and a value of volumetric moisture content at 46.8 % of a measurement recorded using the TDR100 and PCTDR software.

However, with ten couplets of data from ten trials, the results were considered enough for the calibration. The results of the site specific calibration were performed in Table B-2 and Figure B-4 as following.

Table B-2: Results of site calibration.

No. of trial	Oven-dried method				TDR Measurement
	Weight. of Tin (g)	Weight of Tin + Wet soil (g)	Weight of Tin + Oven-dried soil (g)	Gravimetric M.C. (%)	Volumetric M.C. (%)
1	41.08	113.06	110.25	4.06	7.8

2	56.67	122.3	117.73	7.48	9.7
3	56.51	141.61	133.11	11.1	16.8
4	50.92	127.3	118.12	13.66	20
5	55.63	134.87	123.5	16.75	27
6	46.91	126.56	113.16	20.23	35.1
7	45.73	102.39	91.87	22.8	38
8	48.07	109.37	96.85	25.67	41
9	50.25	125.8	109.02	28.55	46.8
10	40.82	100.84	86.45	31.54	50.6

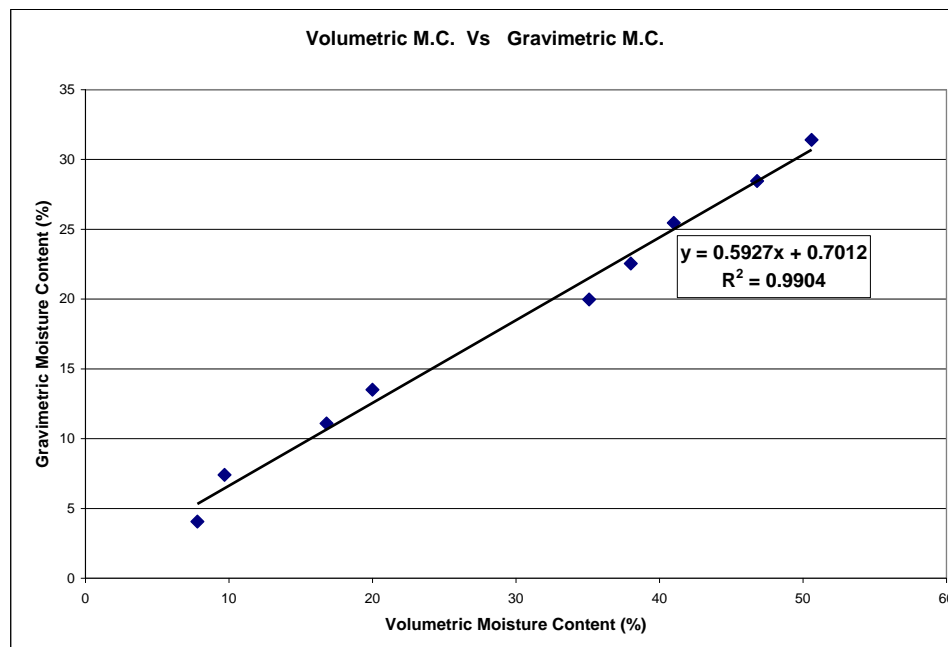


Figure B-4: The relationship between Gravimetric and Volumetric moisture content of the soil obtained from the site calibration.

From the above figure, it can be seen that the gravimetric moisture content increased almost linearly with the increase of the volumetric moisture content. The *Chi-*

*Square* ( $R^2$ ) of value the trendline is approximately equal to (1.00), which means that the data points nearly fit on that trendline and the accuracy of the performing equation is very high. Based on these results, the gravimetric moisture content was considered to be linearly dependent on the volumetric moisture content, and the relationship between these two parameters is expressed through the following equation:

$$\text{Gravimetric M.C (\%)} = \text{Volumetric M.C. (\%)} \times 0.5927 + 0.0712 \quad (\text{Eq. B-3})$$